

BUREAU OF ECONOMIC GEOLOGY
The University of Texas
Austin, Texas 78712
Peter T. Flawn, Director

Report of Investigations — No. 57

**Sedimentary Petrology and
History of the Haymond Formation
(Pennsylvanian), Marathon Basin, Texas**

By

Earle F. McBride



March 1966

BUREAU OF ECONOMIC GEOLOGY

The University of Texas

Austin, Texas 78712

Peter T. Flawn, Director

Report of Investigations—No. 57

**Sedimentary Petrology and
History of the Haymond Formation
(Pennsylvanian), Marathon Basin, Texas**

By

Earle F. McBride



March 1966

Contents

	PAGE
Abstract	1
Introduction	3
Previous and current work	3
Acknowledgments	7
Stratigraphy	8
Problems	8
Lithostratigraphy	8
Age and fossils	15
Megascopic lithologic features	17
Flysch facies	17
Sedimentary structures	18
Structures of current origin	18
Soft-sediment deformation	21
Other structures	22
Allison Ranch facies	22
Coarse sandstone beds	23
Boulder beds	24
South of U. S. Highway 90	24
Clark Butte area	28
Petrography	30
Shale	30
Sandstone of the flysch facies	31
Procedure	31
Quartz	31
Feldspar	31
Rock fragments	32
Carbonate grains and fossils	32
Matrix	32
Cement	33
Texture	33
Fabric	33
Coarse sandstone beds	34
Boulder beds	34
Heavy minerals	37
Cherty limestone bed	39
Stratigraphic petrographic variability	39
Diagenetic features	44
Physical diagenesis	44
Mineralogical diagenesis	44
Deposition of the flysch facies	45
Previous interpretations	45
Present interpretation	45
Comparison with Bouma's turbidite model	46
Problems	47
Allison Ranch facies	48
Origin of the boulder beds	49
Review of previous interpretations	49
Boulder beds south of U. S. Highway 90	49
Origin	49
Source of large fragments	50
Striated and flattened gravel	50
Source and genesis of well-rounded gravel	51
Boulder beds in Clark Butte area	51
Deposition of the coarse sandstone beds	53
Paleocurrents	54
Provenance	57
Summary and sedimentologic history	59
Regional setting	59

Stratigraphy	59
Environment and manner of deposition	59
Paleocurrents	60
Provenance	60
Sedimentologic and tectonic history	60
References cited	62
Appendix A. Petrographic description of erratic and exotic rock types from Haymond boulder beds	65
Appendix B. Location of numbered data localities shown in figure 3	70
Index	100

Illustrations

FIGURES—

PAGE

1. Trend of Ouachita structural belt and location of outcrop areas of flysch units of the Ouachita System	4
2. Generalized section of Paleozoic rocks in the Marathon geosyncline and inferred ages in years of stratigraphic units	5
3. Outcrop and index map of Haymond Formation	6
4. Schematic diagram of major stratigraphic units in the Haymond Formation	9
5. Sketches of stratigraphic details of parts of the boulder bed unit	11
6. Stratigraphic section at the top of the boulder bed unit one-fourth mile northwest of windmill at the base of Housetop Mountain	12
7. Location and thickness of boulder beds in northern part of the Marathon Basin	13
8. Schematic stratigraphic section of boulder beds at section D of figure 7	14
9. Schematic presentation of bedding sequences in Haymond sandstones	19
10. Orientation of soft-sediment faults and sandstone dikes	22
11. Plot of Haymond sandstones showing texture and composition	35
12. Circular orientation histograms based on 100 elongate grains per sample	36
13. Plot of shapes of vein quartz pebbles from the boulder beds south of U. S. Highway 90	52
14. Paleocurrent map	55

PLATES—

PAGE

1. Stratigraphic sections and petrographic variability of flysch and coarse sandstone beds In pocket	
2. Stratigraphic sections of flysch, coarse sandstone, and Allison Ranch facies In pocket	
3. Haymond outcrops showing the flysch character of the formation	72
4. Directional and other sedimentary structures in Haymond sandstones	74
5. X-radiographs and negative print of Haymond sandstones showing internal bedding structure	75
6. Trace fossils, current structures, and soft-sediment faults in Haymond sandstones	76
7. Bedding features of Haymond sandstones	77
8. Sole marks and features of soft-sediment deformation in Haymond sandstones	78
9. Features of coarse (non-flysch) sandstone beds	79
10. Boulder bed member southwest of Housetop Mountain	80
11. Boulder bed member from the vicinity southwest of Housetop Mountain	81
12. Details of the boulder bed member and polished and striated pebbles	82
13. Photomicrographs of Haymond shales	83
14. Photomicrographs of flysch sandstones from below the coarse sandstone and boulder beds	84
15. Photomicrographs of sandstones from below the boulder bed member and of coarse (non-flysch) sandstone	85
16. Photomicrographs of mudstone from the boulder bed member; photomicrograph of the spicule(?) bed from the Dugout Mountain area; photomicrograph of a burrowed sandstone from above the boulder bed member	86
17. Photomicrographs of sandstones from the Dugout Mountain area	87
18. Photomicrographs of sandstones showing diagenetic features	88
19. Photomicrographs and negative print of sandstones showing diagenetic features	89
20. Photomicrographs of sedimentary rocks from the boulder beds	90
21. Photomicrographs of sandstones and metasandstone from the boulder bed member	91
22. Photomicrographs of igneous and metamorphic rocks from the boulder bed member	92
23. Photomicrographs of metamorphic rocks from the boulder bed member	93
24. Photomicrographs of metamorphic rocks from the boulder bed member	94
25. Diagrams showing orientation of directional sedimentary structures	95

Tables

TABLES—

	PAGE
1. Bedding types and sequences in 39 beds from Locality 6	20
2. Average thickness of beds with different types of directional structures	20
3. Maximum and estimated average size of erratic and exotic clasts in the boulder beds	26
4. Estimated percentages of pebbles in polymictic conglomerate from the boulder beds	27
5. Relative abundance of clay minerals in Haymond shales and matrix of sandstone beds	30
6. Mineral composition and average grain size of Haymond sandstones and erratic sandstone pebbles from the boulder bed member	In pocket
7. Percent of non-opaque and non-micaceous detrital heavy minerals in Haymond sandstones	38
8. Data of groups of Haymond sandstones used to test for stratigraphic differences in maximum grain size and mineral composition	40
9. Results of tests of significance of grain size and mineral composition parameters between groups of Haymond sandstones	In pocket
10. Pairs of petrographic parameters of Haymond sandstones that show significant correlation values at 0.05 level of significance	42

Sedimentary Petrology and History of the Haymond Formation (Pennsylvanian), Marathon Basin, Texas

Earle F. McBride¹

ABSTRACT

The Haymond Formation is part of a 12,000-foot sequence of flysch that was deposited in late Paleozoic time in the Marathon segment of the Ouachita geosyncline in Trans-Pecos Texas. The Haymond has a maximum preserved thickness of 4,300 feet and is chiefly a monotonous sequence of intercalated fine-grained sandstone and gray shale beds less than 6 inches thick. This flysch facies has more than 15,000 separate sandstone beds. The shales, chiefly illite with minor quartz silt and minute carbonaceous plant fragments, are mostly burrowed, but they contain no fossils indicative of shallow water. The sandstones, quartzose rocks rich in both feldspar and rock fragments, are characterized by an upward sequence of bedding types (massive-laminated-convolute-cross-laminated) that indicate deposition from waning currents of high initial velocity; in addition, many show graded bedding. The Haymond flysch was deposited in a marine basin that was from several hundred to several thousand feet deep; the shales accumulated slowly as pelagic muds, whereas the sandstones were deposited by turbidity currents which intermittently flowed into the basin.

Mudstone beds and contorted flysch beds that encase exotic and erratic cobbles and boulders up to 130 feet long crop out along the northern and eastern edges of the basin. The interbedded character of mudstone layers, fragmented sandstone and shale beds, and slump structures attest to a sedimentary (syndepositional and prelithi-

fication) origin in contrast to a tectonic (post-depositional and post-lithification) origin for the boulder beds. The latter are interpreted to be the product of submarine slides which originated when masses of Paleozoic rock were dislodged from thrust scarps and slid basinward (P. B. King, 1958). Erratic rock types include angular fragments of rock similar to Paleozoic formations exposed in the Marathon area, but which are normally from 3,000 to 10,000 feet lower stratigraphically, and well-rounded gravel clasts of gneissic granite, metarhyolite porphyry, schist, quartzite, conglomerate, and sandstone. Radiometric dating of a gneissic granite in a pebble suggests the granite formed in late Precambrian time and underwent metamorphism during mid-Paleozoic (late Devonian?) time.

Layers of poorly bedded coarse sandstone are associated with the boulder-bed complex. The coarse sandstones differ from flysch sandstones in that they are coarser, poorly cemented, have less feldspar, and are chiefly massive to poorly laminated. They include a few turbidity-current laid beds but most are probably slide deposits or material deposited from viscous sediment flows with characteristics between those of turbidity currents and gravity slides. Some may have accumulated by sand creep, a process known to operate in steep submarine canyons off the coast of California.

The orientation of more than 500 directional current structures, chiefly groove casts, flute casts, and parting lineations, was measured to determine the paleocur-

¹ Associate Professor of Geology, The University of Texas, Austin.

rent pattern of sediment transport. Data from slope-controlled turbidity currents indicate that most sand detritus was carried down a subsea slope to the west or northwest until the axis of the trough was reached and thence down the regional **plunge to the southwest. Late in the episode** of Haymond deposition, sediment was shed from the uplifted edge of the craton to the northwest and flowed in easterly and northeasterly directions.

The major source of Haymond detritus was a complex positive element to the east-southeast (Llanoria); it had a core of Cambrian-Precambrian granite that was mantled by sandstone, conglomerate, and **shale of probable early Paleozoic age.** Its probable location was in what is now northern Mexico, where a granitic basement-complex with poorly defined limits is

known (Flawn et al., 1961, p. 105). The uplifted edge of the craton (Diablo Platform?) to the northwest of the geosyncline contributed granitic debris and shallow-water carbonate detritus.

The Haymond was the last of three flysch formations (Tesnus, Dimple, Haymond) to be deposited in the Marathon geosyncline; it was succeeded by shallow-water molasse of the Gaptank Formation (Pennsylvanian). The geosyncline was deep throughout most of Haymond deposition but shallowed during later stages as the result of filling of the basin concomitant with uplift of Llanoria and tilting of the paleoslope to the north. At this time sediment probably began spilling into the new deep (Val Verde) basin to the northeast.

INTRODUCTION

This report treats the sedimentary petrology and history of the Haymond Formation, a monotonous sequence of interbedded sandstone and shale that has a maximum preserved thickness of 4,300 feet. The upper part of the formation includes massive coarse sandstone beds and a complex of pebbly mudstones and slumped beds that encase exotic and erratic rock fragments up to 130 feet long. The Haymond is part of a 12,000-foot sequence of flysch that was deposited during late Paleozoic time in the Marathon geosyncline, a part of the Ouachita geosyncline located in Trans-Pecos Texas. The formation is exposed on a structurally high part of the Ouachita structural belt (fig. 1), most of which is known only in the subsurface in Texas (Flawn et al., 1961), within the topographic Marathon Basin, a sub-rectangular area that has dimensions of 50 miles in a NE-SW direction and 35 miles in a NW-SE direction. Deformed Paleozoic rocks trend NE-SW in the Basin and are exposed through a veneer of Quaternary alluvium; the Basin is rimmed by Permian rocks to the northwest (Glass Mountains) and by Cretaceous rocks in other directions.

Paleozoic sedimentary rocks that have a composite thickness of approximately 15,000 feet were deposited in the geosyncline. The rocks were folded and thrust-faulted as the result of crustal shortening that culminated during late Pennsylvanian time and subsequently faulted and domed during Mesozoic and Tertiary time (P. B. King, 1937). Flysch of Mississippian and Pennsylvanian age comprises nearly 12,000 feet of the geosynclinal sequence. The Haymond is the youngest flysch unit; it is separated from the Tesnus, a siliciclastic flysch unit similar in many respects to the Haymond (P. B. King, 1937, Cotera, 1962; McBride and Thomson, 1964), by the Dimple Limestone, a calcarenite-shale flysch unit (Thomson and Thomasson, 1964). Older Paleozoic rocks in the Basin

are chert, novaculite, limestone, and shale, with lesser amounts of sandstone and conglomerate that have a total thickness of approximately 3,000 feet (P. B. King, 1937). A composite stratigraphic section of Marathon Basin rocks, which represent most of Paleozoic time (late Cambrian, Ordovician, Silurian?, Devonian, Mississippian, and Pennsylvanian), is shown in figure 2.

The Haymond is of sedimentologic interest because of the problems of the mode of emplacement of the erratic and exotic rocks of the boulder beds and of the deposition of innumerable alternations of sandstone and shale; in addition, it is of interest as a partial record of the geologic history of the Marathon geosyncline.

This report describes the stratigraphy and petrography of the Haymond and presents interpretations on environments and modes of deposition, provenance, paleocurrent pattern of sediment transport, and sedimentological history. A generalized outcrop map of the Haymond showing the position of sample localities and geographic features mentioned in this report appears as figure 3.

Previous and current work.—The general structure and stratigraphy of the Paleozoic rocks of the Marathon Basin were unraveled chiefly through the classic and monumental work of P. B. King (1930, 1937), in part aided by R. E. King (1930). Earlier reconnaissance studies include reports by Von Streeruwitz (1891), Hill (1900), Udden (1907), and Baker and Bowman (1917). A summary of these reconnaissance reports is given by King (1937, pp. 2–3).

The term "Haymond formation" was applied by Baker (Udden, Baker, and Böse, 1916, p. 46) to rocks exposed near Haymond, a former station on the Southern Pacific Railroad in the eastern part of the Basin (fig. 3). Baker later suggested (Baker and Bowman, 1917, p. 107; Baker, 1928, p. 1114) that the unit called Haymond might be part of an underlying for-

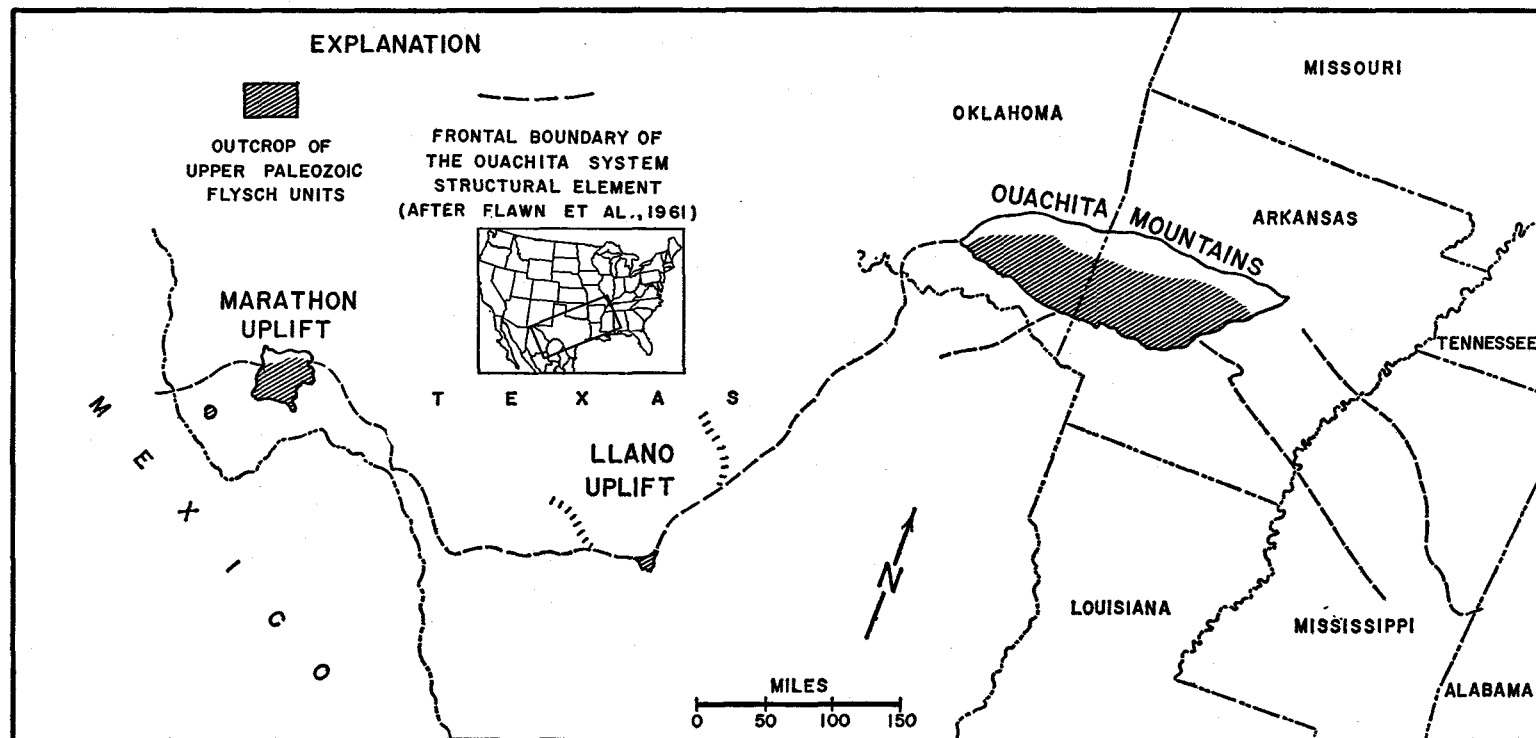


FIG. 1. Trend of Ouachita structural belt and location of outcrop areas of flysch units of the Ouachita System.

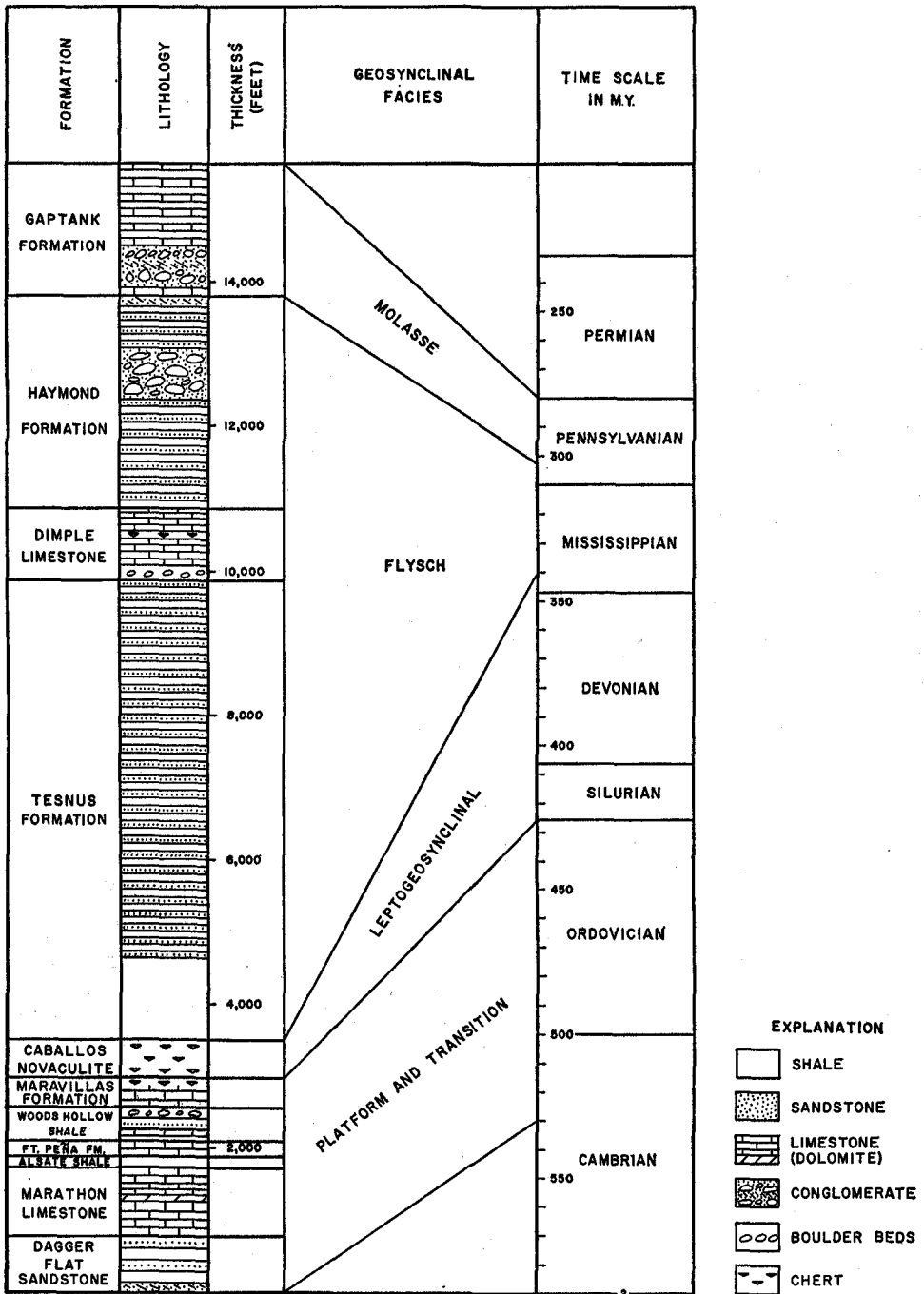


FIG. 2. Generalized section of Paleozoic rocks in the Marathon geosyncline and inferred ages in years of stratigraphic units (modified from Thomson and McBride, 1964).

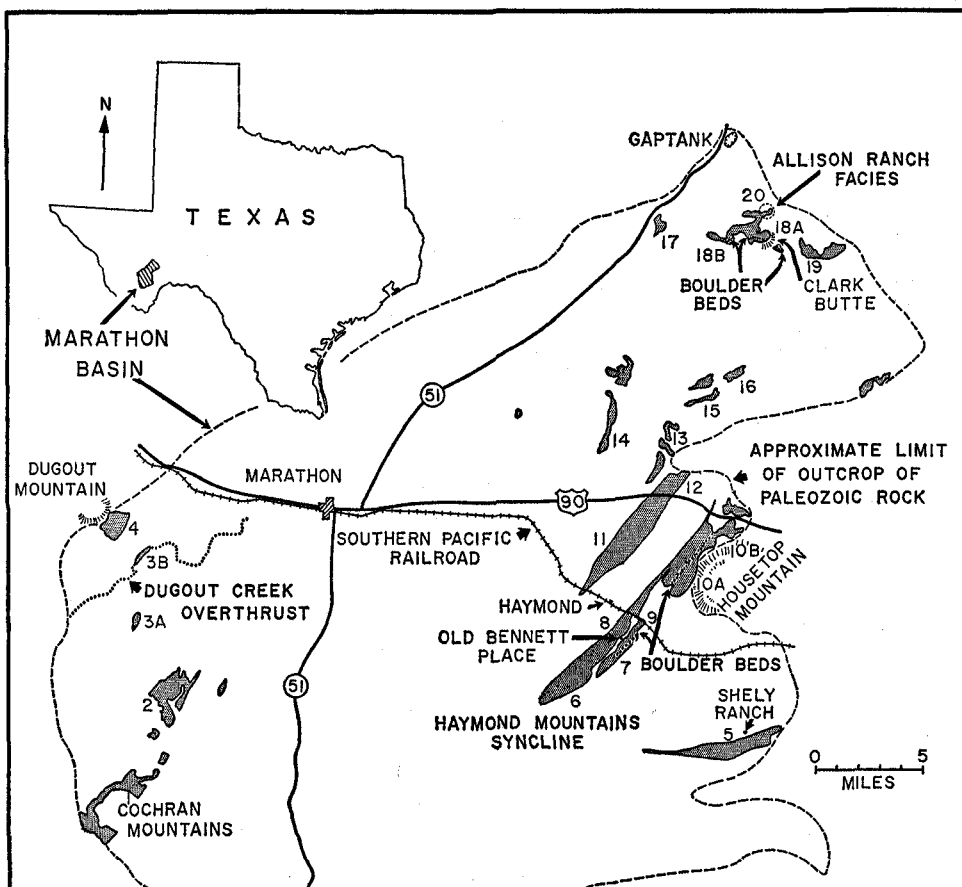


FIG. 3. Outcrop and index map of Haymond Formation (base after P. B. King, 1937). Numerals refer to localities mentioned in the text. Detailed locality descriptions are given in Appendix B.

mation (Tesnus) repeated by thrust faults, although this hypothesis was subsequently disproved by King and King (1928). Brief comments on the stratigraphy or lithology of the Haymond have been made by Schuchert (1927), Baker (1932), Sellards (1933), and Hall (1956). Skinner and Wilde (1954) described a new species of fusulinid from a limestone bed in the Haymond. A statistical study of the thickness of beds in the formation and rate of deposition is described by Dean and Anderson (in press).

Numerous workers have engaged in a controversy over the origin of the boulder beds following their discovery in 1931. The controversy lasted through the 1930's (P. B. King, Baker, and Sellards, 1931;

Sellards, 1931; Baker, 1932; P. B. King, 1932, 1937; Carney, 1934) and has been recently revived (Hall, 1957, 1959; Flawn, 1958; P. B. King, 1958). Flawn (1956, p. 59) studied igneous and metamorphic rocks from the boulder beds as part of a regional study of basement rocks of Texas.

Except for comments on the genesis of the boulder beds by numerous writers, and brief speculation on the environment of deposition of the Haymond by Schuchert (1927, p. 383), Baker (1932), Flawn (Flawn et al., 1961, p. 54), and Goldstein and Hendricks (1962, p. 419), the only treatment of the sedimentologic features of the Haymond has been a few pages in P. B. King's (1937, pp. 65-73, 87-92) lengthy general geologic report.

Field work for the present investigation was accomplished chiefly during the summers of 1960 and 1961. Several days of the summers of 1962 and 1963 were also spent in collecting additional samples. Preliminary results of this study have appeared in abstract (McBride, 1963a) and in a field guidebook (McBride, 1964a).

Acknowledgments.—The writer is indebted to many persons and organizations for help in completing this investigation.

Charles McKetta and Herman Jackson helped with certain aspects of field work, and William Lindemann, Joseph McGowen, Lynn Beeler, and Susan Burton Longacre aided in the laboratory. Much of the final drafting is the work of Eddie Dickerson.

The following ranchers kindly permitted access to their property: Sutton Allison,

David Combs, William Donnell, Warren Henderson (for Catto-Gage Ranch), Gage Holland, Eldon McGonigill, and Travis Roberts. Tom Leary extended hospitality and helped in many ways.

P. T. Flawn and W. R. Muehlberger kindly made available rock samples and thin sections in their possession. Muehlberger provided the age date of the granite pebble from the boulder beds.

Field work was made possible by two summer grants from the Geology Foundation of The University of Texas. The University of Texas Research Institute provided two grants for the purchase of laboratory supplies and equipment.

The writer has also been aided throughout the study by comments from colleagues too numerous to mention; special thanks, however, are extended to Alan Thomson.

STRATIGRAPHY

PROBLEMS

Understanding of the stratigraphy of the Haymond is limited because:

- (1) Nowhere is there a complete section of the formation exposed, and the sections are not evenly distributed geographically. The most nearly complete sections are all in the eastern and northern parts of the Marathon Basin.
- (2) Many outcrops are isolated exposures surrounded by alluvium so that the position of the exposed rocks in the sequence cannot be determined.
- (3) **The formation lacks marker beds.** Although Dean and Anderson (in press) were able to correlate nine siltstone beds in two outcrops 5 miles apart by applying varve-correlation technique, only two beds of distinctive lithology in the formation have been recognized in more than one outcrop. The latter beds occur at only two localities 6 miles apart, and their position in the formation cannot be precisely determined.
- (4) In exposures of interbedded sandstone and shale, commonly only the resistant, thicker sandstone beds crop out well enough to display sedimentary features.
- (5) The fossils in the formation have no stratigraphic value. The only exceptions are fusulinids in the two marker beds referred to in item 3 and possibly fragmental fossils in beds transitional with the overlying Gaptank Formation.
- (6) The outcrops occur in a structurally complex area.

LITHOSTRATIGRAPHY

Although bed-by-bed correlation within the Haymond is not possible, gross stratigraphic relations are known. Below is a synthesis of P. B. King's work (1937) plus more recent observations by the writer.

The outcrop distribution of the Haymond Formation, the location of sample

localities, and the location of geographic features referred to in this report are shown in figure 3. Figure 4 is a schematic fence diagram of gross stratigraphic relations which is based on three measured sections (Pl. 1, in pocket) and restorations.

Interbeds of fine- and very fine-grained sandstone and dark gray shale less than 1 foot thick make up the bulk of the Haymond and are the most distinctive feature of the formation (Pl. 3). More than 65 percent of the thickest section of Haymond measured is composed of such lithology. This aspect, as well as the sedimentary structures of the formation, characterize the Haymond as flysch according to current sedimentologic use of the term (Sujkowski, 1957; Pettijohn, 1957, pp. 634-640; Sanders and Carozzi, 1957). Van der Gracht² (1931, table 3) and P. B. King earlier (1937, p. 87) applied the term flysch to both the Tesnus and Haymond because of their lithology and because they were interpreted to have been deposited directly prior to or contemporaneous with the major diastrophic paroxysm of the Ouachita orogeny. Their usage was based on both lithologic character and tectonic significance, criteria used by numerous other writers.³ In this report flysch will be used in the sedimentologic sense only, and the portion of the Haymond that is composed of such interbeds will be referred to as the "flysch facies." Sandstones of the flysch facies have the same sedimentary textures, structures, and mineralogy throughout the Basin; they are chiefly immature subarkose and sublitharenite sandstone (classification of McBride, 1963b). The flysch sandstones in the Dugout Mountain area are the only major exceptions, in that they contain abundant carbonate rock fragments and sand-sized fossil detritus.

² Van der Gracht grouped the upper Haymond with the Gaptank as molasse, because of the reported occurrence of "conglomerate" (boulder beds) in the upper part of the Haymond.

³ For a discussion of the term flysch, see Eardley and White (1947) and Sanders and Carozzi (1957).

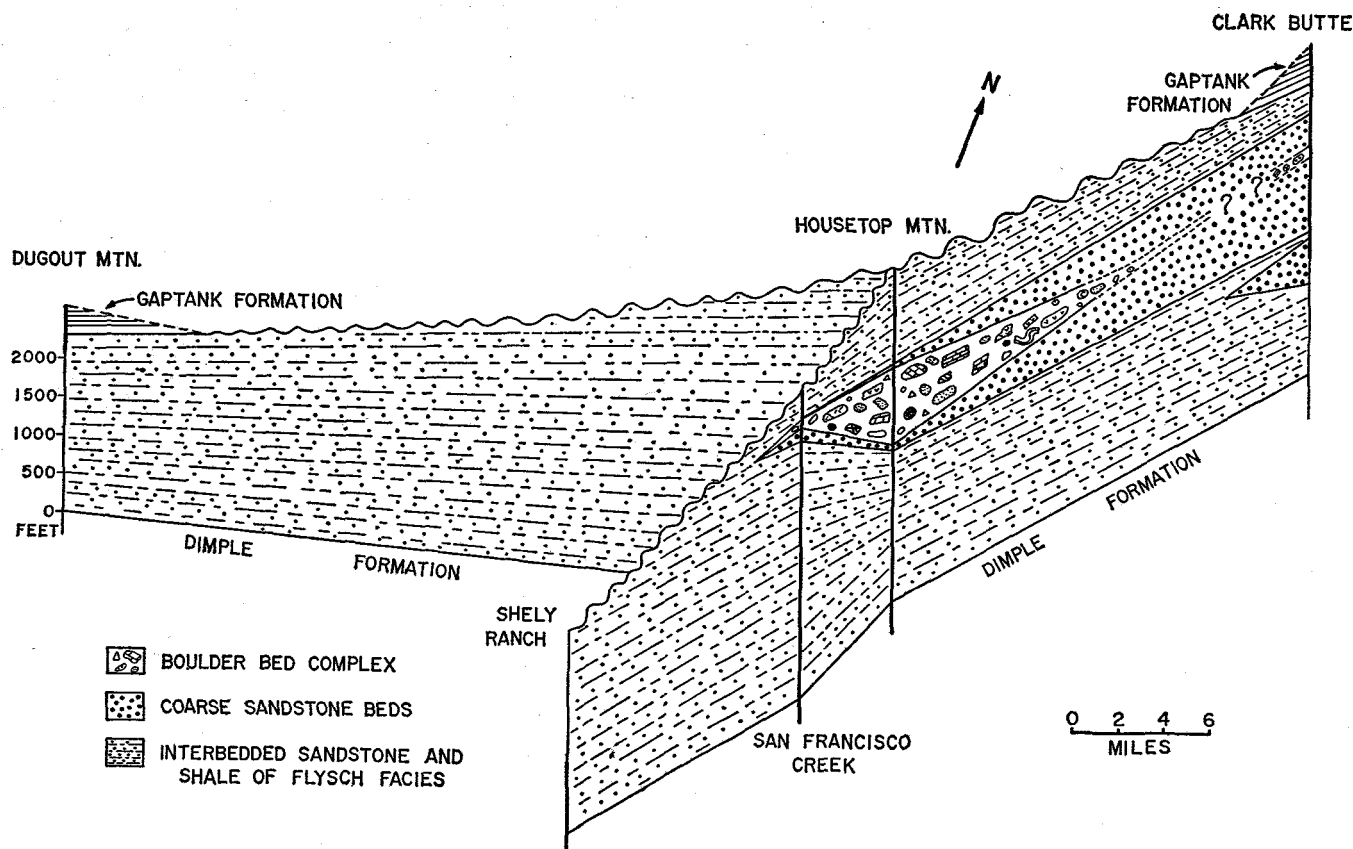


FIG. 4. Schematic diagram of major stratigraphic units in the Haymond Formation. The heavy vertical line at each locality indicates the part of the formation that is exposed; the remainder of each section is inferred.

Rocks exposed in a road cut on the Allison ranch in the northernmost part of the Basin (Loc. 20)⁴ are treated separately from the flysch facies. Although the 70 feet of section exposed there is interbedded sandstone and shale, the sandstones have sedimentary structures that are unlike beds exposed elsewhere in the Basin. This section, which includes the youngest Haymond rocks exposed along the northeastern edge of the Basin, will be referred to as the "Allison Ranch facies."

Within the upper half of the Haymond are boulder beds and coarse sandstone beds that differ markedly from the flysch facies. The boulder beds include mudstone, coarse sandstone, and contorted intercalated sandstone and shale beds that contain fragments of older rocks which range from granules to blocks 130 feet long. The coarse sandstone beds are thicker and coarser (coarse- to very coarse-grained sandstone) and have fewer shale interbeds than the flysch facies. These coarse clastics are known only from a small area around Clark Butte and from exposures along an 8-mile-long belt south of U.S. Highway 90. They form a wedge that thins from north to south; it is approximately 1,200 feet thick at Clark Butte, 1,005 feet thick at the base of Housetop Mountain, and 500 feet thick east of the old Bennett Place. Measured sections of rocks in these areas are shown in Plates 1 and 2 (in pocket).

At Clark Butte are thick structureless beds of coarse sandstone 1 to 55 feet thick that locally contain a few feet of flysch-type interbeds of shale and fine-grained sandstone. Several irregular beds in the upper part of this interval are relatively thin boulder beds (maximum of 30 feet) separated by 30 to 150 feet of structureless coarse sandstone. At the base of Housetop Mountain the non-flysch coarse clastics occupy the third quarter of the 4,272-foot section of Haymond and are chiefly boulder-bearing mudstone and deformed muddy sandstone with minor amounts of chert-pebble conglomerate, coarse sandstone beds, and some flysch-facies inter-

beds of sandstone and shale. All beds are lenticular.

The boulder bed unit thins rapidly southward from Housetop Mountain; it is 87 feet thick at the old Bennett Place section. It can be traced a mile farther south before it disappears in the subsurface, although at this point it appears to be less than 1 foot thick. At the old Bennett Place section approximately 200 feet of normal flysch beds separate the boulder beds from the only structureless coarse sandstone beds in the section. Diagrams and sketches of stratigraphic features of the boulder beds and associated lithologies are shown in figures 5-8 and Plates 10-12 in this report and in figures 23 and 26 in P. B. King's 1937 report.

King (1937, p. 66) applied the term "boulder bed member of the Haymond formation" to the "complex group of interstratified, thin-bedded sandstones and shales, massive arkose, and boulder-bearing mudstone, lying in the upper part of the formation east of the Marathon quadrangle." Problems in terminology exist in that King did not describe the boundaries of the member, nor did he include the boulder-bearing rocks in the northern part of the Basin within the member. Plate 10 of King's report is a map of the boulder beds along the northwestern limb of the Haymond Mountains syncline that shows the size and location of the larger boulders and the formations from which they were derived, and the outcrop of distinctive coarse sandstone ("arkose") and chert breccia beds. The boulder bed member as mapped by King encompasses all beds of mudstone, contorted flysch-facies rocks, and coarse sandstone that contain gravel and block-size erratic rocks. However, coarse sandstone beds crop out below the mapped interval of erratic rocks, and contorted flysch rocks occur above it (fig. 6). Thus, King apparently meant the member to be defined by the upper and lower occurrences of erratic rock fragments, and the procedure is probably not proper to include the boulder-bearing beds in the northern part of the Basin within King's boulder bed member inasmuch as expo-

⁴ The location of numbered localities is shown in figure 3.

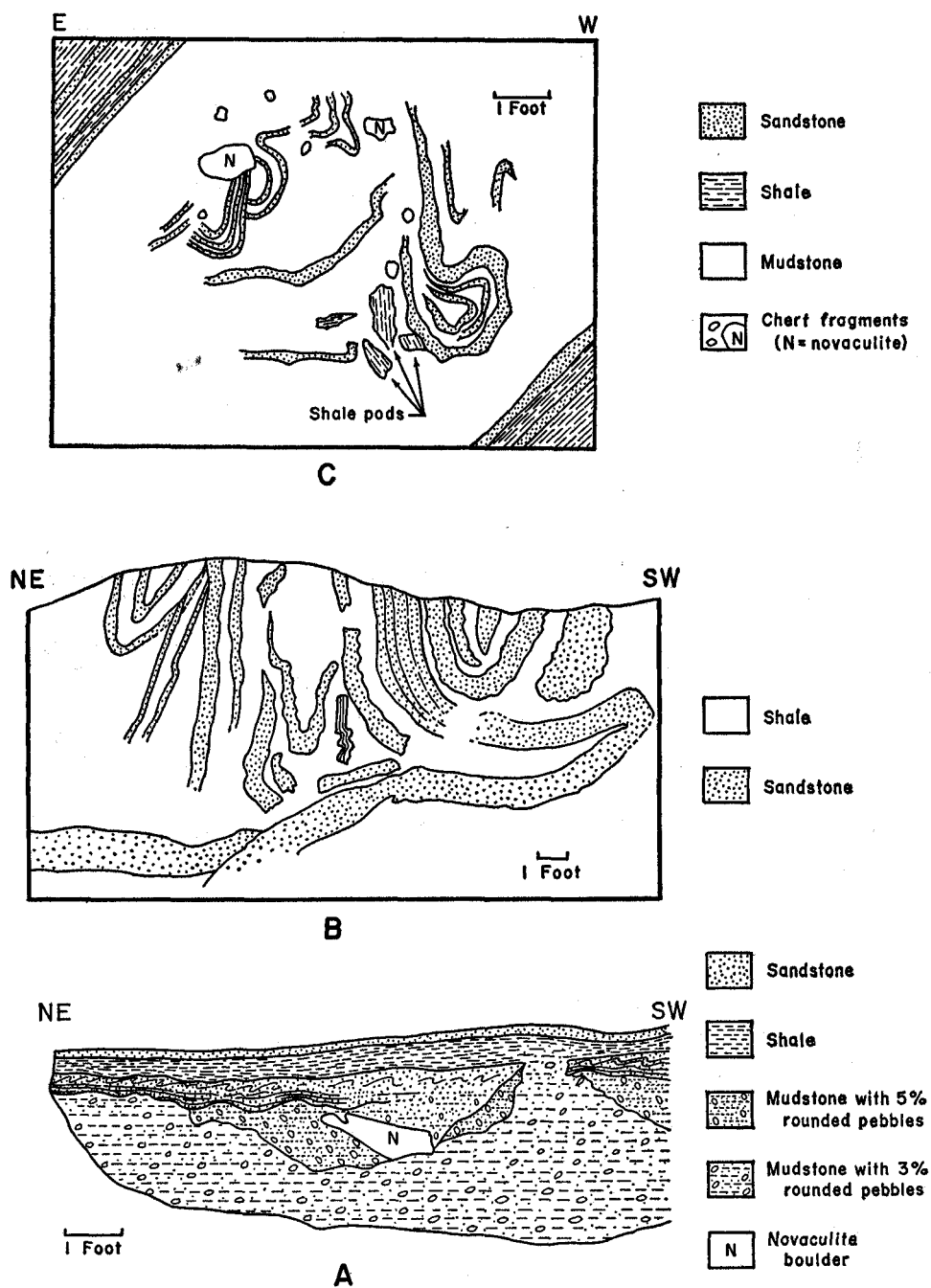


FIG. 5. Sketches of stratigraphic details of parts of the boulder bed unit. All localities at the base of Housetop Mountain.

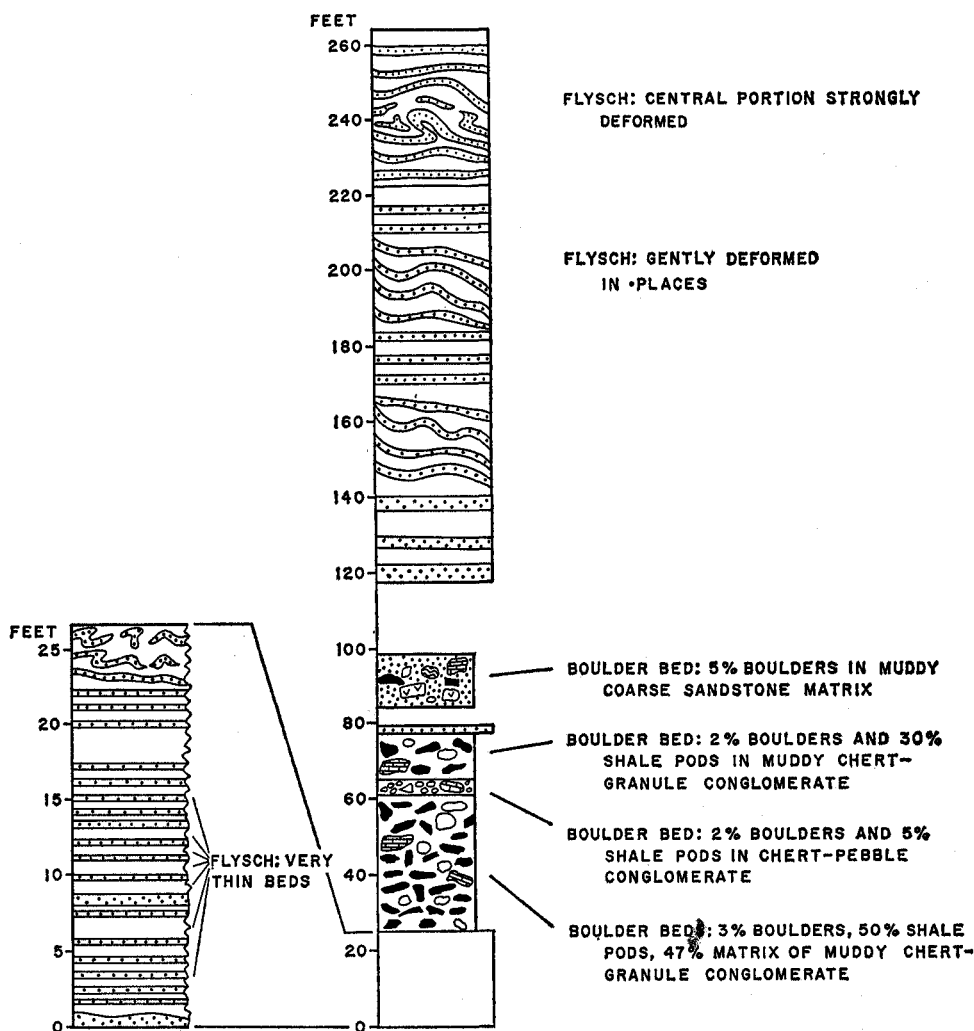


FIG. 6. Stratigraphic section at the top of the boulder bed unit one-fourth mile northwest of windmill at the base of Housetop Mountain. Unpatterned beds are shale.

tures do not permit the northern beds to be “walked into” the area south of U.S. Highway 90. The boulder beds in both areas are herein interpreted as the product of submarine slides (p. 49), and it is likely that they are in part time-correlative on the inference that earthquakes capable of triggering slides would be strong enough to affect both areas simultaneously. However, in this report the term “boulder bed member” will subsequently be used for the rock-stratigraphic unit mapped by King, and “boulder beds” will be used as a

lithologic term without regard to geographic position.

Most exposures of Haymond in the Basin are of flysch facies from below the boulder beds. Except for the Clark Butte area and the northwestern limb of the Haymond Mountains syncline (fig. 3), Haymond beds as young as the boulder beds are probably not preserved in the Basin except at the base of Dugout Mountain.

The Haymond is underlain conformably by the Dimple Formation and is overlain conformably by the Gaptank Formation,

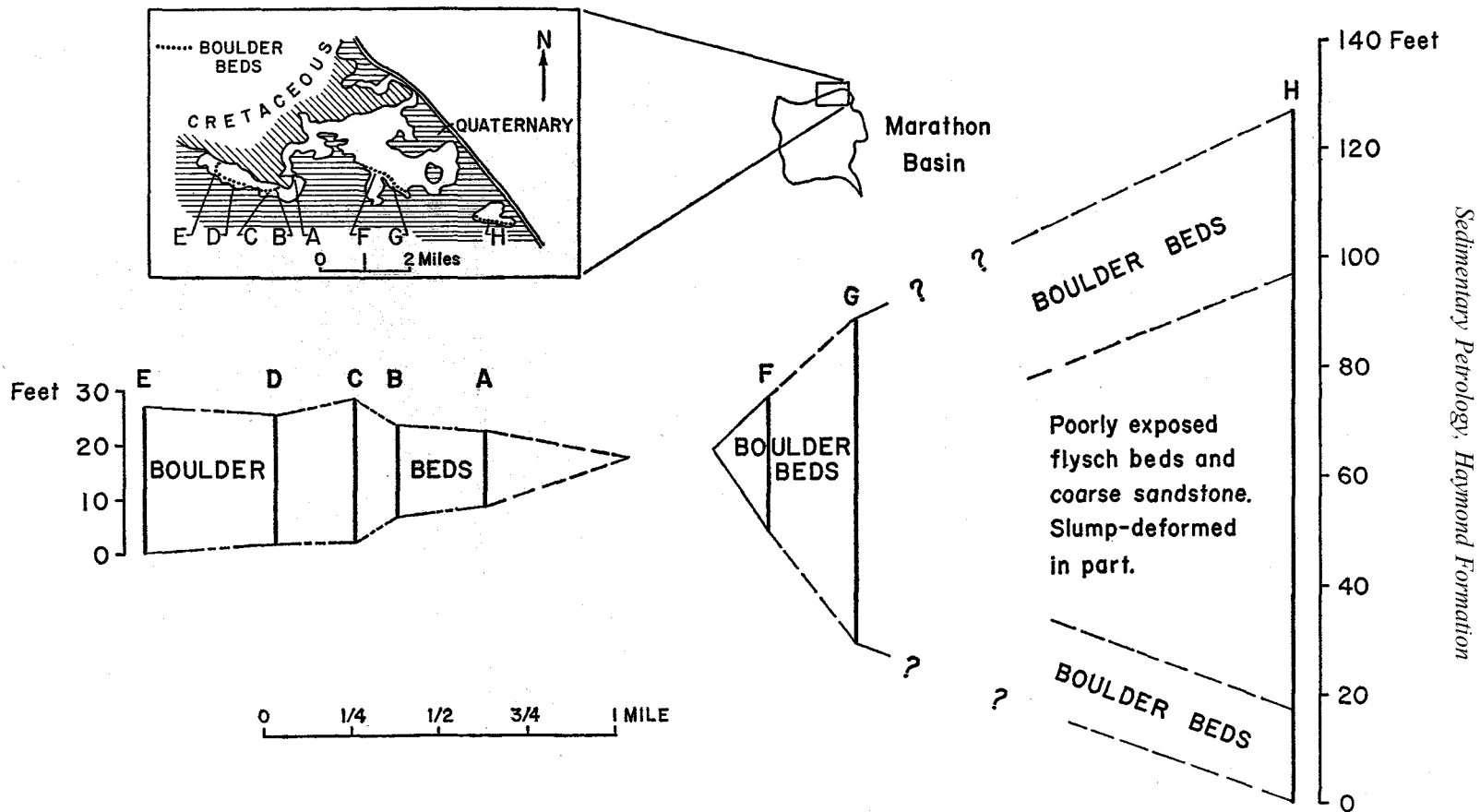


FIG. 7. Location and thickness of boulder beds in northern part of the Marathon Basin.

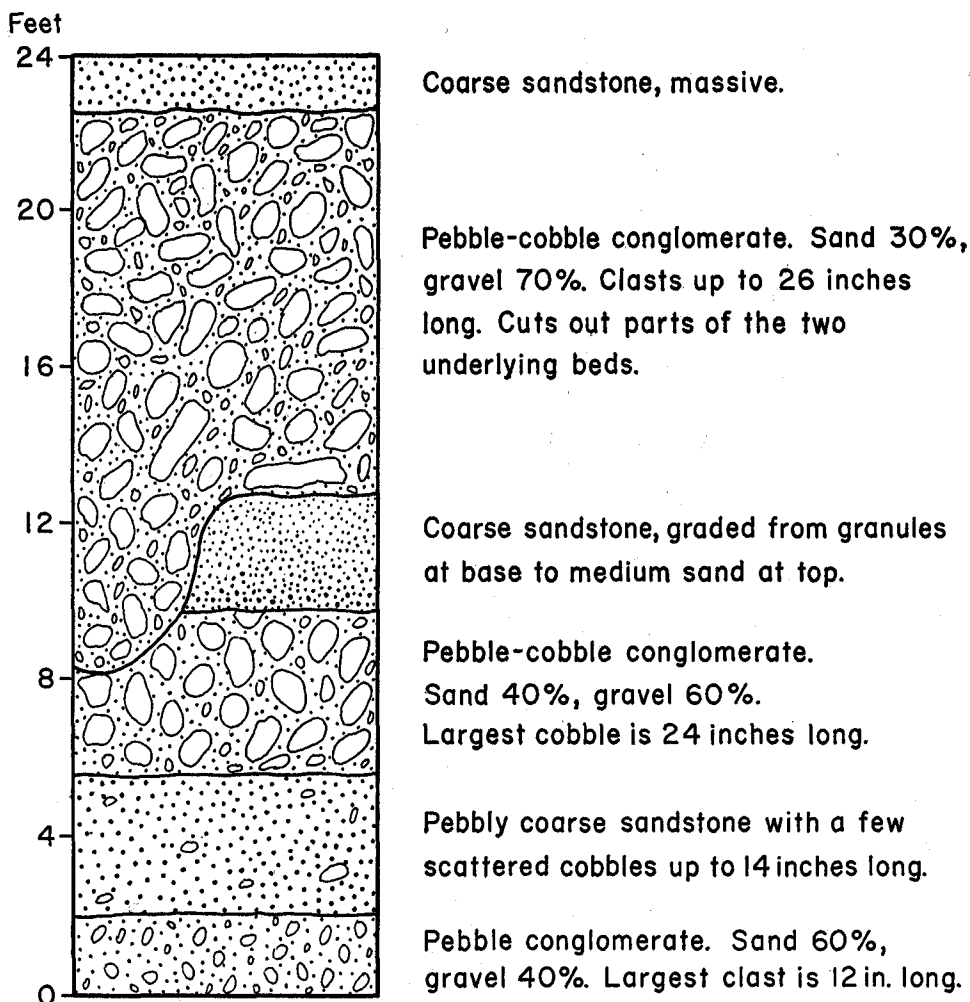


FIG. 8. Schematic stratigraphic section of boulder beds at section D of figure 7.

both of Pennsylvanian age. The Dimple is partly cherty clastic limestone interbedded with chert and shale and has a maximum thickness of approximately 1,200 feet (P. B. King, 1937, Pl. 8). Thomson and Thomasson (1964) described the Dimple as a carbonate flysch composed of a basin facies containing turbidite calcarenites, and a shallow-water shelf facies. The contact with the Dimple is gradational through a thickness of approximately 20 to 50 feet of black shale in which are interbedded thin limestone and sandstone beds of Dimple and Haymond lithology, respectively.

The Gaptank is composed of shale, lime-

stone, sandstone, and some conglomerate that attains a thickness of 1,800 feet (P. B. King, 1937, Pl. 8). In the northern part of the Basin (*Chaetetes* Hill, Loc. 17) interbedded Haymond sandstone and shale are abruptly overlain by fine-grained calcirudite that contains *Chaetetes*. The limestone is succeeded by approximately 50 feet of interbedded sandstone and shale; limestone beds are present higher. P. B. King (1937, p. 73) placed the lower contact of the Gaptank at the base of the *Chaetetes*-bearing limestone.

In the western part of the Basin (Dug-out Mountain area) sandstones of normal Haymond lithology are richer in fossils

and carbonate rock detritus upsection and, through approximately a 200-foot-thick interval of flysch beds, grade into calcarenites of typical Gaptank lithology. P. B. King (1937, pp. 75-76, Pl. 24) apparently placed the Haymond-Gaptank contact at the base of a graded limestone-pebble conglomerate bed present near the top of the gradational interval. Several such conglomerate beds occur in the lower part of the Gaptank.

AGE AND FOSSILS

As is common in many flysch units, the Haymond lacks diagnostic fossils, so that a precise age and correlation with other Pennsylvanian formations cannot be made.

Although an abundant Pennsylvanian fauna has been recorded from exotic⁵ limestone blocks in the boulder beds (P. B. King, 1937, p. 72), the only abundant indigenous fossils in the Haymond are plant remains and animal trails and burrows (*Lebensspuren* or trace fossils). A few sponge spicules and a small foraminifer were recovered from a disaggregated shale sample from the Allison Ranch facies. The only other fossils found in the formation, with one exception, are abraded fragments of fusulinids, echinoderms, brachiopods, mollusks, and probable algae that are common in beds transitional into the overlying Gaptank Formation in the Dugout Mountain area. The exceptions are fusulinids and echinoid fragments that occur in two calcarenite beds several hundred feet above the base of the formation. An early Pennsylvanian⁶ age (P. B. King, 1937, p. 72; Skinner and Wilde, 1954) was assigned to the Haymond based on these fusulinids (*Fusulina* sp. and *Fusulinetta haymondensis* Skinner and Wilde). These beds are similar to turbidite calcarenites of the underlying Dimple Formation described by Thomson and Thomasson (1964). The two beds are turbidites derived, like those

in the Dimple, from a source area to the northwest (Thomson and Thomasson, 1964). The fossils in these beds have been transported from outside the basin of deposition, and it is possible that they, like many fossils in the Dimple, have been reworked. The reworked nature of many Dimple fossils is shown by their occurrence in fragments of limestone. The Haymond limestone beds are too severely weathered for effective study. King, Skinner, and Wilde collected their limestone beds at the writer's Locality 16; what is probably one of the same beds occurs 6 miles southwest at Locality 12. The unique limestone beds are the only known stratigraphic marker beds in the formation.

Plant remains and trace fossils are by far the most abundant Haymond fossils. Impressions or carbonaceous films of plants (up to 8 inches long) occur in approximately 80 percent of the sandstones, and minute carbonaceous particles, including spores, are ubiquitous in shales. Most identifiable plants (floral list in P. B. King, 1937, pp. 71-72) and the largest plants are from the coarse sandstone beds.

The trace fossils include common burrow paths in shale beds and burrow-path casts on sandstone soles and rare burrow paths within sandstone beds. Raised, slightly sinuous, unbranched ridges from 3 to 5 mm wide and 1 to 3 cm long are abundant on the sole of sandstone beds (Pl. 6) throughout the formation. The ridges vary in relief (from 1 to 4 mm) and abundance. Less common forms are small pimple-like mounds and very narrow string-like ridges (Pl. 6, C). Seilacher (1962) stated that most sole-mark fossils in flysch rocks are sandstone casts of burrows subparallel with bedding in shale that have been partially exhumed by turbidity currents and then immediately buried. A similar interpretation is here given for the Haymond sole fossils, because most sandstone beds with organic sole marks are not internally burrowed. If the burrows had been made at the sandstone-shale interface, the covering sandstone would display disturbed textures. The pimple-like mounds are casts of pits that were probably en-

⁵ Exotic is here applied without implication of size to rock types different from rock types exposed elsewhere in the Basin. Erratic is applied to rock fragments of such large size as to preclude their having been transported by currents, but without implication of the mechanism of transportation.

⁶ Atokan (G. L. Wilde, oral communication, 1963).

trances to tunnel systems.

Disturbed zones in shale beds were not recognized in the field, although they are obvious and comprise large portions of five of six thin sections studied. The only sandstones with internal burrows occur near the top of the Haymond in the Allison Ranch facies and in the uppermost 100 feet of section above the boulder beds at the base of Housetop Mountain. In both areas sandstones contain closely spaced vertical and lateral passageways (Pl. 7, D). The burrow fillings generally are sand similar in composition to the burrow matrices, although some are richer in clay than the host rock. Most burrows are less than 3 mm in diameter. The animals that made the burrows were apparently soft-bodied organisms inasmuch as no hard parts have yet been found. More than 100 shale

samples of Haymond collected from exposures along U.S. Highway 90 were disaggregated and sieved by S. P. Ellison (oral communication, 1963) in search of conodonts, but no fossils were recovered on screens as fine as 230 mesh.

Although the precise age of the Haymond cannot be determined from the fossils that it contains, ages of the underlying Dimple and overlying Gaptank Formation, both of which are highly fossiliferous, provide age limits for the Haymond. The Dimple has rocks as young as Atokan (Sanderson and King, 1964), and the Gaptank has rocks as old as Desmoinesian (King, 1930; Ross, 1963; Ellison, 1964). Thus, the Haymond includes rocks equivalent in age to the Atokan (the age of fusulinids in the Haymond) and possibly lower Desmoinesian series.

MEGASCOPIC LITHOLOGIC FEATURES

FLYSCH FACIES

The Haymond flysch facies is a thick sequence of innumerable interbeds of olive- to dark-brown sandstone and dark gray to black shale (Pl. 3). Approximately 3,000 feet of the formation along the eastern edge of the Haymond Mountains syncline where it is thickest is flysch. The formation here is estimated to have more than 15,000 individual sandstone beds greater than 3 mm thick. This figure was obtained by counting all sandstone beds in a 150-foot section of Haymond exposed along U.S. Highway 90 and extrapolating the same ratio (5 beds/foot) to 3,000 feet.

Shale beds range from a millimeter to approximately 12 inches thick, although most are less than 3 inches thick. Sandstone beds range from a few millimeters to 2 feet thick; generally each bed extends the limit of individual exposures with no change in thickness. An exception is beds less than 2 inches thick whose irregular thickness is the result of current ripple marks on the upper surface (Pl. 3, D). As a rule, beds thicker than 2 feet are medium- to coarse-grained sandstone, whereas thinner beds are fine- to very fine-grained sandstone or coarse siltstone.

Extremely thin beds, those only a few millimeters thick (Pl. 3, C), are common throughout the flysch facies. In the freshest exposures, fine sandstone and coarse siltstone laminae as thin as 1 mm can be traced across the outcrop. Owing to the relatively rapid rate of weathering of the very thin beds compared to sandstone beds an inch or more thick, the very thin beds are generally not observable in the average outcrop. One exposure along San Francisco Creek reveals 44 feet of section in which there are only 10 beds between 1½ to 5 inches thick but 650 beds between 1/8 and 1½ inches thick, with an additional estimated 300 beds less than 1/8 inch thick that were not counted.

The thickness of beds in the flysch is not uniform throughout the formation, that is,

some sequences, of 5 to 50 feet thick with a predominance of very thin beds are succeeded by sequences of similar thickness in which beds greater than 6 inches thick are common. To illustrate this feature, the thicknesses of sandstone⁷ beds in two sequences (421 and 122 beds, respectively) exposed in a road cut 15 miles east of Marathon were tabulated. The average thickness of beds in the sequences, which are separated 200 feet stratigraphically, are 1.6 ($\sigma=2.2$) and 6.2 ($\sigma=10.0$) inches, respectively. No particular pattern to the sequences of thicker or thinner beds is apparent within the formation.

With rare exceptions, each sandstone bed, no matter how thin, is overlain by shale. Inasmuch as each sandstone and each shale bed are herein (p. 47) interpreted to represent distinct depositional events, each bed is a sedimentation unit (Otto, 1938). In addition to standing out one-half inch or more in the outcrop face from more eroded shale, sandstone beds commonly have a serrated edge resembling pinkish-shear blades owing to the way the sandstone beds are jointed. The beds commonly have two sets of joints that intersect at approximately right angles. Where neither set is parallel with the trend of the outcrop face, fragments spall off, such that the corners of rectangular-shaped joint fragments project from the outcrop giving the edge of each sandstone bed the serrated pattern.

In order to show details of intercalated sandstone and shale of the flysch facies and to compare them with other parts of the formation, several stratigraphic sections a few feet thick were measured in detail at four localities in the Haymond. Sections B (San Francisco Creek) and C (old Bennett Place) (Pl. 2, in pocket) illustrate the flysch part of the formation; Section A is in the Allison Ranch facies and Section D

⁷ To avoid wordiness when referring collectively to sandstone and coarse siltstone beds in the flysch facies, the coarse siltstone beds will not be specifically mentioned in the following pages.

is of coarse sandstone. Section B is approximately 1,000 feet below the boulder bed complex, whereas Section C is approximately 100 feet below it. The most striking feature of the flysch section, in addition to repetitious interbedding of sandstone and shale, is the repetitious sequence of bedding types in the sandstones.

Sedimentary structures.—The Haymond flysch facies displays an abundance and variety of sedimentary structures, those features of hand-specimen size or larger. The structures include trace fossils, sandstone dikes, slumped sequences of intercalated sandstone and shale, and a number of bedding features in sandstone beds. The latter features include internal structure (or bedding types = horizontal laminations, cross-laminations, structureless bedding, convolute laminations, and graded bedding) and bedding-plane structures (flute and groove casts, load pockets, parting lineation, and ripple marks) that provide important clues to interpreting the sedimentological history of the formation. The structures are described and categorized below according to their mode of origin.

Structures of current origin.—*Graded bedding* is a common but inconspicuous structure in Haymond sandstones; it generally can be detected in the field only by using a hand lens, and commonly it can be found only by examining a thin section (Pl. 5, D). It is, however, the cause of the conspicuous occurrence of sandstones with sharply defined lower bedding planes (soles) and poorly defined tops. The rate of weathering of sandstone beds is faster in the upper part where the clay content is greater, so that there is less contrast between the sandstone and overlying shale than between the sandstone and underlying shale. This differential sharpness of contacts is obvious tens of feet distant from some outcrops.

Graded bedding is best shown in beds less than 3 inches thick and is essentially absent in beds greater than 6 inches thick. Normal graded bedding, in which the framework grains decrease in size upward, is not as common as that produced by an

increase in clay from bottom to top where the framework grains do not decrease upward. The latter type of grading by matrix content is in contrast to normal grading of framework grains; however, both types of grading have been described in turbidites (McBride, 1962, p. 50).

Grading is difficult to detect in the field because the upward change in grain size is slight, grains are coated with limonite that formed upon weathering, or clay, and, owing to the ease with which beds split along bedding planes near their tops, samples with complete bed thicknesses cannot be removed from outcrop. From examination of the freshest outcrops and inspection of numerous hand specimens sawed perpendicular to bedding, it is estimated that 60 percent of Haymond flysch sandstones are graded. In the beds that show framework grading, the grain size decrease is commonly confined to the lower few millimeters of the bed.

Horizontal lamination (Pl. 8, B) is the most widespread internal structure of the sandstones in the field. It is commonest in beds from 2 to 24 inches thick. Laminae are alternations of relatively coarse (sand-rich) and fine (silt- and clay-rich) layers less than a millimeter thick, with the laminae of fine-grained sediment being thinner than the laminae of coarse-grained sediment. Hereafter, beds with horizontal laminae are referred to as laminated beds.

Cross-laminations are common in the upper part of many beds, especially those that are laminated in the lower part (fig. 9). Some thin beds, however, are cross-laminated throughout. In any one bed, sets of cross-laminations dip in the same direction and are rarely more than 1 inch thick. No set thicker than 2 inches has been found. That the cross-laminations were produced by the migration of current-ripples is shown in numerous beds where current-ripple marks are still present on the top of a set of cross-laminae. At least 50 percent of the beds with more than one layer (set) of cross-laminae have climbing-ripple cross-laminae, in which the bedding planes that separate individual cross-laminae sets are inclined in an upcurrent

direction (Pl. 5). This structure develops where sediment is supplied rapidly to migrating ripples (Sorby, 1908, pp. 181-182; Walker, 1963).

Convolute laminations occur in an estimated 40 to 60 percent of the sandstone beds. Deformed laminations characteristic of this structure are present chiefly in the top part of laminated beds; they are uncommon in beds less than 1 inch thick and more than 24 inches thick. Contortions range from oversteepened to overturned cross-laminae and undulatory low-amplitude folds to steep asymmetric anticlines and synclines with amplitudes up to 3 inches (Pls. 5 and 8, B). Owing to the obscurity of the structure in the field, no systematic study of the direction of the overturned folds was attempted. The presence in some beds of undeformed cross-laminae on top of convolute laminae proves that deformation took place during deposition of the bed and before the upper few millimeters of the bed were deposited. Regardless of the degree of contortion of the laminae within beds, the tops of the sandstone beds are smooth and undeformed. Deformed laminae die out upward and are generally covered by an obscure laminated layer 1 to 2 mm thick; rarely by a structureless layer.

Massive or structureless bedding, the absence of all internal structure, is common in the lower part of many beds. Because there are no mottles to suggest that massive bedding is the result of burrowing organisms, the structure is probably produced during deposition of the sand.

Combinations of two or more of the types of bedding mentioned, above are the rule for Haymond sedimentation units. Although several different combinations of structures in individual sedimentation units occur, in all units the structures have a definite sequential arrangement. From bottom to top, the complete sequence is: massive bedding, horizontal laminae, convolute laminae, cross-laminae, and, in some beds, a thin second zone of horizontal laminae. Where grading of framework grains is present it occurs at the base of the bed, whereas grading by matrix con-

tent occurs in the uppermost few millimeters of horizontal or convolute laminae. In only a few beds has the complete sequence been found, but in beds that have two or more types, the sequence is that given above. Figure 9 shows examples of

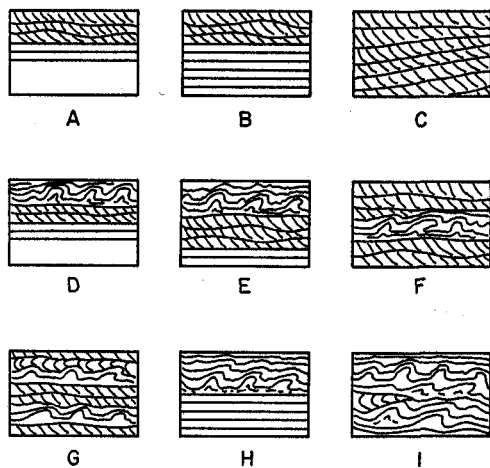


FIG. 9. Schematic presentation of bedding sequences in Haymond sandstones. Massive (un-patterned), laminated, cross-laminated, and convolute layers are shown.

the typical combinations of bedding types observed in the field and sawed surfaces; the sequence of structures recorded in two measured sections is shown graphically in Plate 2.

The relative abundance of the different bedding types and sequences is uncertain owing to the difficulty in seeing the structures in the field. Weathered joint surfaces are coated and stained with limonite which obscures bedding details; even fresh breaks seldom penetrate beyond the limonite stain, and fresh breaks tend to be parallel with bedding rather than perpendicular to it. The only way bedding details can be seen in most beds is to examine a sawed and polished surface wetted with water or an oil such as glycerin. Another technique is to make X-radiographs of sawed slabs⁸ (Pl. 5).

The abundance of different sequences differs from locality to locality, but the

⁸ A Picker Army Field X-ray unit and Kodak Industrial X-ray film were employed. Most slabs are 4 mm thick and were given exposures of 8 seconds at 10 milliamps and 50 kilovolts at 1-meter distance.

thickness of a bed seems to be the single most important factor. Among the beds between 1/4 to 8 inches thick, the thicker beds have more complete sequences. The most common sequence is a thin interval of laminations overlain by thicker intervals of cross-laminations followed by convolute laminations which die out upward into a thin (1—2 mm thick) layer of horizontal laminae. Of the few beds that show anomalous sequences, almost all appear to be beds composed of two or more superposed sedimentation units. Table 1 shows the abundance of bedding types counted for a particularly well-exposed section at Locality 6. Of the 39 beds, five are from 6 to 12 inches thick and the remainder are less than 3 inches thick. In this table the structures of the imperceptible covering layers above convolute laminae are ignored.

TABLE 1.—Bedding types and sequences in 39 beds from Locality 6.

Type of sequence of bedding from base upward	L, X, C	X, C	L, C	C	X
Number of beds	2	28	4	4	1
Percent of beds	5	72	10	10	3

X = cross-laminae, L = horizontal laminae, C = convolute laminae.

All beds show grading by an increase in clay content upward.

Sole marks of current origin include *tool mark casts* and *flute casts*. Tool marks are grooves and other linear marks gouged by objects (tools) transported by currents, whereas flute marks are eroded by the hydraulic force of currents. The marks are eroded in a soft substratum and subsequently covered by sand which preserves their form. Although the objects seen on sandstone soles when the underlying shale spalls away are properly called *molds*, the term *cast* is firmly entrenched in the literature and will continue to be used in sole mark terminology. Although a sophisticated classification of tool mark casts has been proposed (Dzulinski et al., 1959), no attempt was made to classify all the types of Haymond structures.

Groove casts (Pl. 4, A, B) from 1 to 5 mm wide are the most abundant tool mark

casts; lengths range from an inch to about 10 feet, the length of the largest soles exposed. The latter are at the southern end of the Haymond Mountains syncline (Loc. 6), where several vertical beds have over 100 square feet of bedding surface exposed. *Prod casts* and *roll-mark casts* are extremely rare varieties of tool mark casts in the formation.

Flute casts seldom exceed 3 cm in length and 1 cm in width. No giant flute casts were found. *Flute-lineation casts*, symmetrical casts of low relief that lack distinct noses typical of normal flute casts, are common on many beds. In most outcrops where sole marks are visible, beds with groove casts are three to four times more numerous than those with flute casts, although some beds have both (Pl. 4, C). Current sole marks are rare on beds less than 1 inch thick and greater than 12 inches thick. Table 2 shows the average thickness of beds that have different types of sole marks. Beds with flute casts and flute-lineation casts have an average thickness of 8.2 inches, whereas beds with groove casts have an average thickness of 5.7 inches. Comparable average thicknesses and difference between beds with flute and groove casts were found in Ordovician turbidites in the Appalachians, from which it was inferred that flute marks generally form during higher current velocities than groove marks (McBride, 1962, p. 58).

TABLE 2.—Average thickness of beds with different types of directional structures.

Type of directional structures	Average thickness (inches)	Number of beds
Parting lineation	17.3	16
Flute-lineation cast	10.1	18
Flute cast and flute-lineation cast	8.2	35
Flute cast, flute-lineation cast, and groove cast	8.1	67
Groove cast	5.7	149

Ripple marks are scarce, in general, but are abundant in some thin-bedded sequences where sandstones are from one-half to 1½ inches thick (Pl. 3, D). Beds with ripple-marked tops display the cross-laminations in the upper part of the beds and

show that the cross-laminae were produced by migrating current ripples. With few exceptions ripple marks are exposed only in cross section where the plan of the ripples cannot be seen. Of six large bedding surfaces found, only current ripples are present; two beds have longitudinal transverse ripples and four have crescent-shaped ripples. In no beds do the ripple marks or associated cross-laminae suggest wave action.

Oriented plant fragments are visible in many sandstone beds that split along laminae. Carbonized remains or impressions are mostly less than one-half inch long. On most bedding surfaces that expose several square inches with plant fragments, the plants show a preferred orientation parallel to the current that deposited the bed as determined by associated sole marks or parting lineation.

Tiny plant fragments showing a preferred orientation (less than 2 mm long) are found along bedding planes in shale beds. Because bedding surfaces were only rarely exposed when pieces of shale were broken, it is not known how common this feature is.

Soft-sediment deformation.—Structures formed by soft-sediment deformation in the Haymond include slump structures, sandstone dikes and sills, and load deformation features. Features of load deformation other than rare load pockets and slightly load-deformed flute casts are rare. Sandstone dikes have been found in the flysch facies at only one locality (Loc. 5), where thin dikes up to 3 mm wide have been injected down several centimeters into the underlying shale. What appear to be mudstone sills are found at several places above the boulder beds and in the Dugout Mountain area. The beds in question range from one-half inch to 3 inches thick and are distinctive from other beds in an outcrop because they are poorly consolidated (for sandstone) and develop spheroidal weathering. The beds appear structureless megascopically and are composed of fine-grained sand and silt with from 25 to 40 percent clay. Thin sections, however, show faint intricately contorted laminae. The presence of deformed layers

and more clay than occurs in current-deposited sandstones suggests that the mudstone layers were injected as sills of soft sediment in a manner analogous to the formation of sandstone dikes. No mudstone layer was found to pinch out, but exposures do not permit tracing them more than 20 feet.

Slump structures are common in the Haymond, but most are in the boulder beds that are described in a following section (p. 24). Slumps in the flysch facies are small and involve only 1 to 3 feet of stratigraphic section. Most slumps involve only one or two sandstone beds (and adjacent shale) that were deformed into low amplitude folds (Pl. 8, D) and in places broken apart during slump movement.

Owing to tensional forces imparted during slumping, many sandstone beds were broken by a complex system of tiny normal faults (Pls. 6, D; 8, C). The faults are here called microfaults because displacements along the fractures are less than 3 inches. The microfaults are most conspicuous on the sole of sandstone beds because most faults die out within the beds and do not appear on top surfaces. At the time of faulting the sand beds were somewhat stiff but uncemented, because grains are not broken along the fault planes, faults are not mineralized, and the faults die out along and within the beds. Some beds have two microfault sets that intersect at about 60 degrees, whereas others have only one set. In beds with one set of microfaults, generally the most predominant downthrown side is in the direction of the depositional paleoslope as determined by flute casts. The trend of major and minor fault sets and the direction of movement are shown in figure 10. Fault trends are shown after correction for the tilt of the beds, because the faulting occurred before the folding. Many faults trend subparallel to the regional tectonic strike, but there is considerable scatter.

One bed with incipient "ball and pillow" structure (Potter and Pettijohn, 1963, p. 148) was found (Pl. 8, A). In this bed laminae are contorted into a series of steep-walled basins that produce pillow-like

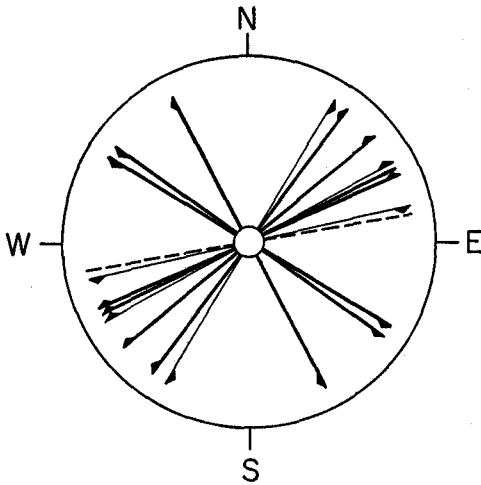


FIG. 10. Orientation of soft-sediment faults (solid lines) and sandstone dikes (dashed lines). Trends of major faults are heavy, trends of minor faults are light. Dip symbols indicate direction of down-slope movement. Orientation corrected to pre-folding attitude.

bodies of sand. Deformation has not been severe enough, however, to pinch off the pillows to form isolated pods.

Other structures.—Additional structures in the Haymond are trace fossils, which have been described more appropriately in the section on fossils (p. 15), and parting lineation. The linear steps between laminae that are produced when beds split (part) parallel with bedding have been termed parting-step lineation to contrast them with linear warps and irregularities (parting-plane lineation) that exist on bedding surfaces (McBride and Yeakel, 1963). Parting-step lineation is common in medium- to coarse-grained Haymond sandstones in beds from 3 to 12 inches thick; it is most abundant in the coarse sandstone beds in the northern part of the Basin (Pl. 4, D).

Mast and Potter (1963), McBride and Yeakel (1963), and Allen (1964) have shown that parting lineation is parallel with the preferred orientation of grain long-axes in several sandstone formations. Grain orientation was studied in three coarse (non-flysch) Haymond sandstones showing parting lineation to test the relationship. Histograms showing the orienta-

tion of 100 quartz grains having elongations of 2:1 (length:width) are shown in figure 12 (I, J, K). The preferred orientation (modal class) and parting lineation direction are nearly parallel in all samples. Parting lineation is parallel with the current which deposited the bed as determined from associated sole marks.

ALLISON RANCH FACIES

The term Allison Ranch facies is applied to rocks exposed in the cut made for the county road 1 mile south of the Allison ranch headquarters (Loc. 20). This section is an unknown distance below the top of the formation and is the northernmost exposure of Haymond in the Marathon Basin. Sandstone beds from 2 to 14 inches thick are interbedded with shale in beds up to 3 inches thick. Because the outcrop is in the stream gap that cuts the northern lip of the Basin, the sandstone and shale have been leached and deeply weathered; hence, they are lighter in color and softer than most flysch rocks. They also differ from typical flysch in that the sandstones are not graded, and they have been strongly churned by animals that burrowed both vertically and horizontally to bedding (Pl. 7, D). Sandstones have either thin sets of current-ripple cross-laminae throughout, or horizontal laminae overlain by cross-laminae. Additional structures include ripple marks; sole impressions of animal trails and burrow entrances; rare short groove casts; parting lineation, present in several laminated beds; irregular network of ridges on upper bedding planes of sandstones that appear to be the traces of sandstone dikes that have broken off at feeder beds; and basin-shaped excavations on top of two sandstones that are questionable gas or spring pits. The latter occur now as pits approximately 5 inches deep that taper evenly from a diameter of 12 inches at the top of the bed to 8 inches at the base of the bed; three such pits are on line about 1 foot apart. Two pits are now empty and the third is filled by sandstone whose bedding conforms to the shape of the pit. The struc-

tures are similar in size and concentric form to spring pits formed by ascending water in loose sand (Quirke, 1930) and to gas rings described from ephemeral lakes by Reeves (1964). The gas rings have only been observed where bottom sediment is mud, however.

Burrows have been found within normal flysch sandstones only sparsely in the youngest beds overlying the boulder beds at the base of Housetop Mountain. Some beds in the Allison Ranch facies are so crowded by sand-filled burrows (Pl. 7, D) that original bedding structures have been destroyed. The burrows are up to 4 mm in diameter and have sinuous patterns where they are visible in bedding planes.

Exposures of Haymond that are gradational into the overlying Gaptank several miles to the west are too poorly exposed to determine whether they have features similar to the Allison Ranch facies.

COARSE SANDSTONE BEDS

The sandstones here referred to as **coarse sandstone beds** are **medium** to very coarse grained and, in places, granule-bearing, that are generally massive or poorly laminated, light brown in color, and poorly cemented. P. B. King (1937) referred to these beds as "arkose" and "arkosic sandstone" in order to distinguish them from other sandstones in the formation. Thin-section study shows, however, that they have no more feldspar than flysch sandstone lower in the section, and actually have less than those higher in the section (table 6, in pocket). However, because they differ in outcrop appearance from sandstones of the flysch facies in that they are lighter in color, more friable, coarser, and occur in thicker beds that have fewer sedimentary structures, they are discussed separately and are hereafter referred to collectively as coarse sandstone beds. In addition to feldspar content, the coarse sandstone beds also differ from flysch sandstones chiefly in that they have less matrix but more calcite cement, micas, and large chert grains.

Coarse sandstone occurs in beds that

range from 2 inches to 5 feet thick. Beds up to 16 inches thick are generally distinctly laminated (Pl. 9, B), and some are cross-laminated in the upper part (Pl. 9, C) and massive in the lower part. No beds display convolute lamination, although one example of contorted laminae that probably originated after deposition was found (Pl. 7, A). Beds thicker than 16 inches are generally massive (Pl. 9, D) or only faintly laminated in the upper part, and many have uneven bases that have up to 3 feet of relief. Such irregular bases are the result of channeling because underlying beds are truncated. In the finer sandstone beds parting lineation is common (Pl. 4, D), and a few flute casts and groove casts have been found. Other sole marks are absent either because the original marks were never present or because the sandstones are too coarse or too poorly cemented to preserve such marks. Many beds less than 12 inches thick are intercalated with shale similar to flysch-type sandstones. However, thicker beds commonly occur in succession and build up a cumulative thickness of as much as 50 feet (Loc. 18A) without a single shale parting.

With one exception, cross-laminae in the coarse sandstone beds are of the small current-ripple type and sets do not exceed 2 inches in thickness. The exception is the occurrence of festoon cross-beds in sets 8 to 16 inches thick in several beds that occur stratigraphically between two boulder-bearing beds in the Clark Butte area (Loc. 19).

Coarse sandstone beds are exposed in the northern part of the Basin around Clark Butte and along the western limb of the Haymond Mountains syncline south of U. S. Highway 90. In the latter area coarse sandstone beds are poorly exposed in or near the stratigraphic interval of the boulder beds. At the base of Housetop Mountain coarse sandstone beds are intercalated with boulder-bearing rocks through 1,005 feet of section, whereas in the section at the old Bennett Place coarse sandstone beds are approximately 200 feet below the boulder bed, which here is 87 feet thick. Some coarse sandstone beds contain up to

5 percent granules and rare pebble-size rock fragments. Mineralogically, the sand fraction of most large boulder-bearing rocks is similar to coarse sandstone beds. In fact, all gradations from granule-bearing, submature (less than 5 percent clay matrix) coarse sandstone to mudstone (40 to 60 percent clay) have been found.

In the Clark Butte area, approximately 60 percent of the 1,000-foot section shown in Plate 1 is coarse sandstone. The section is characterized by shale-free intervals of sandstone from 1 to 50 feet thick; the intervals contain massive beds several feet thick with scattered plant impressions, granules of chert, and other rock fragments. Some beds are crudely graded in that granules decrease in abundance from the base upwards. Such thick massive sandstones are interrupted by thinner sandstone beds intercalated with shale; the former are well laminated and cross-laminated. The cross-laminae, similar to those in flysch sandstones, are current-ripple types in sets less than 2 inches thick and occur above horizontal laminae (Pl. 9, C).

The best examples of erosional contacts at the base of sandstone beds are shown in the conical hill of coarse sandstone 1 block west of Clark Butte (Loc. 18A). A diagrammatic sketch of one example is shown in figure 8.

BOULDER BEDS

South of U.S. Highway 90.—The boulder beds are truly remarkable deposits because of the gigantic size of the larger blocks, the variety of rock types present, and the unusual slump features associated with them. The interval is a complex of grotesquely contorted flysch interbeds, massive coarse sandstone, chert conglomerate, and mudstone and muddy sandstone beds that contain well-rounded pebbles and cobbles of exotic rocks in addition to huge angular blocks from older Paleozoic formations in the Basin. Detailed descriptions of the appearance and stratigraphy of the boulder beds with many excellent photographs are given by Baker (1932) and by P. B. King (1937, pp. 65–72, 89–92). Only a summary of the strati-

graphy and lithology plus features pertinent to the origin of the boulder beds are presented here; outcrop photographs of the boulder beds are shown in Plates 10, 11, and 12 and sketches of stratigraphic details in figures 5 and 6. Brief descriptions of the boulder beds have also been given by King, Baker, and Sellards (1931), Sellards (1931), King (1932, 1958), Hall (1957, 1959), and Flawn (1958).

Because the boulder beds have a large amount of clay in them (in shale and mudstone beds), they break down easily to gentle slopes and are widely covered by a veneer of colluvium. Except for boulders which stand out in relief from their softer matrix (Pl. 10, A, B), good exposures are limited to arroyos that cut across the strike of beds.

Boulder beds and flysch and coarse sandstone beds with which they are interbedded are lenticular and of irregular thickness; the entire complex of beds also has a lenticular form. King, on the basis of plane-table and alidade measurements (1937, p. 66), reported that the boulder bed member has a maximum thickness at the base of Housetop Mountain of about 900 feet, interbedded with thin-bedded sandstones and shales and ledges of massive arkose. Using 5- and 7-foot Jacobs staffs, the writer measured a 1,005-foot section of boulder beds in the same area.

The geologic map of the boulder bed interval presented by King (1937, Pl. 10) is an important contribution that illustrates the interbedded character and lateral continuity of coarse sandstone and boulder beds in the unit and larger-scale stratigraphic features of the unit. Owing to the scale, however, the map is oversimplified in that the boulder bed layers are not single beds but are a succession of beds (or more properly, sedimentation units) that range from 6 inches to 20 feet or more in thickness, and thin boulder-bearing beds also occur in sections shown as arkose. Boulder and arkose (coarse sandstone) beds are lenticular and have irregular thicknesses along strike. Unfortunately, exposures are not sufficient enough to warrant mapping the interval in more detail

than it was mapped by King, and photographs of individual outcrops do not convey a picture of the stratigraphic complexity of the unit. A well-exposed section 260 feet thick at the top of the boulder bed unit at base of Housetop Mountain is shown in figure 6.

An exposure of the basal contact of the boulder-bearing unit was found at only one locality, in an arroyo at the base of House-top Mountain. Here greatly contorted flysch interbeds with local pods of mudstone containing scattered boulders of chert and novaculite rest directly on undeformed flysch beds. A 15-foot block of chert occurs about 5 feet above the base of the unit. Arroyo exposures along strike show that different boulder-bearing lithologies occur at the top of the boulder bed unit. Several areas have 15 to 25 feet of contorted flysch beds above the uppermost boulder bed.

As emphasized by King (1937, p. 66), the most striking feature of the boulder beds is the large size of some of the embedded rocks. Numerous blocks of Caballos Novaculite exceed 50 feet across, and **blocks of Pennsylvanian limestone** (Pl. 10, A) exceed 100 feet in length. The largest block recorded by King (1937, p. 66) and Baker (1932) is a block of Dimple Limestone that is 130 feet across. King's Plate 10 shows the location and lithology of most blocks that exceed 2 feet in diameter. The writer has found additional blocks up to 6 feet long that may have been exposed since King's mapping was done. The map illustrates that the larger boulders are found in clusters and are not evenly distributed along the outcrop. Most large blocks are slab-like with their largest plane parallel to bedding in the block and also to bedding in the outcrop.

Nearly as impressive as size is the variety of rock types. These may conveniently be placed into two groups: (1) sedimentary rocks of older Paleozoic formations exposed within the Marathon Basin and (2) sedimentary, igneous, and metamorphic rocks of uncertain age and unlike older formations in the Basin or immediate vicinity (exotic rocks).

With one exception, rocks larger than 2

feet in longest dimension are those of category 1. The exception is blocks of fossiliferous Pennsylvanian limestone up to 100 feet long that are unlike limestone in the Dimple Formation, its age equivalent. Fragments of Paleozoic rocks range from granules to blocks 130 feet long. Some fragments of pebble- and cobble-size are well rounded, but most pebbles and larger fragments are angular. Some 3- to 5-foot boulders of chert and novaculite are subspherical, although their edges are angular and show no signs of rounding. The chert and novaculite of many boulders have been severely brecciated and later recemented, because the boulders are now composed of angular and splinter-like pieces of chert and novaculite cemented by chalcedony. Slickenside surfaces are exposed on the exterior of a few non-brecciated chert blocks.

Fragments of novaculite and white, black, and green chert from the Caballos Formation are the most abundant rocks in the boulder beds; they comprise an estimated 60 percent of the coarse debris. Sandstone from the Tesnus Formation and chert and limestone from the Dimple are about equally abundant, whereas chert from the Maravillas is rare. Baker (1932, p. 588) reported the presence of limestone from the Maravillas (Upper Ordovician) and Lower Ordovician limestone and chert. Neither King nor the writer has found unequivocal Lower Ordovician rock types.

The maximum and estimated average sizes of each lithology found are given in table 3 (p. 26).

Pennsylvanian limestone fragments are the most abundant single rock type with lithologies unlike those of older rocks in the Basin. The rocks are partly chertified biosparites that were deposited in shallower water than is inferred for the environment of deposition of Dimple limestones (Thomson and Thomasson, 1964). A list of fossils collected from the blocks is given by P. B. King (1937, p. 72).

Other rock types found, in order of abundance, are: (1) several types of sandstone and granule conglomerate; (2) coarse-grained plutonic rocks ranging from muscovite-biotite granite to granodiorite,

TABLE 3.—Maximum and estimated average size of erratic and exotic clasts in the boulder beds.

Rock type	Maximum length		Average (modal) length
	Feet	Inches	Inches
Dimple limestone	130		----
Pennsylvanian limestones	100		6
Caballos chert and novaculite	40		2-12
Tesnus sandstone	35		1- 3
Maravillas chert	5		----
Other sandstones		24	1½
Gneissic granite-granodiorite		10	1
Sheared porphyritic rhyolite		10	1
Vein quartz		6	½
Dimple chert		4	½
Schist		3	½

many with weak foliation; (3) porphyritic rocks, mostly rhyolites but with some rhyodacite, and weakly to strongly sheared equivalents of them (cataclasites); (4) vein quartz; (5) cataclastically altered sandstones; and (6) two types of schist (muscovite schist, graphite schist). King, Baker, and Sellards (1931) found pebbles of aplite and syenite, Flawn (1956) reported one sample of tourmaline-garnet schist, and the writer also found a single pebble of spotted quartz-biotite-sillimanite schist in Flawn's collection. Such rock types are rare, because additional samples were not found in the field. The sandstones and conglomerates, which include quartzite (granule-bearing coarse silicic submature quartzarenite), friable sandstone (medium- to coarse-grained supermature quartzarenite), and well-indurated feldspathic sandstone (medium silicic immature subarkose, probably Tesnus, and coarse silicic immature lithic arkose) show slight to moderate dynamic metamorphism in contrast to the meta-igneous rocks that show textures typical of moderate to severe cataclastic deformation.

Flawn (1956, p. 59) classified the metamorphic rocks of the boulder beds into a higher grade, or Llanoria type, and a lower grade (weakly metamorphosed quartzite), or Ouachita type. In contrast to most Paleozoic rock fragments which are angular, fragments of the exotic rock types are well to very well rounded. Some boulders have a degree of sphericity and roundness seldom found in natural water-worn boulders (Pl. 11, D).

Evidence is presented later that the ex-

otic clasts are fragments of the source land that was situated to the east and southeast of the basin of deposition. The exotic fragments, therefore, provide direct evidence of at least some rock types that made up the source land. Because of their importance to an interpretation of paleogeology, the texture and mineralogy of characteristic rock types have been described in more detail in Appendix A, and photomicrographs of numerous rock types are shown in Plates 20-24. Material for this summary description includes 60 thin sections and more than 200 pebbles, much of which was kindly loaned by other workers.

As mentioned previously, it is rare for clasts in the boulder beds to be in contact. Two exceptions deserve mention, however. Several lenticular beds of chert-pebble conglomerate crop out at the base of Housetop Mountain. King shows the location of the thicker of these "chert breccias" on his geologic map of the boulder beds. These beds are from 1 to 3 feet thick of angular to subangular pebbles of black, white (including novaculite), green, and brown chert from 1 to 5 inches long that form an intact framework (Pl. 11, B). In some beds the interstices are filled with coarse sandstone, but most are partly filled by chalcedony to form resistant beds. Elongate pebbles show a fair alignment parallel with bedding, but no imbrication was observed. A few beds contain sparsely scattered boulders of chert up to 1 foot in diameter.

Another exception is a unique polymictic conglomerate bed 2 feet thick composed almost entirely of well-rounded subspherical pebbles that have an intact framework

and a muddy coarse sandstone matrix (Pl. 11, A). The bed is exposed over a distance of only 25 feet and was not found elsewhere along strike. The types of pebbles present and their estimated abundance are given in table 4. Well-cemented sandstone fragments, largely Tesnus, predominate.

Host rocks to the exotic and erratic debris have a wide range in texture and composition and include the following in order of abundance:

- (1) mudstone
- (2) shale-pod-bearing, muddy coarse sandstone
- (3) muddy coarse sandstone (without shale-pods)
- (4) contorted interbedded flysch sandstone and shale beds

Mudstone is the matrix for approximately 90 percent of the gravel-size material and of all blocks larger than about 10 feet in diameter (Pl. 12, A, B). Few mudstone beds contain more than 50 percent (by volume) material finer than 0.03 mm (mostly clay), although a few beds have as high as 70 percent clay. According to Folk's (1954) textural terminology, most mudstones should be termed highly clayey sandstones. However, the use of mudstone for the Haymond rocks and similar "pebbly mudstone" deposits is well established in the literature and is so used here. Most mudstones have between 40 and 50 percent clay, although they are transitional into normal coarse sandstone beds with a decrease in clay. Mudstones have a framework of medium- to coarse-grained sandstone with randomly oriented grains. The matrix is carbonaceous clay similar to

that in Haymond shales. Plant fragments are sparsely scattered through the mudstones and have no preferred orientation.

Shale-pod-bearing beds have from 30 to 60 percent by volume of semi-elliptical pods of shale encased in massive, slightly clayey coarse sandstone. The shale pods are mostly from 2 to 4 inches long and lie with their bedding (fissility) planes subparallel with bedding, although some are tipped at high angles (Pl. 11, C). Some fragments are bent and thus indicate they were unconsolidated at the time of transportation. This fact, plus the similarity of the shale-pods to normal Haymond shale and associated features formed by slumping, indicates that the shale-pods are fragments of disrupted and brecciated shale beds derived from within the basin of deposition and transported only a short distance. *Muddy sandstone beds without shale-pods* have the same random orientation of grains and massive character as the beds described above. A few sandstone beds that contain fragments no larger than fine-pebble size are crudely laminated, however.

Where boulders occur in flysch-type interbeds of sandstone and shale, the beds are severely contorted and many sandstones pinch and swell and are broken by microfaults (Pl. 10, C, D). Boulders are surrounded by a thin aureole of mudstone made up of a mixture of sand and shale constituents. Flysch beds a few feet thick that do not contain boulders are present between boulder-bearing beds of all types. They range from undeformed beds to those contorted into tight asymmetric disharmonic folds a few feet in amplitude. The

TABLE 4.—Estimated percentages of pebbles in polymictic conglomerate from the boulder beds.

	Percent
Sandstone—	80
Greenish-gray, medium-grained subarkose (Tesus)	55
Light-brown granule-bearing coarse-grained sublitharenite	5
White, coarse-grained quartzarenite	12
Light-brown, medium-grained subarkose	8
Gneissic granite-granodiorite	8
Schist	3
Vein quartz	3
Porphyritic rhyolite (including cataclastic derivatives thereof)	2
Black chert (Caballos?)	2
Green Caballos chert	1
Dimple chert	1

boulder-bearing flysch beds, however, are the most intricately contorted of all. Sketches of two localities at the base of Housetop Mountain are shown in figure 5. Most flysch-type beds are less than 6 inches thick.

The age of the exotic rocks, except for the Pennsylvanian limestone, is uncertain because they contain no fossils and they do not resemble formations known in adjacent areas. King, Baker, and Sellards (1931) assumed them to be of Precambrian age, probably because of the abundance of "crystalline" rocks and the dissimilarity with Paleozoic rocks exposed in the Basin. Flawn (1956) studied the crystalline rocks as possible representatives of Texas basement rocks but did not speculate on their age.

Recently, radiometric ages on a gneissic granite cobble from the base of Housetop Mountain have become available through the courtesy of W. R. Muehlberger, Director of the Crustal Studies Laboratory, The University of Texas (personal communication, 1964). An age of 360 M. Y. was obtained for the age of biotite in the rock by the K-Ar technique, and 570 M. Y. for the whole-rock age using the Rb-Sr technique. The younger age of the biotite indicates that the mineral formed during metamorphism in late Devonian(?) time, possibly when the foliation was developed. The whole-rock age indicates that the granite is at least as old as early Cambrian and is possibly somewhat older, because the younger biotite and possibly other metamorphic minerals were included in the age determination. Dating of additional rocks and minerals from the boulder beds is planned for a future project.

Clark Butte area.—In the northern part of the Basin sparsely scattered boulders occur in chert-pebble conglomerates that are sporadically exposed along a 4-mile-long outcrop belt within the thick section of coarse sandstone beds. No mudstones typical of the beds farther south are present here. King (1937, p. 68) described the boulders as occurring here in a single bed 10 to 25 feet thick. More detailed work done during this study, however, reveals

that the boulders (1) occur in lenticular units with varied thickness along strike, (2) pinch out entirely in places, and (3) are separated by as much as 150 feet of coarse sandstone where more than one bed is present in a section. Pebble- and boulder-bearing beds range from 2 to 60 feet in thickness. Local details of the complicated stratigraphy of these beds are shown in figures 7 and 8. The irregular thickness of the beds is largely the result of deposition on a scoured surface. Since the coarse sandstone beds with which they are interbedded show similar channel-fills, it is possible that boulder beds have been locally removed by erosion. Boulder beds rest on coarse sandstone as well as thin flysch interbeds of sandstone and shale, some of which are deformed into gentle disharmonic folds.

The bulk of the boulder beds are composed of subangular fragments of chert of pebble size and sparsely scattered fragments of boulder size within a coarse sandstone matrix. Pebbles in some beds comprise 70 percent of the rock and are in contact to form an intact framework. These beds are generally partly cemented by chalcedony to form a highly resistant rock. In other beds pebbles form only 40 percent of the rock and are dispersed in a matrix of coarse sandstone. Boulders are mostly between 1 and 3 feet in length; the largest in the area is a slab of novaculite (Caballeros Formation) 10 feet long. This slab, as well as most larger boulders, lies loose in rubble released by weathering of the beds. Some beds contain 20 percent fragments larger than 6 inches in length, whereas others have only rare fragments this large. At several localities beds display a crude grading, in that the boulders are most abundant at the base of the beds, and commonly decrease in abundance, but not size, upward. Only locally do the pebbles and boulders show a preferred orientation parallel with bedding.

The estimated average composition of particles of pebble size and larger for the northern boulder beds is: gray, brown, and black chert, 70 percent; white chert and novaculite, 25 percent; limestone, 4 per-

cent; and chert breccia, 1 percent. King (1937, p. 68) reported trace amounts of Tesnus Sandstone, Maravillas Limestone, fossiliferous Pennsylvanian limestone, and porphyritic rhyolite, and Baker (1932, p. 588) reported the presence of Lower Ordovician chert. Chert and novaculite from the

Caballos Formation are by far the most abundant coarse detritus. An 18-inch piece of petrified wood was found in rubble from one boulder bed. The wood is similar to silicified logs of *Callixylon* cf. *newberryi* which occur in the Caballos Formation south of Marathon (Bennett, 1959, p. 78).

PETROGRAPHY

SHALE

The bulk of the shale in the Haymond is moderately fissile clay-shale that is medium gray to medium light gray (N5-N6) (Rock Color Chart, 1948) in outcrop; unweathered shale has not been found, but relatively fresh samples are darker than weathered ones. Lighter gray shale (N7) occurs in the Allison Ranch facies, but how much of the lighter color is due to leaching during weathering is uncertain. Most good exposures reveal a few shale beds less than 1 inch thick that are coal black (N1) owing to an abnormally large amount of plant debris (Pl. 13, D).

Typical Haymond shale throughout the Basin is highly burrowed clay-rich shale with sparse silt laminations. Except for the exceptionally large amount (15 percent) of plant fragments in the coal-black shales, the chief differences between samples is in silt content, which ranges from 3 to 30 percent. Silt grains occur chiefly randomly distributed through clay beds, although silt laminae averaging 0.02 mm thick make up an estimated 5 to 10 percent of the thickness of layers between recognizable siltstone or sandstone beds. The dearth of laminae in the shales is attributed to the mixing action of burrowing animals, whose activities are shown by swirl orientations of clay particles or rare silt-filled burrows. In addition, clay and plant particles in Haymond shales show only a faint preferred orientation in plain light and feeble mass-extinction in polarized light. In contrast, typical unburrowed shales have a strong preferred orientation of detrital particles parallel with bedding such that thin sections show a strong mass-extinction effect under crossed nicols. The lack of detectable animal hard parts in the shales, in spite of the intensity of burrowing that occurred, suggests that the benthonic animals were worms and other animals without hard parts.

The silt in the shales is chiefly quartz with minor amounts of feldspar and trace

amounts of micas, chlorite, and heavy mineral grains. The clay mineralogy of shales determined by X-ray diffraction of oriented glycolated and heat-treated samples is given in table 5. The relative abundance of clay minerals is based on a visual comparison of the areas beneath first-order basal peaks. Sodium and calcium montmorillonites, well-crystallized illite, and 14-Å chlorite are the only clay minerals, although several samples have trace amounts of mixed-layered clays. Illite predominates in all shales, and chlorite is slightly more common than montmorillonite. Weaver (*in* Flawn et al., 1961) reported small amounts of mixed-layer clay and kaolinite in the lower part of the Haymond.

Carbonaceous debris, probably mostly plant remains, is present in all Haymond

TABLE 5.—*Relative abundance of clay minerals in Haymond shales and matrix of sandstone beds. Stratigraphic position of samples is shown in Plate 1.*

Sample No.	Clay minerals	Comments
Shale		
Hs-4	I = Ch	Chlorite expanded slightly upon glycolation
Hs-5	I > Ch	
Hs-10	I > Ch = M	Ca and Na montmorillonite
Hs-13	I > M, (Ch)	Ca montmorillonite
Hs-16	I > Ch	
Hs-20	I >> Ch	
Hs-22	I > Ch	
Hs-24	I = M, (Ch)	Ca montmorillonite
Hs-27	I > Ch	Sedimentary chlorite
Hs-28a	I > M = Ch	Na and Ca(?) montmorillonite is degraded
Hs-50	I > Ch	Sedimentary chlorite
Hs-53	I > Ch	Sedimentary chlorite Illite is degraded
Sandstone		
H-51	I = Ch ?	Broad peaks
H-52	I = Ch	
H-76	I > Ch	Chlorite expanded slightly when glycolated
H-109	I > Ch	
H-220	I > Ch > M	
H-224	I = Ch	Both have broad peaks

I = illite
Ch = chlorite
M = montmorillonite

shale in amounts of a few percent (by volume), although the coal-black shales have 10 to 15 percent. Most plant particles are less than 10 microns long, but particles up to 2 mm long are present in a few samples. Standard techniques for extracting microfossils other than spores have given negative results in all but one sample. The latter, from the Allison Ranch facies, yielded a small foraminifer and several sponge spicules. S. P. Ellison (personal communication, 1962), in a search for conodonts from more than 100 shale samples from the Haymond, reported negative results. Spores were found in two of four shale samples that were macerated by the writer.

SANDSTONE OF THE FLYSCH FACIES

Procedure.—Flysch sandstones are fine- to very fine-grained, immature to submature quartz sandstones rich in feldspar and containing moderate to large amounts of rock fragments⁹ and are bound together by a combination of interlocking matrix and framework grains with minor quartz and calcite cement. The chief textural and composition features of 25 sandstone samples were determined by making 100 point counts per thin section to determine the relative amounts of framework grains, matrix, and cement, and then making additional counts until the mineral composition of a total of 100 framework grains (excluding micas and heavy minerals) had been determined. Point-count data are given in table 6 and are summarized in figure 11. Representative sandstone samples are illustrated in Plates 14, 15, and 17.

Framework grains fall into the following categories: quartz, polycrystalline quartz, metaquartzite rock fragments, chert, plagioclase, K-feldspar, sedimentary rock fragments, metamorphic rock fragments, volcanic rock fragments, muscovite, biotite, and other accessory minerals. Percentages of these constituents are given in table 6 (in pocket).

The sandstones were classified on the

composition of framework grains following the writer's classification (McBride, 1963b). This classification has the following end-members: Q-pole (quartz, chert, and metaquartzite), F-pole (feldspar), and R-pole (fine-grained fragments of igneous, metamorphic, and sedimentary rocks). Figure 12 shows that most sandstones fall in the arkose, subarkose, and lithic subarkose field; they are quartzose sandstones rich in feldspar and containing moderate amounts of rock fragments.

Quartz.—Quartz is the most abundant framework constituent in all sandstones; it ranges from 57 to 80 percent and averages 67 percent. The bulk of it is common quartz—that which shows straight to slightly undulose extinction and which has few bubble inclusions. Highly undulose grains or those with abundant mineral inclusions are rare. Most grain shapes have been altered since deposition either by the addition of small amounts of quartz cement or by pressure-solution along contacts with adjacent clay and quartz grains; consequently, no detailed study of grain shapes or roundness was made. Most grains have typical subequant shapes, although a few slivers are common in each thin section. Subangular to subrounded grains predominate, but all grain shapes are represented. Similar to most sandstones, the coarser grains are the better rounded.

The number of polycrystalline quartz grains in each slide was counted because such grains are most abundantly derived from metamorphic source rocks. Although a few rocks have as high as 6 percent (of framework) polycrystalline quartz, there is no significant regional or stratigraphic trend.

Feldspar.—The sandstones have from 7 to 31 percent feldspar and average 19 percent. Sodic plagioclase (albite-oligoclase) is the most abundant feldspar; it is present in all samples and ranges from 4 to 24 percent. K-feldspar is present in only trace amounts or absent in 9 of the 25 samples, and only in 5 does it exceed 5 percent. The relative abundance of feldspar types may be due to the paucity of K-feldspar in the source rocks or may reflect the greater re-

⁹ Although all terrigenous mineral grains are true rock fragments, the term here refers to sand-size polygranular aggregates of fine-grained igneous, metamorphic, or sedimentary rocks such as basalt, schist, or claystone.

sistance to weathering of sodic plagioclase over K-feldspar when released from source rocks. Evidence to support the latter situation is that K-feldspar shows more alteration than plagioclase in thin sections. Although most plagioclase grains show some degree of alteration, most rocks have a few fresh, twinned grains. Alteration of plagioclase generally proceeded first by sericitization followed by vacuolization. Some grains are so highly sericitized they are difficult to distinguish from matrix sericite.

To aid in identifying untwinned feldspars, thin sections were etched in hydrofluoric acid fumes and immersed in a saturated solution of sodium cobaltinitrite prior to point counting. K-feldspars stained yellow and are readily distinguishable from plagioclase and quartz. In four unstained slides no attempt was made to distinguish feldspar types. Untwinned K-feldspar, probably mostly orthoclase, predominates over grid-twinned (microcline) feldspar. Although a few K-feldspar grains are still fresh, most show partial to complete replacement by calcite or siderite-ankerite (Pl. 15, A). A few K-feldspar-rich rocks have sand-sized grains of kaolinite and generally some kaolinite cement (Pl. 19, A). The kaolinite grains are pseudomorphs after K-feldspar and their undeformed shape shows that the argillation took place after deposition. Inasmuch as K-feldspar grains are replaced to a greater degree than plagioclase, grains of calcite that completely replace feldspars as pseudomorphs were tabulated as K-feldspar grains, even though their parentage could not be proved.

Feldspar clasts are chiefly subhedral to euhedral, angular to subangular grains that average slightly smaller in size than the average associated quartz grains.

Rock fragments.—Sand-size fragments of shale and fragments of the schist-phyllite (Pl. 15, C, D) group make up the bulk of the fine-grained rock fragments in the sandstones. Minor rock types in order of abundance include chert, siltstone, sandstone, metaquartzite, silicic and mafic volcanic rock fragments, and granitic plutonic rocks. The shale grains range from

well-indurated and rounded particles that have been only slightly elongated (Pl. 15, B) and distorted due to post-depositional framework compaction and condensation, to soft grains that have been so strongly squeezed (Pl. 18, D) that they cannot always be distinguished from clay matrix and in fact have become clay matrix.

The shale grains and most sandstone and siltstone grains are similar in texture and mineralogy to Haymond rocks and most are thought to have been derived from beds within the basin of deposition. Silicic volcanic rock fragments are composed of feldspar microlites or a mosaic of anhedral grains (Pl. 15, 6) and are only slightly altered. In contrast, mafic rock fragments are composed chiefly of secondary chlorite or serpentine and minor plagioclase microlites.

Carbonate grains and fossils.—Carbonate rock fragments, chiefly micrite and algal biomicrite, and fossils have been found only in the Dugout Mountain area in sandstones transitional into the Gap-tank Formation. In these beds (Pl. 17) fragmental remains of echinoderms, crinoids, brachiopods, algae, small foraminifers, fusulinids, and pelecypods(?) are present, as are a few oolites. The fossils have all been transported from shallower water, and some, as shown by their occurrence in rock fragments, have been reworked from older rocks.

Matrix.—Figure 11 shows the relative percentages of framework grains, cement, and matrix of individual samples. Detrital grains coarser than 0.02 mm are classified as framework grains, whereas finer detrital constituents or their reconstituted products are considered matrix. The matrix is chiefly muscovite-type clay with minor quartz silt and a trace of chlorite. Samples range from those in which the muscovite-type clay is nearly all illite to those in which one-half the matrix is muscovite fibers (sericite). The latter is certainly authigenic, because fibers penetrate some framework grains, and probably is reconstituted illite. Six sandstones were crushed and sieved in order to separate matrix constituents. X-ray diffraction (table 5) pat-

terns of the fractions finer than 0.06 mm show the presence of subequal amounts of illite and 14-Å chlorite, and one sample has a trace of montmorillonite. Owing to the crushing process, fine-grained rock fragments may have contributed some grains to the sieved fraction. The percent of matrix in sandstones ranges from 5 to 30, although most have less than 20 (average 13 percent).

Samples shown in figure 11 with more than 30 percent matrix are mudstones. In parts of some thin sections it was impossible to determine whether clay patches are matrix grains or whether they are soft shale fragments that have been smashed between more resistant grains. In the point-counting procedure such grains were divided equally between *matrix* and *shale rock fragments*.

Cement.—Quartz overgrowths (Pl. 18, A) on detrital grains are the chief cementing material of Haymond sandstones throughout the Basin. Carbonate minerals are present in trace amounts in many sandstones and are the only cement in sandstones immediately below the Gaptank Formation in the Dugout Mountain area. In the latter beds, carbonate minerals not only fill primary pores but also replace the margins of some framework grains (Pl. 17). Because it was not possible to determine whether some patches of carbonate originated as pore filling or by replacement, all authigenic carbonate was arbitrarily classified as cement during point-counting and is so plotted in figure 11. Sandstones plotted with more than 10 percent cement all contain some authigenic carbonate. The latter is chiefly euhedral rhombs of ankerite-siderite, in part altered to limonite, that are scattered throughout the rock where they have replaced both framework grains and matrix. Clear patches of sparry calcite are common minor constituents. The most common cement paragenesis is quartz, calcite, ankerite-siderite.

If the amount of cement in the sandstones is interpreted to be the porosity of the rocks prior to cementation, Haymond sandstones had original porosities far

lower than modern sands (20 to 40 percent). The lower porosity of Haymond sandstone is in part due to the presence of silt- and clay-sized detritus in pores but is probably largely due to condensation of framework grains accompanying compaction. Evidence for condensation includes sutured quartz grains and smashed rock fragments (Pl. 18, C, D).

Texture.—Mechanical grain-size analyses could not be made owing to the well-indurated character of the beds. Although a procedure has been described for converting size distributions made by measuring grain diameters in thin section to equivalent sieve (weight) distributions (Friedman, 1958), the procedure will not work for sandstones containing appreciable clay. Inspection of thin sections indicates that the framework fractions of most beds are moderately well sorted, but the overall sorting of the rocks is significantly less owing to the presence of matrix clay particles. The clay imparts a negative skewness to all samples. In the absence of size analyses, the best concept of sorting is given by photomicrographs (Pls. 14, 15, and 17).

Flysch sandstones, with few exceptions, have average and modal sizes of fine to very fine sand. Grains of coarse silt are common in very fine sandstones, and some very thin beds (less than 5 mm thick) are true siltstones. Many beds grade upward from very fine sand to coarse silt but have modes in the very fine sand size.

The uniformity of grain size in flysch sandstones is illustrated by using the average diameter of the ten largest grains in a thin section as a measure of the mean size of a sample (p. 40). Few average values exceed the fine-sand limit (Pl. 1).

Fabric.—Under hand-lens inspection the only apparent preferred orientation of sand grains is mica flakes and flat rock fragments (Pl. 15, C, D) whose long dimensions are subparallel with bedding. However, most thin sections cut perpendicular to bedding show that elongate quartz and feldspar grains also have a preferred orientation subparallel with bedding (Pl. 14, A, B), and 10 percent of the

thin sections show a distinct upcurrent imbrication of grains. In order to illustrate quantitatively representative sandstone fabrics, the orientation of long axes of quartz and feldspar grains having lengths at least twice their widths (elongation ratio $> 2:1$) was determined in sections cut perpendicular to and parallel with bedding from five beds from which paleocurrent directions were known from sole marks. Grain orientation data are shown as circular histograms having 20-degree class intervals (fig. 12). Each histogram is based on at least 100 grain orientations.

Sections cut perpendicular to bedding (fig. 12, A-C) and parallel with the current direction show very strong modes; in one sample the grains are parallel with bedding whereas in the others the grains have an upcurrent imbrication¹⁰ of 30 to 40 degrees. The imbrications are not apparent upon inspection of the thin sections. Sections cut parallel with bedding (fig. 13, D-H) show that the samples have, at best, very feeble preferred orientations; the histograms are polymodal and do not have strong principal modes.

COARSE SANDSTONE BEDS

The prominent megascopic differences between flysch sandstones and the coarser and thicker sandstone beds in the northern and eastern parts of the Basin have been mentioned previously (p. 23). Point counts of 12 thin sections show that coarse sandstone beds have on the average less feldspar and matrix than flysch sandstones but more chert and non-carbonate sedimentary rock fragments. Although P. B. King (1937) refers to "coarse arkose beds" to contrast them from flysch sandstones, the coarse sandstones actually have less total feldspar (average of 16.9 percent) than the average flysch sandstone (average of 19.0 percent). Statistical tests (table 9, in pocket) show that the only significant difference in average feldspar content is between the flysch beds above the boulder bed member and the coarse sandstone beds

($p = < 0.05$). Feldspar is more conspicuous and K-feldspar is more abundant in the coarse sandstone beds than in flysch beds.

The lower matrix content of the coarse sandstones combined with less hematite-limonite stain results in lighter shades of brown than prevail in flysch sandstones.

Detailed fabric studies were made only on three coarse sandstone beds to test the relation between grain orientation and parting lineation (fig. 12, G-K). The results are discussed on page 22. Inspection of thin sections perpendicular to bedding shows a distinct orientation of long axes parallel to bedding in laminated beds but feeble or no orientation in massive beds. No imbrication is apparent. The coarsest particles in the sandstones are fragments of plants up to 6 inches long, known only from impressions. Although scarce, some bedding planes have numerous fragments which generally have a distinct preferred orientation parallel with the paleocurrent as determined from associated current structures.

BOULDER BEDS

Rocks unique to the boulder beds include mudstone and the erratic and exotic gravel- and block-size fragments. One pebble of each different rock type (excluding Caballos and Maravillas chert) was chosen from collections made by the writer from the boulder beds and from other collections available to the writer; a thin-section description of each is given in Appendix A (p. 65). Photomicrographs of different rock types are shown in Plates 20-24.

Thin sections of mudstones from the boulder bed reveal a mixture of poorly sorted framework grains in from 30 to 60 percent organic-rich clay matrix. Both the framework grains, which are identical mineralogically to coarse sandstone beds, and the clay have a random orientation and together show no vestiges of bedding. Although the sand-sized grains in mudstone layers now all appear to have intact frameworks, beds with greater than 50 percent clay probably had dispersed fab-

¹⁰ The direction of imbrication, by convention, is the direction a grain is inclined downward from the bedding (reference) plane.

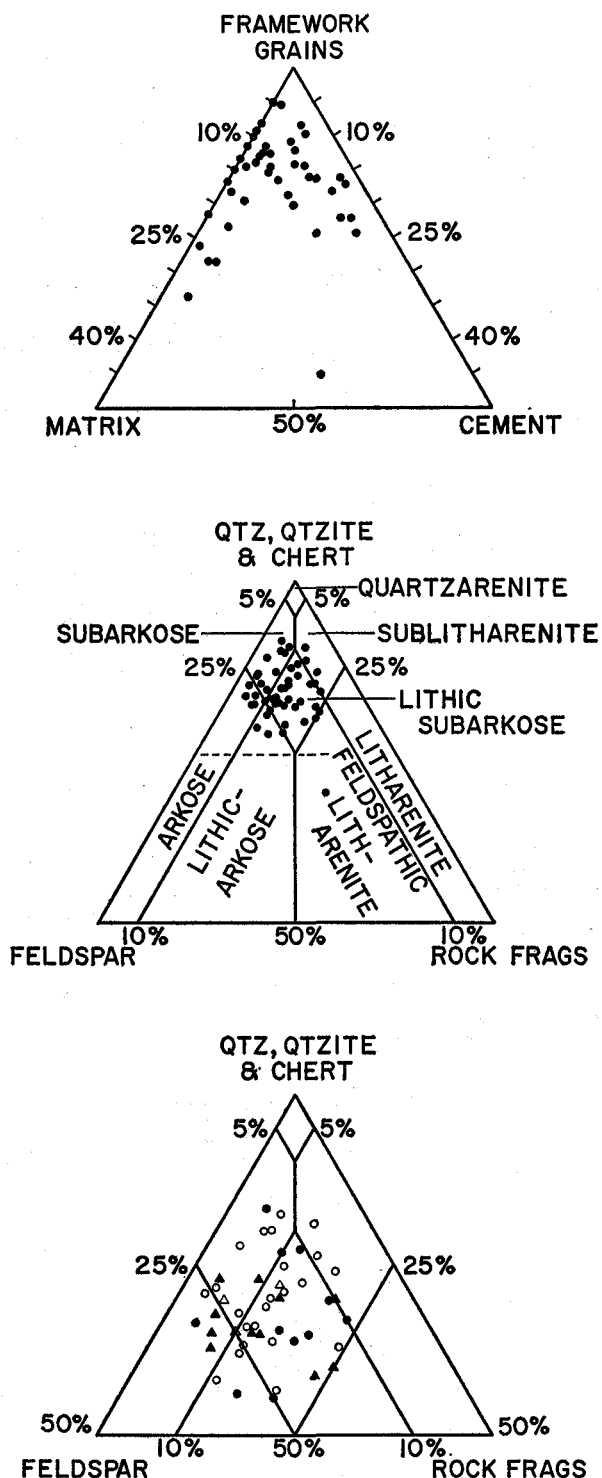


FIG. 11. Plot of Haymond sandstones showing texture and composition. Lower diagram is an enlarged view of the center diagram. Open circles = below the boulder beds; solid circles = above the boulder beds; open triangles = Dugout Mountain area; solid triangles = coarse sandstone beds.

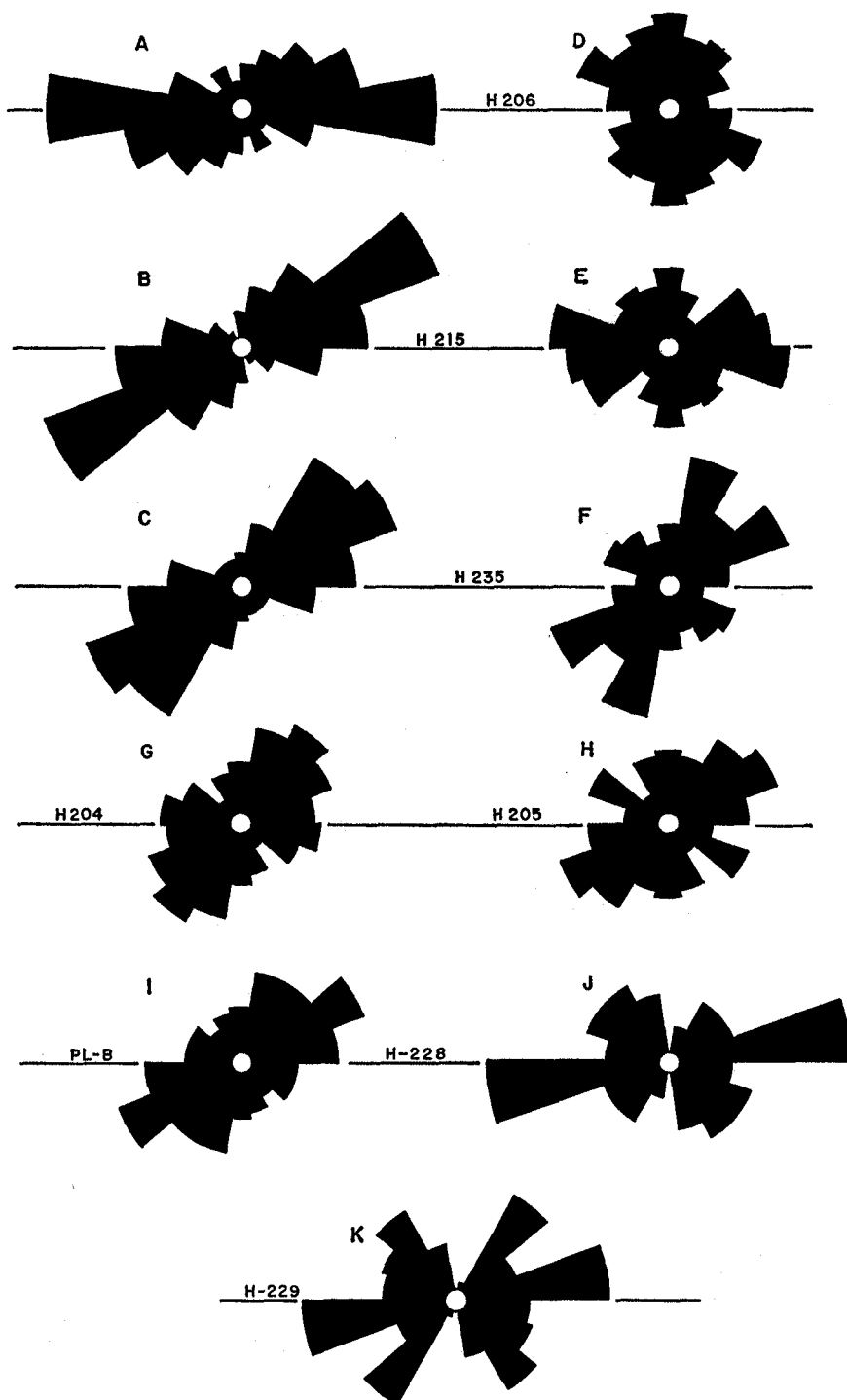


FIG. 12. Circular orientation histograms based on 100 elongate grains per sample. Samples A, B, and C show orientations perpendicular to bedding; the remainder are in the plane of bedding. The horizontal reference line in Samples D-H is the trend of the depositing current; the horizontal line in Samples I-K is the trend of parting lineation.

rics (grains surrounded by clay) prior to compaction. Large rock fragments show the greatest results of compaction; soft grains are flattened, whereas resistant grains have sutured boundaries. Many smaller, resistant grains that were probably cushioned by adjacent soft shale grains during compaction show no signs of suturing and display original shapes outlined against the dark clay matrix (Pl. 16, A, B).

Gravel-size chert clasts are abundant in the northern boulder beds and in several chert-pebble conglomerates (breccias of King) in the boulder beds south of U.S. Highway 90. A thin section study reveals the following types of chert to be common in the northern boulder beds (in order of abundance):

1. Clear, colorless chert; traces of hematite grains less than 2μ in diameter. Uniform even-textured chalcedony grains less than 1μ in diameter except for recrystallized spicules and radiolarian tests(?) that are coarser-grained chalcedony (5 percent).

2. Brown phosphatic chert; chertified and phosphatized fossiliferous limestone. Relict texture of laminated fossil detritus (identifiable sponge spicules, molluscs, foraminifers); now 55 percent silica (microcrystalline quartz and chalcedony) and 45 percent fine-grained cellophane.

3. Brown chert; chertified silty calcarenite(?) about 90 percent brown cryptocrystalline chalcedony, 10 percent quartz silt grains, and a trace of spicules and hematite.

4. Cherty cellophane; 90 percent brown colloform cellophane, 10 percent chalcedony, a trace of authigenic hematite. Cellophane has replaced chert. Relict spicules visible in cellophane.

HEAVY MINERALS

Heavy minerals were separated from 22 sandstone samples. Owing to the high degree of induration and cementation of the sandstones, it was necessary to crush the samples to disaggregate the grains. Approximately 60 grams of each sample were

crushed and screened to remove particles coarser than 0.5 mm. Heavy minerals were separated in tetrabromoethane (sp. gr., 2.89) using conventional techniques. Magnetite, comprising up to 30 percent of some concentrates, was removed with a hand magnet.

Only 5 of the 22 samples yielded clean separations of several hundred grains; all are from sandstones whose average maximum grain size is 0.5 mm or coarser. Sandstones with abundant authigenic hematite yielded floods of hematite-coated light minerals. Fine- and very fine-grained sandstones commonly yielded less than 50 grains per sample. Apparently, the crushing process did not sufficiently disaggregate the rock into constituent grains and thus heavy minerals remained cemented to clusters of light minerals and did not sink in the heavy liquid.

Although the data on hand are too meager to provide a detailed treatment of the heavy minerals, the data are summarized below. Counts of 100 grains along line traverses were made for the five good samples, and data are given in table 7. Opaque minerals, which predominate in most slides, and micaceous minerals (biotite, muscovite, and chlorite) were excluded from the counts; the former owing to the difficulty in identification of specific minerals, and the latter owing to their inconsistent degree of separation. Barite occurs in 5 samples ranging from a trace to 64 percent of the total heavy grains. Because it is obviously authigenic, occurring as large irregular-shaped angular grains crowded with fluid and mineral inclusions, it is not included in the discussion of heavy detrital grains.

Heavy minerals identified in the Haymond in order of abundance are: zircon, garnet, tourmaline, rutile, monazite, apatite, sphene, and epidote(?). The assemblage is characterized by zircon and garnet, which comprise from 50 to 90 percent of each sample.

Zircon, the most abundant mineral in most samples, is present 95 percent as rounded to well-rounded subspherical grains and 5 percent as euhedral grains

TABLE 7

Percent of non-opaque and non-micaceous detrital heavy minerals in Haymond sandstone.

Sample	Average Max. Grain Size ¹	ZIRCON				Rutile	Tour- maline	Garnet	Apatite	Alterite	Monazite	Sphene	Epidote?	
		Colorless Round	Metamict Round	Colorless Euhedral	Metamict Euhedral									
H - 14*	0.47	38	43		2			8		4	3	2		*based on 50 counts
H - 26	0.55	25	26	5	1	14	8*	6	4	5	4	2		*1% indicolite
H - 81	0.92	38	27	2	2	2	4	6	3	6	2	5	3	
H - 97*	0.78	19	34			1	3**	40	2	1				*sample has 64% barite not included in the data in the table. **1% indicolite
H - 100	0.80	17	19	2		1	2	51	2	3	3			

¹

This is the average of the 10 largest grain-diameters in the thin section.

showing only incipient rounding. Metamict (cloudy) and clear grains are equally abundant. Most clear grains are colorless but a few are pale pink.

Garnet occurs as the largest grains in the assemblage. Grains have angular projections typical of etched surfaces, and numerous grains are partly replaced by calcite.

Tourmaline occurs chiefly as subrounded grains larger than other grains except for garnet. Tourmaline grains are brown and yellow brown; a trace of purple (indicolite) grains is present.

Apatite, rutile, monazite, sphene, and epidote(?) occur as rounded and well-rounded grains that are, with the exception of some sphene, devoid of original crystal faces.

All slides from which counts were made contain a few grains that are so obscured by surface or internal alteration that they could not be identified. Such grains were tabulated as alterites.

Heavy minerals in the Haymond are those yielded chiefly by silicic igneous rocks and sedimentary rocks; minerals diagnostic of moderate to high-grade metamorphic and mafic igneous rocks are absent. Garnet is a possible exception, but its occurrence as an accessory mineral in cobbles of gneissic granite from the boulder beds indicates the mineral may be of igneous provenance. The high degree of roundness and sphericity of the tiny zircon grains in association with nearly unworn euhedral grains is evidence of at least two types of source rocks. The worn zircon grains were probably released from sedimentary rocks, whereas the euhedral grains are first-cycle from crystalline source rocks. Thus, more than one-half of the grains of each separation were contributed by older sedimentary rocks. The relatively large size of the garnet and zircon grains suggests they may be first-cycle; both occur as primary accessory minerals in schist pebbles collected from the boulder bed member. The sizes of the other heavy minerals yield no clue to their immediate source rocks, but rutile, apatite, and sphene also occur as accessory miner-

als in pebbles of basement rock collected from the boulder bed member.

CHERTY LIMESTONE BED

A unique limestone bed was found in the Dugout Mountain area (Loc. 4) at an unknown distance below the Gaptank Formation. The bed is approximately 3 feet thick, massive, and weathers dark orange brown. A summary description of the bed, which resembles the top portion of some thick turbidites in the Dimple in cuts along U.S. Highway 90, is given below and is illustrated in Plate 16, C.

Chertified silty limestone (spiculite?); calcite (50%), chalcedonic quartz (40%), quartz and feldspar silt (10%). Calcite includes the following: silt-sized micrite clasts (25%), slender spicule-like, slightly curved rods or plates with a maximum length of 0.4 mm (20%), euhedral rhombs of ankerite-siderite less than 20 μ in diameter that are largely replaced by hematite (5%), and a trace of spicules or spines.

The calcite plates or rods show a strong preferred orientation of long axes; the objects are probably spines or spicules. Quartz and feldspar silt grains are scattered throughout but are locally concentrated in probable burrowed zones. A sawed surface reveals a blotchy color mottling in the rock.

STRATIGRAPHIC PETROGRAPHIC VARIABILITY

Differences in mineralogy, both vertically and areally within a formation, can provide important clues to the position and composition of source areas and to the time of certain events (volcanic eruptions, new exposure of basement rocks by faulting, etc.). Field and thin-section inspection of Haymond sandstones reveals an obvious difference between the coarse sandstones and all flysch sandstones and between flysch sandstones of Dugout Mountain and all other areas. In order to evaluate apparent differences in mineralogy, and to look for subtle differences not apparent to inspection, a statistical test of comparison

TABLE 8.—Data of groups of Haymond sandstones used to test for stratigraphic differences in maximum grain size and mineral composition. Statistics are based on data where each mineral constituent tabulated by point-counting to equal zero percent was reported as 1 percent.

	Size(mm)	Cement	Matrix	Quartz	Plagioclase	K-feldspar	Total feldspar	SRF	MRF	Polyquartz
Dugout Mountain area										
SUM	1.64	57.00	104.00	385.00	119.00	35.00	156.00	43.00	12.00	9.00
SSQ	.47	799.00	3702.00	24811.00	2585.00	357.00	4278.00	389.00	32.00	15.00
\bar{X}	.27	9.50	17.33	64.17	19.83	5.83	25.76	7.17	2.00	1.50
S	.07	7.18	19.49	4.62	6.71	5.53	6.66	3.76	1.26	.55
n = 6										
Flysch above boulder beds										
SUM	5.26	86.00	313.00	1448.00	328.00	44.00	372.00	134.00	105.00	46.00
SSQ	.52	241.00	1914.00	40836.00	4068.00	87.00	4943.00	903.00	368.00	69.00
\bar{X}	.22	4.10	13.00	63.80	19.20	2.30	21.50	8.30	5.00	2.50
S	.07	2.85	4.99	3.82	6.51	1.95	5.97	4.88	3.62	.85
n = 10										
Coarse sandstone beds										
SUM	6.39	78.00	62.00	728.00	108.00	66.00	174.00	93.00	65.00	26.00
SSQ	5.26	906.00	464.00	49038.00	1292.00	498.00	3066.00	1069.00	605.00	90.00
\bar{X}	.58	7.19	5.64	66.18	9.82	6.00	15.82	8.45	5.91	2.36
S	.39	5.94	3.38	9.26	4.81	3.19	5.60	5.32	4.70	1.69
n = 11										
Flysch below boulder beds										
SUM	5.26	86.00	313.00	1448.00	328.00	44.00	372.00	134.00	105.00	46.00
SSQ	1.73	1032.00	5797.00	10058.00	5908.00	332.00	7434.00	1048.00	661.00	141.00
\bar{X}	.25	4.10	14.90	68.95	15.62	2.10	17.71	6.38	5.00	2.19
S	.14	5.83	7.52	6.10	6.26	3.39	6.50	3.11	2.61	1.47
n = 21										
All flysch beds										
SUM	7.44	127.00	443.00	2086.00	520.00	67.00	587.00	217.00	155.00	71.00
SSQ	2.25	1273.00	7711.00	50894.00	9976.00	419.00	12377.00	1951.00	1029.00	210.00
\bar{X}	.24	4.10	14.29	67.29	16.77	2.16	18.94	7.00	5.00	2.29
S	.12	5.01	6.78	5.93	6.46	2.97	6.49	3.79	2.91	1.30
n = 31										

Abbreviations and symbols: SUM = total of measurements; SSQ = sum of squares; \bar{X} = average; S = sample standard deviation; n = total number in sample; SRF = sedimentary rock fragments; MRF = metamorphic rock fragments; polyquartz = polycrystalline quartz.

was used to establish rigorously significant differences. For this study the average mineralogical composition of sandstone frameworks, matrix, and cement content, and maximum grain size¹¹ (table 8) were computed for the following groups: (1) flysch sandstones below the boulder bed member, (2) flysch sandstones above the boulder bed member, (3) all flysch beds (excluding Dugout Mountain beds), (4)

flysch sandstones of the Dugout Mountain area, and (5) coarse sandstone beds.

A comparison of each particular parameter was made by testing the null hypothesis that "there is no difference in the average abundance of item x between group A and B" using Student's T-test. If the hypothesis could be rejected at a level of significance of $p = < 0.05$, then an important difference is assumed to exist. Table 9 (in pocket) shows which parameters were tested and gives values for significant tests. Table 8 gives the mean values for the parameters tested.

The flysch sandstones of the Dugout

¹¹ The average of the ten largest grains in each thin section was used. Pettijohn (1957, p. 249) has shown that a straight-line correlation exists between the maximum and average grain size of gravel samples. Pelletier (1958) and Yeakel (1962) have shown that the average of the 10 largest pebbles in an outcrop can easily be used to study areal differences in grain size.

Mountain area have, on the average, the greatest amounts of K-feldspar, total feldspar, and cement among flysch sandstones and the only carbonate fossils and carbonate rock fragments of sand-size in the formation. In other respects, the Dugout Mountain beds are not significantly different from other flysch beds.

Another striking difference is between the flysch beds (excluding the Dugout Mountain area) and the coarse sandstone beds. The latter are significantly coarser than flysch beds (average of 0.58 mm compared to 0.24 mm) and have more K-feldspar but less matrix, plagioclase, and **total feldspar**. Visual inspection shows that they also have more calcite cement, micas, and **large chert grains**.

A comparison of flysch sandstones below the boulder beds with those above shows that a decrease in quartz (from 68.9 to 63.8 percent) is the only significant difference.

The mineralogic differences noted can be due to any one or a combination of the following: (1) differences in grain size, (2) geographic differences in source area, and (3) differences in source area with time (secular differences). Data available show that different geographic source areas account for the chief compositional differences of the Dugout Mountain beds. Differences in grain size were thought to account for the differences between coarse sandstone beds and flysch sandstones, but this is not borne out by statistical data (table 9). The cause of the decrease in quartz upsection in the flysch beds is not apparent. It must be kept in mind that the statistical significance test was applied to mineral *percentages*, and a percentage system is a closed system in that all ingredients must total 100 regardless of the size of the sample. It is possible that a chance increase in three ingredients (for example, K-feldspar, plagioclase, and SRF) could lower the quartz percentage sufficiently to yield a positive test for significance, the cause of which may not have been important.

The comparisons made above were for the *average* values of parameters from

groups of sandstones. Gradual secular changes are not brought out by this method. In order to look for vertical changes in mineralogy and grain size, vertical variability diagrams were constructed for three measured sections. Percentages of quartz, plagioclase, K-feldspar, SRF, MRF, and the average grain size of each sample were plotted at the stratigraphic positions from which samples were collected, and tie-lines drawn between samples. Visual inspection of the variability diagrams attests to the remarkable uniformity in mineralogy and texture that was predicted from field work; no consistent secular trends are apparent.

In order to determine the dependency of mineralogy on grain size, correlation coefficients (r) were calculated for the relation between average maximum grain size and the following: matrix, cement, quartz, plagioclase, K-feldspar, total feldspar, MRF, SRF, and polycrystalline quartz. Correlation coefficients testing the **interdependence of these pairs** (and all other pair combinations) were made for the following sample groupings: Dugout Mountain beds, flysch above the boulder beds; flysch below the boulder beds, all flysch beds; coarse sandstone beds, all Haymond beds. Inasmuch as computations cannot be made for samples wherein an ingredient is absent (i.e., zero percent), it was necessary to consider each ingredient tested to comprise at least 1 percent of the sample. False data were recorded for cement, K-feldspar, SRF, MRF, and polycrystalline quartz for several samples; however, inasmuch as these ingredients are present in most thin sections, although in trace amounts, this procedure of modifying the data is not sufficiently drastic to change the results. All computations¹² were made by a CDC 1604 computer operated by the Computation Center, The University of Texas. Table 10 lists the paired parameters that show significant correlation values at the 0.05 level of significance and indicates whether the correlation is positive (direct) or negative (inverse).

¹² Employing program ZITZ, on file in the Department of Geology, The University of Texas.

TABLE 10

Pairs of petrographic parameters of Haymond sandstone that show significant correlation values (r) at 0.05 level of significance. (+) = direct correlation, (-) = inverse correlation. Parameters that were tested for correlation are: maximum grain size, cement, matrix, quartz, plagioclase, K-feldspar, total feldspar, SRF, MRF, and polycrystalline quartz.

Dugout Mountain area	(+) Size - Cement			
	(-) Size - Matrix			
	(-) Cement - Matrix			
	(+) Plagioclase - Matrix			
Flysch above boulder bed member	(-) Size - Matrix	(-) Total feldspar - SRF		
	(-) Cement - Matrix	(-) Cement - Polyquartz		
	(+) Plagioclase - Total feldspar			
	(-) Plagioclase - SRF			
Coarse sandstone beds	(+) Plagioclase - Total feldspar			
	(+) Quartz - SRF			
	(+) Polyquartz - K-feldspar			
	(+) Polyquartz - Total feldspar			
Flysch below boulder bed member	(-) Size - Matrix	(-) Quartz - Total feldspar		
	(+) Size - Quartz	(+) Plagioclase - Total feldspar		
	(+) Matrix - Plagioclase	(+) MRF - SRF		
	(-) Quartz - Plagioclase			
All flysch beds	(-) Size - Matrix	(-) Matrix - K-feldspar	(-) SRF - Total feldspar	
	(-) Plagioclase - Quartz	(-) Total feldspar - Polyquartz	(+) MRF - SRF	
	(+) Size - Quartz	(+) Total feldspar - Plagioclase		
	(+) Plagioclase - Matrix	(-) SRF - Plagioclase		
All Haymond beds	(-) Size - Matrix	(+) Matrix - Total feldspar	(-) Quartz - MRF	(-) Plagioclase - SRF
	(-) Size - Plagioclase	(-) Quartz - Plagioclase	(-) Quartz - Polyquartz	(-) Total feldspar - SRF
	(-) Cement - Matrix	(-) Quartz - K-feldspar	(-) Plagioclase - K-feldspar	(-) Total feldspar - Polyquartz
	(+) Matrix - Plagioclase	(-) Quartz - SRF	(+) Plagioclase - Total feldspar	(+) SRF - MRF
	(-) Matrix - K-feldspar			

In only one sample group (all Haymond beds) does grain size correlate with mineralogy; plagioclase is inversely related to grain size. All groups but one show an inverse correlation of grain size with matrix, **a situation that is apparent by inspection.** It is concluded that grain size is not an important factor controlling mineralogic differences between flysch sandstones and coarse sandstone beds.

Inspection of table 10 shows that significant correlation exists between ingredients that could be predicted to be correlative owing to nature of the closed system of data reported by percentage, and also other

correlations that would not be predicted and for which no geologic interpretation is apparent. The former situation is shown by the inverse correlation between quartz and each of the following: plagioclase, K-feldspar, SRF, MRF, and polycrystalline quartz in the "all Haymond beds" group (i.e., the greater the amount of quartz in a sample, the less there can be of one or more other constituents). The latter situation is exemplified by the positive correlation of matrix with both plagioclase and total feldspar and the negative correlation of matrix with K-feldspar.

DIAGENETIC FEATURES

Diagenesis includes all changes that take place in a sediment or sedimentary rock from immediately after the time of deposition to the time that weathering begins. Most diagenetic changes of Haymond rocks have been mentioned previously in this report so that only a summary is presented here.

Physical diagenesis.—Compaction and induration are the most significant sedimentologic changes that Haymond sediments have undergone. Tectonic deformation including folding, jointing (Pl. 19, D), and faulting of beds is well developed but has not been responsible for many mineralogic changes. Compaction has decreased the original thickness of shale beds by expulsion of connate water (thereby destroying all original porosity) and caused many soft rock fragments in sandstones to be flattened (Pls. 14, C, and 18, D) by more resistant neighboring grains.

Slumping prior to consolidation resulted in the formation of microfaults in sandstone, folding of sandstone and shale beds, and physical mixing of the constituent grains of clay and sand beds to form mudstone.

Mineralogical diagenesis.—Mineralogic changes include precipitation of cement in pores, pressolution (solution induced by pressure at grain contacts, Pl. 18, C), and reprecipitation, replacement and recrystallization of minerals, growth of new miner-

als, weathering, and possible intrastratal solution.

Minerals that occur as pore-filling cement in Haymond sandstones in order of abundance are: quartz, calcite, kaolinite (Pl. 19, A, B), hematite (Pl. 18, D), chalcedony (in chert), and possibly barite.

Replacement phenomena include the partial replacement of feldspar grains by carbonate minerals (Pl. 19, C) and kaolinite.

Recrystallization is indicated in some carbonate rock fragments in calc lithic sandstones in the Dugout Mountain area and most probably took place in some clay particles in the shales and matrix of sandstones.

The following minerals are present as authigenic grains in occurrences other than as cementing agents: calcite, ankerite-siderite (Pl. 18, D), pyrite, kaolinite, barite, and hematite.

Intrastratal solution (solution by migrating fluids prior to weathering) is suggested by the etched surfaces of garnet grains observed in heavy mineral mounts, but the process has not been extensive.

Combined physical and chemical diagenesis has produced indurated sandstones and shales that are devoid of intergranular porosity and permeability. The formation is considerably fractured, but the Haymond is not known to be a reservoir rock for either water or hydrocarbons.

DEPOSITION OF THE FLYSCH FACIES

PREVIOUS INTERPRETATIONS

The problems that early workers faced in interpreting the environment of deposition of interbedded Haymond sandstone and shale were similar to those encountered by students of all flysch sequences prior to 1950. The general absence of marine fossils, the abundance of land plants, and the presence of sandstone beds were considered unquestionable evidence for shallow water. This evidence led Baker (1932, p. 581) to suggest that the Haymond was of deltaic origin and P. B. King (1937, p. 89) to suggest that the sandstones and shales were laid down in brackish or fresh water and that couplets of sandstone and shale might be varves. In 1950 Kuenen and Migliorini recognized that marine turbidity currents were capable of transporting sands far from shore into deep water and suggested that interpretations of shallow-water origin for flysch units in general should be reconsidered.

In *The Ouachita System* (Flawn et al., 1961) both Flawn and King suggested that the Haymond was deposited in deep water. Flawn's interpretation (p. 54) was based chiefly on world-wide evidence that flysch deposits in general are deposited in deep-water troughs between tectonic ridges. King (p. 184) argued similarly but also noted that sedimentary structures suggested that much clastic material in both the Tesnus and Haymond favored deposition by turbidity currents in "moderately deep to very deep water." A few years earlier, in a discussion of the origin of the boulder beds, King (1958, p. 1734) mentioned that he favored deposition of the Haymond in a "deep, rapidly subsiding trough" in contrast to his first interpretation. From analogy with other flysch sequences, Goldstein and Hendricks (1962, p. 419) speculated that Haymond sandstones were deposited by turbidity currents.

PRESENT INTERPRETATION

In this report the shales of the flysch

facies are interpreted as having accumulated slowly as pelagic layers in a deep-marine basin into which turbidity currents periodically deposited sand beds. Although the interpretation cannot be proved by any single criterion, it best explains the combination of association of rock types, absence of sedimentary features and fossils that occur only in shallow water, thickness and extent of the formation, and tectonic setting at the time of deposition. The most compelling evidences that the sandstones are turbidites (that is, deposited by turbidity currents) are: (1) they are interbedded with shale that is best interpreted as a deep-water deposit, and (2) internal structures suggest that they were deposited by waning currents that initially had high velocities. In addition, the sandstones have groove and flute casts, graded bedding, convolute lamination, and slump structures—an assemblage of features that is common in other turbidites.

(1) The interpretation that the Haymond flysch sediments accumulated in deep water is based on (a) the presence of quiet-water muds (shales), (b) the lack of textures or structures that form only in shallow-water environments, such as large-scale cross-beds, mud cracks, wave ripple marks, etc., and (c) the absence of shallow-water fossils in the shales—land plant fragments can float, and mud-burrowing animals have been found in modern oceans at abyssal depths. The latter two lines of reasoning employ negative evidence, but they are important aspects where no reliable faunal depth indicators are present. Thus, although definitive depth criteria are lacking, evidence favors the possibility that the basin was several hundreds of feet and possibly several thousands of feet deep. It is not assumed that the depositional basin was everywhere the same depth at all times; certainly the part of the basin along the structural axis was deeper than the flanks. A shallowing of the basin late during deposition of the Haymond is suggested by the presence of well-burrowed

beds in the youngest flysch exposed above the boulder beds at the base of Gap Peak (Loc. 10B) and by the assemblage of structures (ripple marks, intensely burrowed sandstones, possible spring pits) of the Alhson Ranch facies. The overlying Gap-tank further records conditions of successively shallower-water deposition (Ross, 1963; McBride, 1964b).

(2) Sequences with bedding types similar to Haymond sandstones have been described as typical of turbidites (Bouma, 1962; McBride, 1962). The types of structures produced under different regimens in hydraulic flume experiments support the concept that the common sequence of structures in alleged turbidite beds is the result of deposition from a current of waning velocity (McBride and Kimberly, 1963, p. 1852). Although the complete sequence of graded (or massive)-laminated-cross-laminated-convolute-laminated structures has not yet been produced experimentally, it has been shown (Gilbert, 1914, pp. 32–33; Simons and Richardson, 1961) that horizontal laminae (plane-bed forms) develop during higher velocities than cross-laminae (ripple-mark forms) if all other variables remain constant. In the Haymond, cross-laminae always overlie horizontal laminae where both are present in the same bed. Extrapolation of these data suggests that the structures present in a bed were not produced by currents separated in time but were the product of a current that changed its flow characteristics (regimen) as its velocity decreased. Convolute laminae of the type found in turbidites have not yet been produced in flumes, so the exact hydrodynamic significance of the structure is unknown. Numerous authors (ten Haaf, 1956; Sanders, 1960; Dzulinski and Walton, 1963) have speculated on how it forms and there is agreement that it is formed during deposition of a turbidite layer and is caused directly or indirectly by forces generated by the turbidity current.

The reason for the difference in bed sequences shown by sandstone beds is uncertain. Bouma (1962, pp. 50–51) suggested that partial sequences are the product of two turbidity currents that flow to-

gether and interfere, or the sudden diversion of a turbidity current to follow a new path, or the erosion of part of one turbidite by a later current.

Sanders (1965) suggested that much sediment transported by fast-moving turbidity currents is not carried in turbulent suspension but moves as "bed load" in the form of flowing-grain layers or moving viscous suspensions. Sanders would apply the term turbidite only to that part of a bed known to have been deposited by a "density current caused by turbulently suspended sediment." He gives criteria whereby such beds can be recognized, but several concepts have not yet been documented in flume experiments. In view of the uncertain hydrologic significance of massive bedding and other structures, in this report the term turbidite is applied to all sediment inferred to have been deposited by currents that were generated as suspended-sediment turbidity currents.

Comparison with Bouma's turbidite model.—From a study of turbidites in several formations in Europe, Bouma (1962) proposed a type sequence of structures that characterized the ideal turbidite. From bottom to top they are: (a) graded or massive layer; (b) laminated layer; (c) cross-laminated and/or convolute layer; (d) laminated layer; and (e) pelite layer. The pelite layer is the accumulation of fine material that settles out of suspension from the dying current and is distinct from the overlying pelagic layer. Since Bouma's type sequence (or model) has been used as a standard reference, the relation of Haymond sequences to the model should be mentioned. The typical discernible Haymond sequence includes only layers (a), (b), and (c) of Bouma's model. Laminations of layer (d) have not been observed, except for the laminae that smooth out the surface of convolute laminae, and these do not exceed 2 mm in thickness. Bouma's layer (e) has also not been observed, with the exception of an interval approximately 2 mm thick where graded beds pass into shale. In contrast to the sharp basal contact of sandstone (turbidite) on shale (pelagite), the top of graded beds cannot be lo-

cated more precisely than the thickness of the gradational interval. It is a moot question, however, as to what part of the shale represents the last clay that settled out of the turbidity current versus the portion of pelagic clay. In the Haymond it is extremely difficult to examine the upper parts of graded beds because they generally spall off with the overlying shale. Dean and Anderson (in press) suggested that more than 50 percent of the shale beds were deposited by dying turbidity currents.

Problems.—Problems common to an explanation of turbidites of the Haymond and other flysch formations include an explanation for the triggering mechanism of the turbidity currents, the direction and distance the currents traveled, and whether **there are sandstone beds in the section that were deposited by currents other than by turbidity currents.**

Earthquakes are important triggering agents for large recent turbidity currents (Heezen and Ewing, 1952, 1955), and it is likely that they played a major role in starting turbidity currents during Haymond deposition. Flysch basins in general are tectonically unstable.

The direction that turbidity currents traveled can be determined by mapping **directional current-structures.** Because of meager knowledge of paleogeography during deposition of Haymond sediments, it is impossible to determine how far individual turbidity currents traveled. A minimum distance can be determined for any bed that can be correlated from one outcrop to the next. The only diagnostic beds in the Haymond that have been so correlated are the calcarenites of Dimple lithology and the nine sandstone beds recognized by Dean and Anderson (in press). The calcarenites are now separated by 6 miles and the sandstones by 5 miles, although the original distances were somewhat greater prior to crustal shortening. Another estimate of minimum distance is given by the distance from the edge of the present Haymond outcrop to the inferred center of the sedimentary basin; present distances are from 1 to 7 miles.

According to the interpretation pre-

sented here, each sandstone bed which has a sequence of internal structures, either partial or complete, was deposited by a turbidity current during a nearly instantaneous geologic event. In contrast, each shale bed represents sediment that settled out of suspension slowly and records deposition over thousands of years. Thin sections of shale reveal layers of silt or fine sand that are less than 1 mm thick. These laminae are structureless except for rare graded bedding, and it is uncertain whether such layers are feather-edges of turbidity-current deposits or material that settled out of suspension following severe storms.

Hsu (1964) has pointed out that the abundance of ripple-marked and cross-laminated tops of sandstone beds in some flysch formations suggests that strong marine bottom currents were able to rework turbidite layers. Evidence for the existence of deep-sea currents with velocities up to 40 cm/sec have been measured, and photographs of ripple marks and current-scour features suggest even greater velocities (Heezen and Hollister, 1964). Hsu also questioned whether turbidity currents are capable of forming cross-laminae. That turbidity currents can deposit small-scale cross-beds is accepted by many investigators (Kuenen, 1953, p. 1052; Bouma, 1962, p. 97) and, in fact, is proved for beds in which convolute layers are formed of and interlayered with cross-laminae. Some of the latter show oversteepened cross-laminae truncated and overlain by undeformed cross-laminae. If it is accepted that such convolute laminae form during deposition from a turbidity current, then the cross-laminae interlayered with them must have formed at the same time.

The problem that remains is whether it is possible to distinguish cross-laminae formed by a turbidity current from cross-laminae formed by other bottom currents. Hsu (1964) suggested that clean, well-sorted sandstones and beds several inches thick that are cross-laminated throughout are probably reworked beds. Relatively well-sorted sandstones occur in the Allison Ranch facies but are not known in the

flysch facies. However, many thin flysch sandstones, including beds as thick as 4 inches, are cross-laminated throughout. It is not denied that such beds in the Haymond may not be reworked turbidites; however, it is important to note that many sets of cross-laminae in these beds (and in most Haymond flysch sandstones) are the climbing-ripple type. It is generally agreed that this type of cross-bedding forms under conditions of rapid deposition of sediment;¹³ hence ripple avalanche-faces climb the stoss sides down-current from them. These are exactly the conditions that should exist during deposition from a turbidity current. The writer accepts Hsu's contention that bottom currents can rework turbidite layers and produce cross-laminae but maintains that except for well-sorted beds, the evidence seldom permits such beds to be distinguished from unreworked turbidities. For the Haymond specifically, it is likely that bottom currents reworked the tops of some turbidite layers, but it is uncertain how widespread this event was.

Allison Ranch facies.—As mentioned previously, the better sorting and intensely burrowed character of sandstone beds in

the Allison Ranch facies suggest the shallowest deposition which prevailed during accumulation of the Haymond. Relatively shallow conditions are also supported by the questionable spring pits or gas rings and the apparent upward gradation of the facies into the shallow-water Gaptank Formation. Evidence of the depth range is lacking. No evidence of subaerial conditions or wave action is present.

The agent of deposition of the sandstone beds in this facies is uncertain. The fact that many beds have groove casts and that many beds show the upward sequence of laminations overlain by small-scale cross-bedding similar to many flysch sandstones indicates that the beds may also be turbidites. However, beds have equally sharp upper and lower contacts and are not graded. Such a situation would be expected, however, if bottom currents reworked and sorted the top part of a turbidite layer. It can only be stated that the sandstones were deposited by currents (with characteristics of upper and lower flow regimes) in an environment where soft-bodied animals burrowed actively and where the water was not favorable to open-marine forms of life.

¹³ Sanders (1965) termed this deposition by "traction plus fallout."

ORIGIN OF THE BOULDER BEDS

REVIEW OF PREVIOUS INTERPRETATIONS

The origin of the boulder beds, particularly those south of U.S. Highway 90, has been a controversy since their discovery in 1930. The history of their discovery and the subsequent controversy have been summarized by P. B. King (1958). Of the many investigators of the boulder beds, only Hall (1957, 1959) has argued that they are entirely tectonic in origin, representing the denuded cores of faulted folds. Hall's interpretation has been criticized by King (1958) and Flawn (1958). The writer agrees with King (1932; 1937, p. 90; 1958, p. 1732) that the boulder beds "west of Housetop Mountain show so clearly the sedimentary interbedding of the characteristic thin-bedded sandstones and shales of the Haymond Formation with the arkoses, boulder-bearing mudstones, and chert breccias of the boulder bed member that no special defense need be offered for the sedimentary nature of the deposit." The stratigraphic evidence in the northern part of the Basin is equally compelling.

Although all published descriptions of the boulder beds except that of Hall recognize the sedimentary origin of the unit, there has been disagreement among investigators as to the derivation of the large blocks and their mode of emplacement. Baker (1932) and Carney (1934) both favored a glacial origin for the boulder bed complex. Carney published only an abstract of the results of his study before his death. Baker concluded, and recently reaffirmed (personal communication, 1962), that the large blocks most probably were transported by ice rafts to their site of deposition. He suggested that some of the complex stratigraphy of the boulder bed interval might have been produced in part by the grounding of large blocks of ice in shallow water and subsequent shedding of detritus on melting. Baker (1932) described the presence of "soled" and striated pebbles in the boulder beds but noted that

they are not conclusive evidence for glaciation. Powers (footnote in Van der Gracht, 1931, p. 1040) considered the entire boulder bed complex to be a deltaic or beach deposit.¹⁴

Although his views have changed somewhat since his earlier reports, King has consistently argued for a non-glacial sedimentary origin of the beds, and his views have been supported recently by Flawn (1958; in Flawn et al., 1961, pp. 184-185). King (1937) originally suggested that the flysch facies was laid down in brackish or fresh water (p. 89) and that the boulder beds in the eastern part of the Basin were deposited as a series of mudflows which spread out along the northwest base of advancing overthrust blocks, and that the boulder bed in the north was probably an outwash of debris spread in front of a large mudflow (p. 92). In the intervening years much has been learned about the sedimentary and tectonic history of geosynclines. More recently, King (1958; in Flawn et al., 1961, pp. 184-185) suggested that the Haymond was deposited in (1958, p. 1734) "a deep, rapidly subsiding trough, with tectonically unstable, probably faulted margins," into which turbidity currents carried sands and that "the blocks, boulders, well-rounded cobbles, and muds were carried from the unstable shelves in subaqueous landslide which developed proximally into turbid flows." This interpretation, with slight modifications, best explains the features of the flysch sandstones and boulder beds and is compatible with the evidence of strong tectonic disturbances of intermittent catastrophic character.

BOULDER BEDS SOUTH OF U. S. HIGHWAY 90

Origin.—The unusual textures in the boulder bed member are best explained as

¹⁴ Following a brief description of the boulder beds, Van der Gracht stated, "Sidney Powers believes the entire deposit is a deltaic or beach formation." The context implies Powers' statement referred only to the boulder bed complex and not to the entire Haymond Formation.

the product of (1) submarine slumps and mudflows and (2) soft-sediment deformation produced during emplacement of erratic blocks of moderate to gigantic size. Crowell (1957) demonstrated that many pebbly mudstones originate when gravel transported by turbidity currents is laid down on soft, water-saturated mud, then becomes unstable, slumps downslope, and mixes with mud. A similar origin for some of the pebbly mudstone beds in the Haymond is likely, although the successive stages described by Crowell are not completely recorded in the Haymond. The large blocks in the Haymond are too heavy to have been transported by turbidity currents. It is inferred that blocks of Paleozoic formations were sloughed from submarine thrust-fault scarps, as suggested by King (1958, p. 1734), slid downslope through unconsolidated sand and clay, and churned the sediments into dense mud that moved with the blocks and buoyed them during movement. The largest blocks must have moved by sliding, whereas smaller cobbles and boulders may have been carried in suspension in mudflows. As emphasized by Crowell (1957), a continuous series is envisaged between turbidity currents, slumps, and slides of gigantic proportions in subaqueous environments, so it is not always possible to infer the exact transporting mechanism of individual beds. Deposits of all such mechanisms, in addition to beds ripped up and churned by the large blocks as they came to rest, are probably represented in the boulder bed sequence. The presence of numerous recognizable sedimentation units shows that there were many episodes of submarine slumping and sliding followed by periods of normal deposition of flysch-facies beds and coarse sandstone.

Source of large fragments.—The writer agrees with King that the fragments of Paleozoic rock were derived from high-standing thrust blocks. The occurrence of chert and novaculite breccia boulders, the presence of slickensided surfaces on boulders, the mammoth size of the large blocks, and the presence of fragments of formations that normally lie 3,000 to 10,000 feet

stratigraphically below the boulder beds favor this interpretation. It cannot be determined whether the fault scarps were submarine or subaerial, but blocks dislodged from submarine scarps seem more likely to have generated submarine slides.

The distance that the erratic and exotic blocks traveled is likewise uncertain. Their proximity to the eastern edge of the basin suggests the source was in that direction. King (1958) and Flawn (1958) have suggested that some boulders may have come from western sources; boulders of Dimple and Maravillas limestone in the boulder beds more closely resemble exposures west of their present occurrence, and granite is also known in the basement to the west. However, a westerly source is unlikely in view of the paleobathymetry inferred from paleocurrent data (p. 54). The deepest part of the geosyncline during most of Haymond deposition was to the west of the boulder bed exposures. Furthermore, paleocurrent data from turbidites above and below the southern boulder beds show the paleoslope was to the west. It can only be concluded that the blocks came from beyond the present limit of surface outcrops of Paleozoic rocks in the Marathon Basin, a distance of from 1 to 12 miles. The inferred water depths of the Basin during Haymond deposition is that encountered today several miles or tens of miles from shore.

Striated and flattened gravel.—Baker (1932) and King (1937, p. 66) have recorded the presence of striated and flattened pebbles and cobbles in the boulder bed interval, and Baker (p. 595) believed some of the pebbles with flat sides were probably till stones. King (p. 91) noted that most fragments with flat surfaces owe their shape to joints within the rock, and during this study no pebbles with flat surfaces were found that did not appear to have a similar origin. The only striations observed, except for slickensides, are on highly polished pebbles (Pl. 12, C, D) embedded in mudstone. The polished areas cover up to 75 percent of the surface area of the pebbles, but striations cover only a few square millimeters. The striations are

all parallel shallow markings mostly less than 5 mm long. Baker, however, reported (p. 586) **intercrossed striae on one pebble**. As noted by Baker (p. 595), no particular significance need be attached to "scratched, grooved, soled and polished pebbles in strata which have been compacted and strongly tilted during severe deformation ... because such phenomena can be caused through interstitial movements grinding together, under great pressure, the pebbles and boulders." All striated and polished pebbles collected by the writer were embedded in mudstone layers; no polished or striated pebbles were found in sandstone matrix. Judson and Barks (1961) studied striations on pebbles of many ages and from numerous Recent environments and concluded that "parallel microstriations" must be formed during compaction tectonism. In the Haymond, the presence of polished and striated pebbles only in the strongly compactable mudstone layers strongly supports the origin of the features by similar means. Quartz, feldspar, and chert silt grains in the mudstone were the probable abrasive and polishing grains.

Source and genesis of well-rounded gravel.—The rounded gravel-size exotic rocks in the boulder beds present a problem as to their source, the environment in which they were rounded, and how they were incorporated in the boulder beds.

The same evidence for an easterly source for the blocks of Paleozoic age argues for a similar source for the exotic gravel. Sand-sized fragments of most lithologies represented by the gravel clasts also occur in turbidite sandstones that had an easterly source.

The gravel particles were obviously abraded during stream transport or on a beach prior to their deposition in the boulder beds; the pebbles are well rounded, and some have an unusually high sphericity (Pl. 11, D). Unpublished work by R. L. Folk (personal communication, 1963) and published data (Blatt, 1959) show that vein quartz pebbles larger than 6 mm tend to abrade to rod-shaped particles in a fluvial environment and to disc-shaped pebbles in a beach environment.

Unbroken vein quartz pebbles were collected from the boulder beds, their axes measured with a caliper, and the data plotted on Sneed and Folk's (1958) shape diagram. The plot of 150 pebbles from the Haymond cluster in a field typical of stream-abraded pebbles (fig. 13). Theoretically, only structurally isotropic pebbles show shape differences similar to vein quartz pebbles, so that other lithologies could not be similarly studied. It is concluded that vein quartz pebbles in the Haymond were rounded in streams and then transported into deeper water before they underwent sufficient beach abrasion to impart beach characteristics to them. It seems likely that other crystalline rocks had a history similar to the vein quartz.

Whereas the blocks of Paleozoic rocks were most likely shed directly from fault scarps, the exotic gravel was not. The gravel could have reached its ultimate site in the boulder bed by either (1) having traveled as slide debris from a starting point in shallow water or (2) having been first transported into deep water by turbidity currents, then scattered in mudstone during later slumping. The well-rounded gravel clasts in the Haymond probably do not exceed the maximum size that can be transported by turbidity currents; most are no larger than clasts in inferred turbidity-current-laid conglomerates in California and elsewhere (Crowell, 1957). In either case, gravel transported from the sourcelands to the east must have been initially deposited close to or at the shoreline of the Marathon Basin and subsequently dislodged, probably by earthquakes, and carried seaward by turbidity currents or slides. During this time the sourceland must have had a steep gradient to the sea, and possibly a rocky shoreline.

BOULDER BEDS IN CLARK BUTTE AREA

Mudstone beds and large slump features, common in the boulder beds to the south, are absent in the Clark Butte area. The size of the larger boulders here indicates they were not transported by normal marine currents. It is likely that the boulders and

associated pebble-size debris were emplaced as submarine slides. The presence of chalcedony cement in the pores of several boulder-bearing chert conglomerate beds is a feature difficult to explain in a slump deposit. Chalcedony generally occurs as a diagenetic pore-filling cement, whereas the spaces between gravel particles in slumped beds are filled by a finer-grained matrix of mud or sand as, in fact, most Haymond beds are. It is possible that a matrix existed at the time of deposition and was later winnowed out, or, less

likely, that chalcedony entirely replaced all original matrix constituents.

Although the boulder beds in this area cannot be traced into those to the south, their uniqueness in the Haymond suggests the beds in both areas formed from catastrophic events that simultaneously affected both areas. The character of the coarse sandstones intercalated with the boulder beds in this area suggests the basin was shallower here than in the area of boulder deposition to the south.

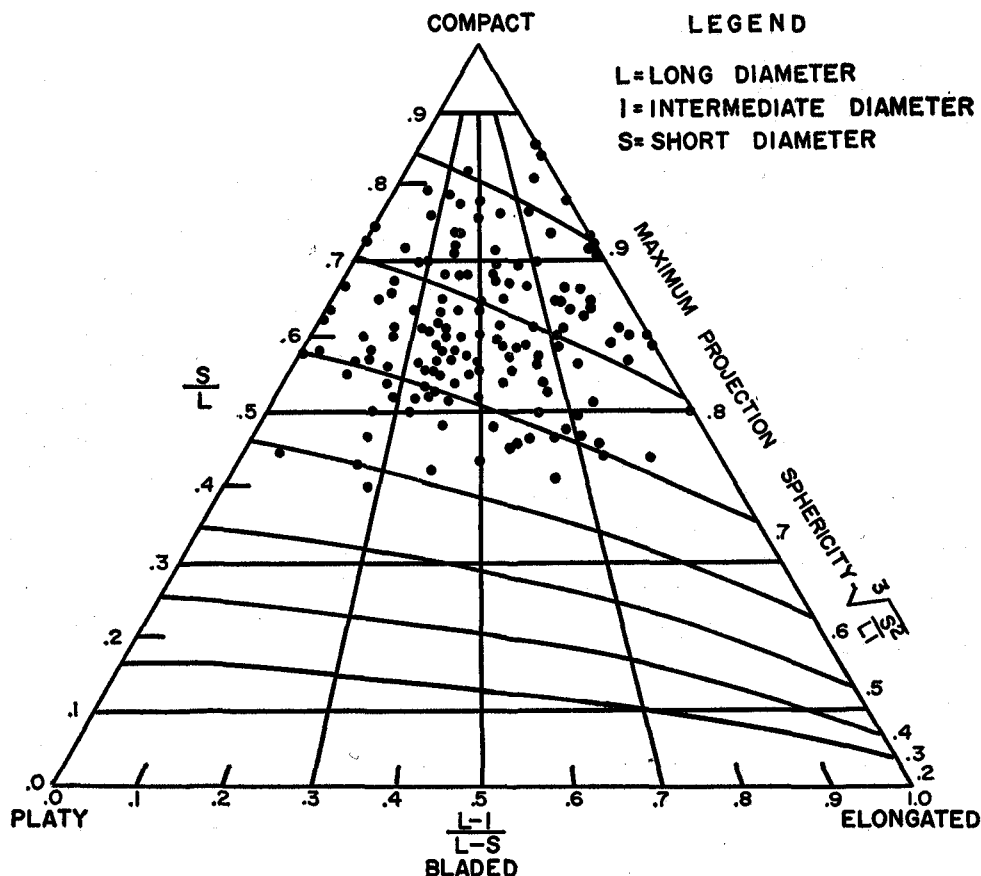


FIG. 13. Plot of shapes of vein quartz pebbles from the boulder beds south of U. S. Highway 90.

DEPOSITION OF THE COARSE SANDSTONE BEDS

The agent of deposition of many of the coarse sandstone beds is uncertain. Thin beds have structures similar to flysch sandstones and for similar reasons are interpreted as turbidity current deposits. Thicker beds, however, differ from typical turbidites in that some occupy channel-fills, are massive or crudely laminated, and lack sole marks and convolute lamination. On the other hand, some are crudely graded, and some are intercalated with typical turbidites. Thus, from their stratigraphic position interbedded with probable deep-water deposits, the inference is that they too must have been deposited in deep water. The only contrary evidence is (1) the channeled bases of some beds, which are irregular surfaces of only a few feet of relief, and (2) several festoon cross-beds up to 2 feet thick that occur between the two boulder-bearing conglomerate beds in a small hill south of Clark Butte (Loc. 18A). Channels in turbidity current deposits have been described (Wood and Smith, 1959), although they are not common. Channelways have been found on the Atlantic sea floor in areas traversed by modern turbidity currents, although the sediments have been studied only in a few widely spaced cores. Thus, the low-relief channels in the coarse sandstone beds do not necessarily preclude a deep-water interpretation.

Festoon cross-beds as great as 2 feet thick are typical of river and tidal channels and tidal flats traversed by swift water. The scarcity of shale in this part of the section in the Clark Butte area suggests that the rate of accumulation of coarse sandstone

and associated boulder beds was fast, and it is possible that sediment built up so rapidly that it produced shoal water where tidal currents were effective sediment movers. Shoal conditions can also account for the apparent winnowed chalcedony-cemented boulder-bearing chert conglomerates that occur 50 feet lower in the section. The scarcity of such conglomerates and of festoon cross-beds indicates that shoal conditions existed only a short time; normal deep-water flysch beds occur above and below the problematic sequence.

The greater part of the coarse sandstone beds are laminated or massively bedded. Possible modes of transportation of laminated and structureless sediment include creep, mass slumps, and masses of sediment that moved with characteristics intermediate between slumps and turbidity currents (fluxoturbidites). Dill (1963) described the slow creep of sand down steep submarine canyons off California, although it is not known what type of bedding forms in the sand. Creep requires slopes steeper than are encountered in most areas of the sea floor, however. Some coarse layers of sediment in other flysch deposits have been interpreted to be fluxoturbidites (Dzulinski et al., 1959, p. 1114; Thomson and Thomasson, 1964), and it is probable that some massive layers in the Haymond are deposits of this kind. Thick laminated beds are an additional problem, because most laminae in sands form during upper flow-regime conditions (Harms and Fahnestock, 1964), which suggest high-velocity currents.

PALEOCURRENTS

Numerous sedimentary structures in Haymond sandstones provide information on the direction of current flow when the beds were deposited. The orientation of flute and groove casts, flute-lineation casts, and parting lineation were recorded wherever possible in order to determine the regional paleocurrent pattern of sediment transport. Readings were not taken on cross-laminae because of the difficulty in obtaining accurate readings on the small sets in the field or on the few rare ripple marks. The predominant current trend was determined for all beds; a single reading was taken for each bed recorded, even where more than one directional feature was present.

Because of their symmetry, groove casts and parting lineation give an orientation but not a direction; hence, in some beds the dip direction of cross-laminae was used to determine the down-current direction of the orientation. It is assumed that few beds were reworked by bottom currents to produce cross-laminae dips that indicate directions opposite those actually followed by turbidity currents. Because the beds had been deformed during Late Pennsylvanian time, the orientation of structures in the field had to be corrected for post-depositional tilting. This was done in the following manner: a strike line was marked on the sandstone sole; a 5 × 7-inch sheet of plexiglas was placed parallel with bedding and its long edge aligned along the strike-line; a pencil held in place by rubber bands was oriented parallel with the directional sole marks; the plexiglas sheet was then rotated to a horizontal position using the strike-line as a hinge-line; and the orientation of the pencil was measured with a Brunton compass. This corrects for post-depositional tilting around an axis parallel to strike only; inasmuch as folds in the Haymond have gentle plunges, other rotational movements are assumed to be negligible. Beds in overthrust plates may have been rotated somewhat from their original position, but it is unlikely that this un-

corrected error is more than a few degrees.

The orientation of directional features is shown graphically in Plate 25. On each diagram the orientation of parting lineation, groove casts, and flute-lineation casts is shown in the outer circle; groove casts for which the direction is known from cross-laminae and flute casts are shown in the middle circle; and plant fragments are shown in the inner circle.

In order to show the regional current trend, the modal current direction or directions of each locality are shown in figure 14. For this map, only data from flute casts and groove casts whose current sense was ascertained from associated cross-laminae were used. Multiple arrows that diverge from a common point represent a fan-wise spread of directions, whereas arrows that are not connected at their ends represent individual modes at the same station. On the paleocurrent map, the arrows point in the direction of current flow, and the thickness of each arrow is proportional to the number of readings it represents.

The assumptions are made that Haymond turbidity currents move downslope; that the modal current directions define regional slopes, although the orientation of submarine canyons and irregular submarine topography may produce local slope anomalies; and that upslope directions led to source-land masses. The paleocurrent map yields the interpretation that the chief source area lay to the east-southeast of the Marathon Basin, although there were significant contributions from the northwest. Along the entire eastern edge of the Basin, currents flowed toward the west; this includes directions ranging from northwest to southwest in a fan-like distribution. In the northern part of the Basin the currents flowed nearly perpendicular to the tectonic strike, and presumably also to the basin axis, whereas progressively southward the currents range from oblique to nearly parallel with the strike (and basin axis).

In the Dugout Mountain area (fig. 14, shown in circle), currents flowed predomi-

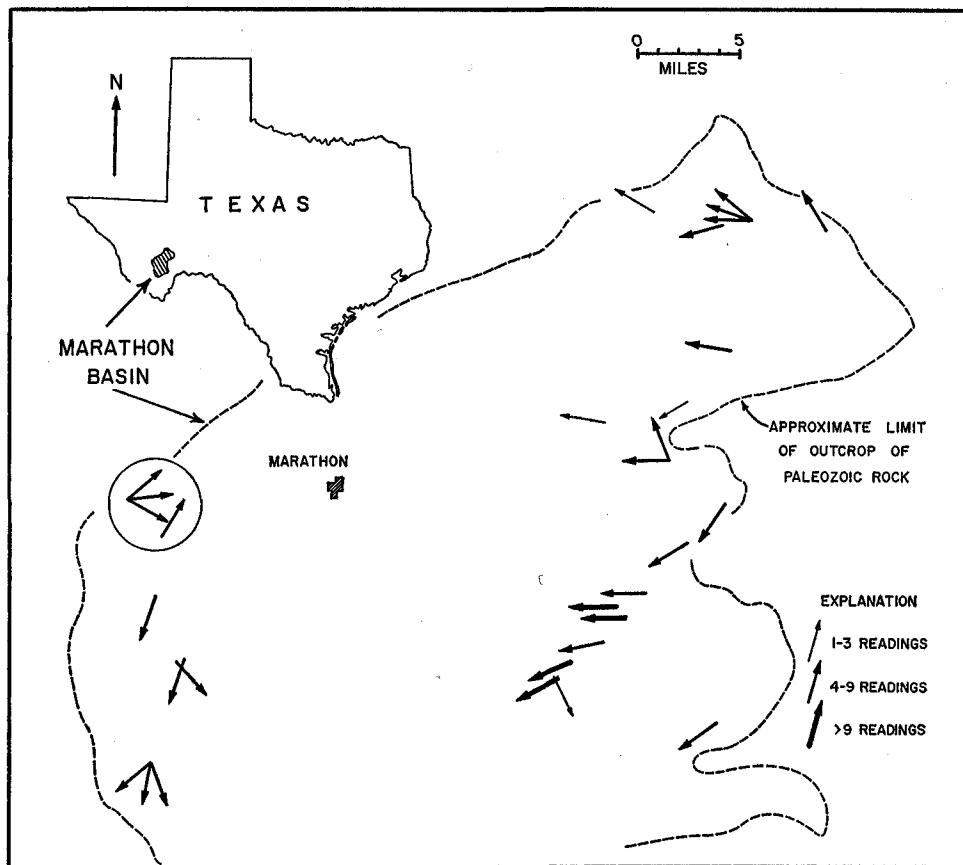


FIG. 14. Paleocurrent map. Arrows show the average direction of current-flow at each locality. Arrows fanning from a common point indicate diverging flow directions; arrows not connected at a common point define separate modes at a locality.

nantly northeastward; at one locality currents were parallel to the basin axis, at the other locality the currents had a fan-like spread. The beds deposited by these currents are calcarenitic sandstones that are probably younger than beds elsewhere in the Haymond with the exception of the Allison Ranch facies.

South of Dugout Mountain in stratigraphically lower (older) Haymond beds, currents flowed both parallel (southwest) and oblique (southeast) to the basin axis. Although the current pattern suggests these sandstones were derived from the northwest, they are not calcarenitic like the Dugout Mountain beds. In fact, they are similar in mineralogy to the sandstones in the eastern part of the basin. Inasmuch as the sandstones in question are older than the cal-

carenitic Dugout Mountain beds, it is possible they were derived from a granitic terrain on the craton before the craton became a site of carbonate deposition. Longitudinal currents, however, may have brought some detritus from the eastern side of the basin.

Paleocurrent studies of flysch turbidites have introduced a controversy—were flysch basins filled predominantly by detritus derived from sides of the trough by “lateral” currents, or were they filled from the ends of the trough by “longitudinal” currents (Dzulinski et al., 1959)? Assuming that the long axis of the basin was more or less parallel with the present tectonic strike, Haymond paleocurrents are mostly oblique; longitudinal currents are present but of minor importance. It seems

probable that most turbidity currents initially flowed transversely into the basin, and upon reaching the basin axis, were deflected to flow longitudinally down the axial slope, which was first to the southwest, then later to the northeast. This change in basin-axis slope is inferred from the fact that the young beds in the Dugout Mountain area show current transport to the northeast, in a direction opposite that shown by older beds. Almost all other paleocurrent data in the Marathon Basin are from beds stratigraphically below the boulder beds, except in the Clark Butte area where data are about equally abundant from below and above the boulder beds. During most of Haymond deposition, the sedimentary basin was deeper along the medial part of the basin parallel with the present tectonic strike and was deepest at the southwestern end of the basin. The change of slope from southwest to northeast probably reflects the approaching peak of orogenic activity during which the southeastern edge of the geosyncline underwent deformation and uplift.

Plate 25 shows that at some localities the directional readings are uniform in one modal orientation, whereas at others there are several distinct modes or a fan-like scatter. Inasmuch as readings at most localities were taken from within separate structural elements (one limb of a fold, edge of a thrust plate, etc.), the spread in current directions is real and not the result of

grouping data from beds that have undergone different degrees and directions of structural rotation. Since turbidity currents are slope-controlled, localities with uniform currents probably had steeper slopes, and hence less deviation of currents, than sites where there was a spread in current directions. Inasmuch as the directional readings at any locality represent a considerable time span, another interpretation is that localities with a large current spread were sites where the paleoslope changed with time due to unequal amounts of sediment accumulation or possibly tectonic movements of the sea floor.

Flute casts at several localities (3, 4, 10A) show the interesting fact that several turbidity currents flowed in a direction opposite to the predominant trend. These anomalous beds were rechecked to be sure a mistake had not been made. The explanation of such occurrences is unknown, but it is unlikely that the slopes of the sea floor at these sites were reversed for short periods. It has been pointed out (McBride, 1962, p. 85) that other factors, such as the orientation of submarine gullies and canyons, slope of subsea fans, and irregular submarine topography, can affect the course of turbidity currents in addition to the regional slope. A comparison of the mineralogy of the anomalous turbidites with the normal beds reveals no significant differences.

PROVENANCE

The mineralogy of Haymond rocks and the paleocurrent pattern of sand dispersal provide clues to the geologic character and **location (provenance) of the sourcelands** that shed the detritus which makes up the formation. An analysis of paleocurrent data on slope-controlled turbidity currents yields the interpretation that the Haymond was deposited in a trough elongate in a NNE-SSW trend with sourcelands to the ESE and WNW. The sourceland to the ESE was a positive element throughout all of Haymond deposition and contributed the bulk of the detritus. The sourceland to the WNW contributed considerable detritus late in the time of Haymond deposition but probably was not an important source **in earlier times.**

The name Llanoria¹⁵ has been applied for many years to the positive element inferred to have shed detritus into the Marathon geosyncline throughout much of Paleozoic time, **although opinions as to the nature of the sourceland range from that of a landmass of continental proportions to narrow anticlinal welts derived from within the geosyncline** (Branner, 1897; Willis, 1907; Schuchert, 1910; Dumble, 1920; Powers, 1920; Miser, 1921; King, 1937, p. 21; Morgan, 1952; Woods, 1956). Different opinions have also been expressed on the location of the landmass and its continuity between Mexico and the southern Appalachians. Since the early speculations, data from geophysical studies and deep wells (Flawn et al., 1961) enable a more accurate interpretation to be made. But because of the scarcity of deep wells east of the Marathon region in Texas and northern Mexico, interpretations in this area are tentative and the boundaries of sourceland and basin are yet to be established.

The mineralogy of Haymond sandstones and fragments of exotic rocks in the boulder

beds indicate that the sourceland was a complex of sedimentary rocks (chiefly sandstone, conglomerate, and shale), igneous rocks (granite, granodiorite, rhyolite), and low-grade metamorphic rocks (schist, phyllite, cataclasite). Incorporating the age-dates of the gneissic-granite pebble, a logical interpretation is that the positive element had a core of Cambrian-Precambrian granite and silicic volcanic rocks of unknown age that was mantled by sedimentary rocks, chiefly of early Paleozoic age. The granite, volcanic rocks, and sediments underwent low-grade metamorphism with a high local shearing component during late Devonian(?) time, and the complex was later uplifted to form the chief source of first Tesnus (Cotera, 1962; Johnson, 1962) and later Haymond detritus. As the mass was uplifted, streams stripped off the mantle of sedimentary and low-grade metamorphic rocks to reach the Precambrian granitic core prior to deposition of the Haymond. Later, the sourceland was uplifted further and shoved northwestward along thrust faults at the margin of the basin; near-shore Haymond sediments were exposed to cannibalistic erosion, and older rocks of the Marathon sequence (Maravillas, Caballos, Tesnus, Dimple) were exposed or situated so that large chunks were dislodged from thrust plates **and slid seaward.** The areal extent of the sourceland cannot be determined because the distribution and volume of Haymond-age rocks have not been traced in the subsurface. The large volume of detritus in the Haymond and the complex mixture of rock types indicate that the streams must have drained either a large area or a small constantly rising mass with considerable relief. The coarseness of the gravel from the boulder beds favors prominent relief during part of the time.

How far to the east of the present Haymond outcrop the sourceland lay is uncertain, because outcrops of pre-Pennsylvanian rock are few, and deep wells are scarce southeast of the Marathon region. Flawn

¹⁵ The concept of the landmass was apparently first stated by Branner (1897). Willis (1907) named it Llano, and Dumble (1920) renamed it Llanoria in order to distinguish it from the outcrop area of the Llano region. The term Llanoris appeared in P. B. King's 1930 paper (p. 114), but this is probably a typographical error.

(in Flawn et al., 1961, p. 105) summarized evidence to indicate the presence of "a major pre-Mesozoic granitic terrane in northern Mexico lying on the east side of the Coahuila peninsula," which is in a feasible location to have been the sourceland. Flawn (p. 105) delimited the terrane as "south of the highly sheared low-grade metamorphic rocks . . . that form an interior zone of the Ouachita structural belt in west Texas and northernmost Mexico and outcrop in the Sierra del Carmen; it is east of the Permian deformed belt of the Las Delicias—Acatita area; and is west of the highly sheared slate and metagraywacke encountered in the No. 101 Chapa [well] in Nuevo Leon."

The sourceland to the west of the geosyncline was the chief source of detritus for

the underlying Dimple Formation (Thomson and Thomasson, 1964) but apparently contributed little to the Haymond until late in its history. The source contributed granitic debris and fossils and carbonate rock detritus of shallow-water facies. Carbonate rocks apparently accumulated on the shallow southeast margin of the craton, which was uplifted to shed carbonate detritus and Precambrian (?) granitic detritus into the geosyncline via turbidity currents. The cratonic mass may have been a southeast prong of the Diablo Platform, a structural element which extends northwest from western Brewster County (Flawn, in Flawn et al., 1961, p. 145). Uplift of the source or downwarp of the trough late in the history of Haymond deposition changed the slope of the Marathon trough to the northeast.

SUMMARY AND SEDIMENTOLOGIC HISTORY

Regional setting.—The Haymond Formation is part of a thick section of Paleozoic flysch that was deposited in the west Texas part of the Ouachita geosyncline during part of Pennsylvanian time. The formation is exposed on a structurally high portion of the Ouachita structural belt in the topographic Marathon Basin, a subrectangular area that has dimensions of 50 miles in a northeast-southwest direction and 35 miles in a northwest-southeast direction. Deformed Paleozoic rocks trend NE-SW in the Basin and are unconformably overlain by Cretaceous rocks to the northeast, southeast, and southwest, by Permian rocks to the northwest, and in places by Quaternary alluvium within the Basin.

Stratigraphy.—A uniform sequence of interbedded greenish-gray fine-grained sandstone and gray shale of flysch characteristics makes up the bulk of the Haymond throughout the Basin. The formation conformably overlies the Dimple Limestone and underlies the Gaptank Formation and has a maximum preserved thickness of 4,300 feet at the base of Housetop Mountain. Coarse sandstones without flysch characteristics form a wedge-shaped body that tapers from approximately 600 feet thick in the north to a feather edge at the south. Boulder-bearing beds occur adjacent to and interbedded with the coarse sandstone beds. The boulder beds are a complex of contorted flysch beds and mudstone lenses that encase fragments of erratic and exotic blocks having a wide range of sizes. The largest fragments (maximum length, 130 feet) were derived from Paleozoic sedimentary formations, some of which normally occur 3,000 to 10,000 feet lower stratigraphically. Exotic cobbles and boulders of granite, granodiorite, metarhyolite, schist, quartzite, sandstone, and conglomerate, at least part of which are Precambrian(?), are well rounded in contrast to the angular and commonly brecciated character of sedimentary rock fragments of indigenous formations.

Environment and manner of deposition.

—The flysch part of the formation was deposited in a deep-marine basin in which muds (now shale) accumulated slowly as pelagic layers and into which sediment-laden density currents (turbidity currents) flowed periodically and deposited sand beds. The interpretation of a deep-water environment is based on the combination of (1) the presence of quiet-water muds (shale), (2) the lack of textures or structures that are restricted to shallow-water environments, and (3) the absence of marine fossils in the shales that are restricted to shallow water. The only fossils recovered from shale are carbonaceous plant fragments, spores, and siliceous spicules (from one bed); laminae disturbed by burrowers are ubiquitous. Evidence that the sandstone beds were deposited by turbidity currents is: (1) the sandstones were deposited in deep water, and (2) internal structures show the sandstone beds were deposited by waning currents that initially had high velocities; many beds are graded, and many pass upward from massive bedding to horizontal laminae to cross-laminae. The record of more than 15,000 separate turbidity currents is preserved in the flysch part of the formation.

Direct evidence as to the depth of water is lacking, but from an analogy with modern sediments and paleoecologic interpretations of other flysch units, the depth is inferred to have been from at least several hundred to possibly several thousand feet deep. In the entire formation evidence of shoal water occurs only near the top of the Haymond (Allison Ranch facies) and possibly in coarse sandstone beds at Clark Butte.

The *boulder beds* ("wild-flysch") are the product of catastrophic submarine slides generated on numerous occasions when masses of rock were dislodged from (submarine?) fault scarps and slid seaward to come to rest in deep water. The presence of fragmented flysch beds, boulders encased in mudstone, and slump fea-

tures, indicates that the chaotic features of the boulder beds are sedimentary (depositional and pre-lithification) in origin and not tectonic (post-lithification). However, faulting was responsible for bringing older Paleozoic rocks (represented by erratic debris in the beds) to the surface of the sourceland that lay to the east, as attested by fragments of brecciated Caballos Novaculite, a formation that is normally 10,000 feet below this part of the Haymond.

Pebbles and cobbles of rocks foreign to the Marathon region are detrital constituents derived from the tectonic sourceland that lay to the east and provide evidence of the lithology of the mass. Cataclastic rhyolite, gneissic granite and granodiorite, several types of sandstone, and vein quartz pebbles are common, whereas schist is rare among the exotic gravel fragments. The particles were rounded by streams or on beaches before they were incorporated in the Haymond submarine slides. A radiometric age-determination on a pebble of gneissic granite from the boulder bed at the base of Housetop Mountain gave 360 M.Y. for the biotite (K-Ar technique) and 570 M.Y. for the whole-rock age (Rb-Sr technique). The rock is probably a granite of Cambrian or Precambrian age that underwent metamorphism (and recrystallization of biotite) during late Devonian(?) time.

The coarse sandstone beds present a problem in interpreting the agents of deposition owing to a general scarcity of features diagnostic of known processes. Most coarse sandstone beds were deposited in water equally as deep as flysch beds, although the presence of a few large-scale festoon cross-beds in the Clark Butte section implies shoal conditions with strong currents. Most beds appear to have been deposited from slurries of moving sediments ("fluxoturbidite") intermediate in character between a subaqueous slide and a turbidity current; they are structureless to faintly laminated beds, commonly with channeled bases, and attain a thickness of 15 to 20 feet. An alternate hypothesis is that sand moved by slow creep in the manner of sediment now moving down subma-

rine canyons in California. A few beds have the sequence of structures diagnostic of turbidites.

Paleocurrents.—The regional paleocurrent pattern of sediment transport was reconstructed from measurements of more than 500 directional structures, chiefly from groove casts, flute casts, and parting lineation. During most of Haymond deposition, turbidity currents flowed down a prominent subsea slope to the northwest until they reached the axis of the trough, where they were deflected down the regional plunge to the southwest. During the later stages of deposition, currents flowed into the basin from the northwest and the east and were deflected to the north. The change in current pattern reflects the filling of the geosyncline and tilting to the north accompanying the heightened pulse of late Paleozoic diastrophism.

Provenance.—The sourceland to the east (Llanoria) was a positive element with a core of Cambrian-Precambrian(?) granitic rocks, rhyolite, and schist and a mantle of sandstone, conglomerate, and shale, of probable early Paleozoic age. The granite and some sediments show moderate regional metamorphism, whereas most rhyolite shows severe cataclastic deformation. The sourceland was of sufficient relief for streams to cut through the veneer of sedimentary cover to transport sand-sized granitic detritus, and, at times, cobbles and boulders of all types of bedrock, to the shoreline. The exact position and size of the sourceland are uncertain, but Flawn (*in* Flawn et al., 1961, p. 105) outlined the limits of a granitic basement complex in northern Mexico that is a likely source in part.

The craton to the northwest, probably the southern end of the Diablo Platform, provided granitic debris to the Haymond late in its history. The shelf-edge of the craton was the site of carbonate deposition; with uplift of the shelf, carbonate detritus was mixed with granitic debris and swept into deep water by turbidity currents.

Sedimentologic and tectonic history.—The record of Haymond deposition is but

one episode in the remarkable sedimentologic history in the Marathon part of the Ouachita geosyncline. Details of this history, although only sketchily known for the early Paleozoic, have been summarized by Thomson and McBride (1964). The geosyncline underwent a period of gradual deepening during early Paleozoic time. During this "forming stage" of its history, the Basin received relatively little sediment (3,600 feet in 250 million years (fig. 2)); the last phase was deposition of siliceous oozes of the Caballos Novaculite under "starved" or leptogeosynclinal conditions (King, *in* Flawn et al., 1961, p. 181; Thomson, 1964). The forming stage episode was succeeded by an interval of rapid deposition, constituting the "filling stage" of the geosyncline, during which 12,000 feet of flysch (Tesnus, Dimple, Haymond) and 1,800 feet of molasse (Gaptank) were deposited in approximately 60 million years.

The Tesnus Formation is a thick (6,500 feet) wedge of siliciclastic detritus that was derived from the same sourceland (Llanoria) that later provided detritus for the Haymond (Johnson, 1962; Cotera, 1962). The bulk of the Tesnus was deposited below wave base in quiet water; the formation has records of numerous episodes of submarine slumps and deposition by turbidity currents (Cotera, 1962; McBride and Thomson, 1964). Tesnus sandstones in general have more matrix and metamorphic rock fragments but less feldspar than Haymond sandstones.

The dominantly calcarenitic detritus of the Dimple Formation was derived from a sourceland to the northwest. The bulk of the Dimple was deposited in deep water as turbidites and pelagic layers, although shallow-water shelf deposits are interpreted to be present in exposures in the northwestern part of the area (Thomson and Thomasson,

1964).

Deposition of the Haymond began as the positive element (Llanoria) to the east again rose to provide a source of siliciclastic detritus. The cratonic elements to the northwest subsided from the time of Dimple deposition but rose late during Haymond history as the source of the turbidites in the Dugout Mountain area. Two calcarenite turbidites in the lower part of the Haymond were also derived from this source.

During most of Haymond deposition the geosyncline had a regional slope to the southwest. As the pace of tectonism increased during Pennsylvanian time, the trough was concomitantly filled and tilted to the north. Shallow-water deposition during late Haymond history is shown by the Allison Ranch facies. At this time, detritus was apparently being transported northeastward into the Val Verde basin, a recently formed deep-water trough whose existence is known from deep wells (Flawn, *in* Flawn et al., 1961, pp. 136-137). In the Marathon area, Haymond sediments were succeeded by molassic carbonates, conglomerates, sandstone, and shales of the Gaptank Formation.

Several workers have attempted to date closely the time or times of diastrophism recorded in the Marathon region (Van der Gracht, 1931; Hall, 1956, p. 2254). However, the writer agrees with King (*in* Flawn et al., 1961, p. 184), who stated that the sedimentary rocks "record pulsation of a continuing process of orogeny, by which the original geosynclinal area was being converted into an orogenic system." Although the orogeny was continuous, boulder beds and conglomerates in the Tesnus, Dimple, Haymond, and Gaptank attest to episodes of stronger than usual tectonic activity.

REFERENCES CITED

- ALLEN, J. R. L. (1964) Primary current lineation in the Lower Old Red Sandstone (Devonian), Anglo-Welsh Basin: *Sedimentology*, vol. 3, pp. 89-108.
- BAKER, C. L. (1928) Date of major diastrophism and other problems of the Marathon Basin (discussion): *Bull. Amer. Assoc. Petrol. Geol.*, vol. 12, pp. 1111-1116.
- (1932) Erratics and arkoses in the middle Pennsylvanian Haymond Formation of the Marathon area, Trans-Pecos Texas: *Jour. Geol.*, vol. 40, pp. 577-607.
- and BOWMAN, W. F. (1917) Geologic exploration of the southeastern Front Range of Trans-Pecos Texas: *Univ. Texas Bull.* 1753, pp. 61-177.
- BENNETT, R. E. (1959) Geology of East Bourland and Simpson Springs Mountains, Brewster County, Texas: Master's thesis, Univ. Texas, 172 pp.
- BLATT, HARVEY (1959) Effect of size and genetic quartz type on sphericity and form of beach sediments, northern New Jersey: *Jour. Sed. Petrology*, vol. 29, pp. 197-207.
- BOUMA, A. H. (1962) Sedimentology of some flysch deposits: Elsevier, Amsterdam, 168 pp.
- BRANNER, J. C. (1897) The former extension of the Appalachians across Mississippi, Louisiana, and Texas: *Amer. Jour. Sci.*, 4th ser., vol. 4, pp. 357-371.
- CARNEY, FRANK (1934) Glacial beds of Pennsylvanian age in Texas (abst.): *Geol. Soc. Amer., Proc.*, p. 70.
- COTERA, A. S. (1962) Petrology and petrography of Mississippian-Pennsylvanian Tesnus Formation, Marathon Basin, Trans-Pecos Texas: Ph.D. dissertation, Univ. Texas, 186 pp.
- CROWELL, J. C. (1957) Origin of pebbly mudstones: *Bull. Geol. Soc. Amer.*, vol. 68, pp. 993-1010.
- DEAN, W. E., JR., and ANDERSON, R. Y. (in press) Slope stratification of the Pennsylvanian Haymond Formation, Marathon region, Texas: *Bull. Geol. Soc. Amer.*
- DILL, R. F. (1963) Contemporary erosion in the heads of submarine canyons (abst.): *Geol. Soc. Amer. Spec. Paper* 76, p. 45.
- DUMBLE, E. T. (1920) The geology of East Texas: *Univ. Texas Bull.* 1869 (Aug. 10, 1918), 388 pp.
- DZULINSKI, ST., KSIAZKIEWICZ, M., and KUENEN, PH. H. (1959) Turbidites in flysch of the Polish Carpathian Mountains: *Bull. Geol. Soc. Amer.*, vol. 70, pp. 1089-1118.
- , and WALTON, E. K. (1963) Experimental production of sole markings: *Trans. Edinburgh Geol. Soc.*, vol. 19, pt. 3, pp. 279-305.
- EARDLEY, A. J., and WHITE, M. G. (1947) Flysch and molasse: *Bull. Geol. Soc. Amer.*, vol. 58, pp. 979-990.
- ELLISON, S. P. (1964) Conodonts of the Gaptank Formation: 1964 Field Trip Symposium and Guidebook, Pub. 64-9, Permian Basin Section, Soc. Econ. Paleontologists and Mineralogists, pp. 45-46.
- FLAWN, P. T. (1956) Basement rocks of Texas and southeast New Mexico: *Univ. Texas Pub.* 5605, 261 pp.
- (1958) Genesis of Haymond boulder beds (discussion): *Bull. Amer. Assoc. Petrol. Geol.*, vol. 42, pp. 1734-1735.
- , GOLDSTEIN, AUGUST, JR., KING, P. B., and WEAVER, C. E. (1961) The Ouachita system: *Univ. Texas Pub.* 6120, 401 pp.
- FOLK, R. L. (1951) Stages of textural maturity in sedimentary rocks: *Jour. Sed. Petrology*, vol. 21, pp. 127-130.
- (1954) The distinction between grain size and textural maturity in sedimentary rock nomenclature: *Jour. Geol.*, vol. 62, pp. 344-359.
- FRIEDMAN, G. M. (1958) Determination of sieve-size distribution from thin-section data for sedimentary-petrological studies: *Jour. Geol.*, vol. 66, pp. 394-416.
- GILBERT, G. K. (1914) The transportation of debris by running water: *U. S. Geol. Survey Prof. Paper* 86, 236 pp.
- GOLDSTEIN, AUGUST, JR., and HENDRICKS, T. A. (1962) Late Mississippian and Pennsylvanian sediments of Ouachita facies, Oklahoma, Texas, and Arkansas, in *Pennsylvanian System in the United States, a symposium*: *Amer. Assoc. Petrol. Geol.*, pp. 385-430.
- HAAF, E. TEN (1956) Significance of convolute lamination: *Geol. en Mijnbouw*, vol. 18, pp. 188-194.
- HALL, W. E. (1956) Marathon folded belt, Big Bend, Texas: *Bull. Amer. Assoc. Petrol. Geol.*, vol. 40, pp. 2247-2255.
- (1957) Genesis of "Haymond Boulder Beds," Marathon Basin, West Texas (note): *Bull. Amer. Assoc. Petrol. Geol.*, vol. 41, pp. 1633-1637.
- (1959) Genesis of "Haymond Boulder Beds," Marathon Basin, West Texas (discussion): *Bull. Amer. Assoc. Petrol. Geol.*, vol. 43, pp. 238-239.
- HARMS, J. C., and FAHNESTOCK, R. K. (1964) Stratification, bedforms and flow phenomena with an example from the Rio Grande (abst.): *Bull. Amer. Assoc. Petrol. Geol.*, vol. 48, p. 530.
- HEEZEN, B. C., and EWING, MAURICE (1952) Turbidity currents and submarine slumps, and the 1929 Grand Banks earthquake: *Amer. Jour. Sci.*, vol. 250, no. 12, pp. 849-873.
- , and ——— (1955) Orleansville earthquake and turbidity currents (abst.):

- Bull. Amer. Assoc. Petrol. Geol., vol. 39, pp. 2504-2505.
- , and HOLLISTER, C. (1964) Deep-sea current evidence from abyssal sediments: *Marine Geology*, vol. 1, no. 2, pp. 141-174.
- HILL, R. T. (1900) Physical geography of the Texas region: U. S. Geol. Survey Topo. Atlas, folio 3, 12 pp.
- HSU, K. J. (1964) Cross-laminations in graded bed sequences: *Jour. Sed. Petrology*, vol. 34, pp. 379-388.
- JOHNSON, K. E. (1962) Paleocurrent study of the Tesnus Formation, Marathon Basin, Texas: *Jour. Sed. Petrology*, vol. 32, pp. 781-792.
- JUDSON, SHELDON, and BARKS, R. E. (1961) Microstriations on polished pebbles: *Amer. Jour. Sci.*, vol. 259, pp. 371-381.
- KING, P. B. (1930) The geology of the Glass Mountains, Texas, Part I, Stratigraphy: Univ. Texas Bull. 3038, 167 pp. (Published January 1931.)
- (1932) Large boulders in the Haymond Formation of West Texas (abst.): *Bull. Geol. Soc. Amer.*, vol. 43, p. 148.
- (1937) Geology of the Marathon region, Texas: U. S. Geol. Survey Prof. Paper 187, 148 pp. (Published August 1938.)
- (1958) Problems of boulder beds of Haymond Formation, Marathon Basin, Texas (discussion): *Bull. Amer. Assoc. Petrol. Geol.*, vol. 42, pp. 1731-1735.
- , BAKER, C. L., and SELLARDS, E. H. (1931) Erratic boulders of large size in the West Texas Carboniferous (abst.): *Bull. Geol. Soc. Amer.*, vol. 42, p. 200.
- , and KING, R. E. (1928) The Pennsylvanian and Permian stratigraphy of the Glass Mountains: Univ. Texas Bull. 2801, p. 113.
- KING, R. E. (1930) The geology of the Glass Mountains, Texas, Part II, Faunal summary and correlation of the Permian formations with description of Brachiopoda: Univ. Texas Bull. 3042, 146 pp. (Published August 1931.)
- KUENEN, P. H. (1953) Significant features of graded bedding: *Bull. Amer. Assoc. Petrol. Geol.*, vol. 37, pp. 1044-1066.
- , and MIGLIORINI, C. I. (1950) Turbidity currents as a cause of graded bedding: *Jour. Geol.*, vol. 58, pp. 91-127.
- MAST, P. F., and POTTER, P. E. (1963) Sedimentary structures, sand shape fabrics, and permeability. II: *Jour. Geol.*, vol. 71, no. 5, pp. 548-565.
- MISER, H. D. (1921) Llanoria, the Paleozoic land area in Louisiana and eastern Texas: *Amer. Jour. Sci.*, 5th ser., vol. 2, pp. 61-89.
- MCBRIDE, E. F. (1962) Flysch and associated beds of the Martinsburg Formation (Ordovician), Central Appalachians: *Jour. Sed. Petrology*, vol. 32, pp. 39-91.
- (1963a) Sedimentology of the Haymond Formation (Pennsylvanian flysch), Marathon Basin, Texas (abst.): *Geol. Soc. Amer. Spec. Paper* 73, p. 204.
- (1963b) A classification of common sandstones: *Jour. Sed. Petrology*, vol. 33, pp. 664-669.
- (1964a) Sedimentology and stratigraphy of the Haymond Formation, Marathon Basin, Texas: 1964 Field Trip Symposium and Guidebook, Pub. 64-9, Permian Basin Section, Soc. Econ. Paleontologists and Mineralogists, pp. 35-40.
- (1964b) Stratigraphy and sedimentology of the Gaptank Formation, Marathon Basin, Texas: 1964 Field Trip Symposium and Guidebook, Pub. 64-9, Permian Basin Section, Soc. Econ. Paleontologists and Mineralogists, pp. 41-44.
- , and KIMBERLY, J. E. (1963) Sedimentology of the Smithwick Shale (Pennsylvanian), eastern Llano region, Texas: *Bull. Amer. Assoc. Petrol. Geol.*, vol. 47, pp. 1840-1854.
- , and THOMSON, ALAN (1964) Sedimentology of the Tesnus Formation, Marathon region, Texas: 1964 Field Trip Symposium and Guidebook, Pub. 64-9, Permian Basin Section, Soc. Econ. Paleontologists and Mineralogists, pp. 17-21.
- , and YEAKEL, L. S. (1963) Relationship between parting lineation and rock fabric: *Jour. Sed. Petrology*, vol. 33, pp. 779-782.
- MORGAN, H. J. (1952) Paleozoic beds south and east of Ouachita folded belt: *Bull. Amer. Assoc. Petrol. Geol.*, vol. 36, pp. 2266-2274.
- OTTO, G. H. (1938) The sedimentation unit and its use in field sampling: *Jour. Geol.*, vol. 46, pp. 569-582.
- PELLETIER, B. R. (1958) Pocono paleocurrents in Pennsylvania and Maryland: *Bull. Geol. Soc. Amer.*, vol. 69, pp. 1033-1064.
- PETTJOHN, F. J. (1957) *Sedimentary rocks*: Harper and Co., New York, 718 pp.
- POTTER, P. E., and PETTJOHN, F. J. (1963) *Paleocurrents and basin analysis*: Springer-Verlag, Berlin, 296 pp.
- POWERS, SIDNEY (1920) The Sabine Uplift, Louisiana: *Bull. Amer. Assoc. Petrol. Geol.*, vol. 4, pp. 117-136.
- QUIRKE, T. T. (1930) Spring pits, sedimentation phenomena: *Jour. Geol.*, vol. 38, pp. 88-91.
- REEVES, C. C., JR. (1963) Gas rings from Terry County, Texas: *Jour. Sed. Petrology*, vol. 34, pp. 190-193.
- ROCK COLOR CHART (1948) National Research Council, Washington, D. C.
- ROSS, C. A. (1963) Standard Wolfcampian series (Permian), Glass Mountains, Texas: *Geol. Soc. Amer. Memoir* 88, 205 pp.
- SANDERS, J. E. (1960) Origin of convoluted laminae: *Geol. Mag.*, vol. 97, pp. 409-421.
- (1965) Primary sedimentary structures formed by turbidity currents and related sedimentation mechanisms, in *Primary sedi-*

- mentary structures and their hydrodynamic interpretation: Soc. Econ. Paleontologists and Mineralogists Spec. Pub. No. 12, pp. 192-219.
- , and CAROZZI, ALBERT (1957) Flysch and molasse (abst.): Bull. Geol. Soc. Amer., vol. 68, p. 1770.
- SANDERSON, G. A., and KING, W. E. (1964) Paleontological evidence for the age of the Dimple Limestone: 1964 Field Trip Symposium and Guidebook, Pub. 64-9, Permian Basin Section, Soc. Econ. Paleontologists and Mineralogists, pp. 31-34.
- SCHUCHERT, CHARLES (1910) Paleogeography of North America: Bull. Geol. Soc. Amer., vol. 20, pp. 427-606.
- (1927) Pennsylvanian-Permian systems of western Texas: Amer. Jour. Sci., vol. 14, pp. 381-401.
- SEILACHER, ADOLF (1962) Paleontological studies of turbidite sedimentation and erosion: Jour. Geol., vol. 70, pp. 227-233.
- SELLARDS, E. H. (1931) Erratics in the Pennsylvanian of Texas: Univ. Texas Bull. 3101, pp. 9-17.
- (1933) The pre-Paleozoic and Paleozoic systems in Texas, in *The geology of Texas*, Vol. I, Stratigraphy: Univ. Texas Bull. 3232 (Aug. 22, 1932), pp. 15-238.
- SIMONS, D. B., and RICHARDSON, E. V. (1961) Forms of bed roughness in alluvial channels: Proc. Amer. Soc. Civil Engineers, Jour. Hydraulics Div., HY 3, pp. 87-105.
- SKINNER, L. W., and WILDE, G. L. (1954) New Early Pennsylvanian fusulinids from Texas: Jour. Paleont., vol. 28, pp. 796-803.
- SNEED, E. D., and FOLK, R. L. (1958) Pebbles in the lower Colorado River, Texas: A study in particle morphogenesis: Jour. Geol., vol. 66, pp. 114-150.
- SORBY, H. C. (1908) On the application of quantitative methods to the study of the structure and history of rocks: Geol. Soc. London Quart. Jour., vol. 64, pp. 171-233.
- SUJKOWSKI, Z. L. (1957) Flysch sedimentation: Bull. Geol. Soc. Amer., vol. 68, pp. 543-554.
- THOMSON, ALAN (1964) Genesis and bathymetric significance of the Caballos Novaculite, Marathon region, Texas: 1964 Field Trip Symposium and Guidebook, Pub. 64-9, Permian Basin Section, Soc. Econ. Paleontologists and Mineralogists, pp. 12-16.
- , and McBRIDE, E. F. (1964) Summary of the geologic history of the Marathon geosyncline: 1964 Field Trip Symposium and Guidebook, Pub. 64-9, Permian Basin Section, Soc. Econ. Paleontologists and Mineralogists, pp. 52-60.
- , and THOMASSON, M. R. (1964) Sedimentology and stratigraphy of the Dimple Limestone, Marathon region, Texas: 1964 Field Trip Symposium and Guidebook, Pub. 64-9, Permian Basin Section, Soc. Econ. Paleontologists and Mineralogists, pp. 22-30.
- UDDEN, J. A. (1907) A sketch of the geology of the Chisos country, Brewster County, Texas: Univ. Texas Bull. 93, 101 pp.
- , BAKER, C. L., and BÖSE, EMIL (1916) Review of the geology of Texas: Univ. Texas Bull. 44, 178 pp.
- ULRICH, E. O. (1911) Revision of the Paleozoic systems: Bull. Geol. Soc. Amer., vol. 22, pp. 281-680.
- VAN DER GRACHT, W. A. J. M. VAN WATERSCHOOT (1931) Permo-Carboniferous orogeny in south-central United States: Bull. Amer. Assoc. Petrol. Geol., vol. 15, pp. 991-1057.
- VON STREERUWITZ, W. H. (1891) Report on the geology and mineral resources of Trans-Pecos Texas: Texas Geol. Survey, 2d Ann. Rept. (1890), pp. 669-738.
- WALKER, R. G. (1963) Distinctive types of ripple-drift cross-lamination: Sedimentology, vol. 2, pp. 173-188.
- WILLIS, BAILEY (1907) Discoidal structures of the lithosphere: Bull. Geol. Soc. Amer., vol. 31, pp. 247-302.
- WOOD, ALAN, and SMITH, A. J. (1959) The sedimentation and sedimentary history of the Aberystwyth Grits (Upper Landoverian): Geol. Soc. London Quart. Jour., vol. 114, pp. 163-196.
- WOODS, R. D. (1956) The northern structural rim of the Gulf Basin: Trans. Gulf Coast Assoc. Geol. Soc., vol. 6, pp. 3-11.
- YEAKEL, L. S., JR. (1962) Tuscarora, Juniata, and Bald Eagle paleocurrents and paleogeography in the Central Appalachians: Bull. Geol. Soc. Amer., vol. 73, pp. 1515-1540.

APPENDIX A

PETROGRAPHIC DESCRIPTION OF ERRATIC AND EXOTIC ROCK TYPES FROM HAYMOND BOULDER BEDS

Presentation of data.—This appendix contains a description of individual pebbles and cobbles that were chosen as representative of the various rock types (exclusive of Maravillas and Caballos chert) collected from boulder-bearing units of the Haymond Formation. The materials for this study include rocks and 19 thin sections of the writer's collection, rocks and 39 thin sections belonging to the Bureau of Economic Geology and collected by P. T. Flawn, and rocks collected by W. R. Muehlberger.

Rock types are described below in the following order: sedimentary rocks (carbonate rocks, sandstones), metasandstones, igneous rocks, and metamorphic rocks. Estimates of the modal mineral compositions were made of igneous rocks and appear in parentheses. Point counts were made of five sandstone samples; complete percentage data for each are given in table 6 (in pocket) and summary data are given in the descriptions below. Estimates of the different feldspar types were generally not made owing to the difficulty in identifying individual grains on the flat stage. Attempts to stain K-feldspar in thin section using sodium cobaltinitrite were not successful.

The sample listed as No. 1 is from the northern boulder beds at Clark Butte; samples 10, 13, and 17 are from the old Bennett ranch locality south of the Southern Pacific Railroad tracks; the remainder are from the vicinity of Housetop Mountain. Field sample numbers of the rocks described are given in parentheses at the end of each description. For samples from the Bureau of Economic Geology collection, the thin section number is also given in parentheses.

1. Limestone. Alternating layers of dark brown microsparite and light brown biosparite in layers 1 to 8 mm thick. Several layers are truncated by others at low angles. The microspar has a wide grain-size range and includes scattered grains of

spar; calcite spicules or spines and other fragmental fossils comprise 1 percent of the layers. Biosparite layers are made of medium-grained well-sorted fossil fragments with interstitial micrite and spar cement. The unequal grain size of spar suggests it is recrystallized micrite. Echinoderm fragments are the most abundant grains; other recognizable forms are ostracodes, trilobites, phosphatic brachiopods, and spines or spicules. Elongate particles have a strong preferred orientation parallel with bedding.

The pebble is similar to rocks in the Marathon and Maravillas Formations. (BB-1; Pl. 20, A)

2. Chertified limestone (calcarenite). The original rock was a coarse (maximum grain size, 4.0 mm; median, 0.7 mm) calcarenite composed of limestone (40%), phosphate (20%), and chert (10%) rock fragments and abraded skeletal grains (30%). Chalcedony has replaced whatever primary cement was present and large portions of most skeletal grains and carbonate rock fragments. Introduction of dolomite rhombs (3% of rock) to replace both calcite and chert was the last diagenetic process. Identifiable skeletal grains include echinoderms, brachiopods, and spines or spicules of brachiopods and sponges. Elongate grains are subparallel with bedding.

The hand specimen is a mottled compact pebble that is bluish gray where fresh and orange white where weathered.

The texture and composition of this pebble are similar to beds in the Dimple Formation. (BB-9; Pl. 20, B)

3. Limestone (oosparite). Framework (60% of rock) is composed largely of amber-colored oolites (maximum size, 0.5 mm; 92% of framework) that have both concentric and radial structure. Other grains are well-rounded skeletal debris of echinoderms, bryozoa, brachiopods, and corals(?) and micrite pellets or intraclasts. Fragments of this group of fossils and whole tests of foraminifers form nuclei of the oolites. Some particles have only a superficial oolite coating. Framework grains are loosely packed; the only evidence of grain condensation or compaction is a few "pig-tail" oolites. Calcite spar-cement generally has the form of fine crystals rimming grains, grading to coarser grains (0.05 mm) in the last-filled pore space between grains.

The hand specimen is a light-gray pebble (3 inches long) without bedding.

The texture and composition of the rock are similar to many formations of Mississippian-Pennsylvanian age in the United States but unlike rocks exposed in the Marathon region. (BB-11; Pl. 20, C)

4. Limestone (intraclastic biomicrite). Tightly packed framework (85% of rock) of rounded skeletal grains (75% of framework) and limestone rock fragments (25%) cemented by dark brown micrite (15%). Fossils include (in order of abundance) particles of echinoderms, bryozoa, brachiopods, pelecypods, and questionable corals. Rock fragments are biomicrites and micrite with a few dark-brown organic-rich sparry calcite grains. Glauconite and cellophane particles occur in trace amounts. Strong grain condensation is shown by broken and collapsed shells and deeply sutured grains. Stylolites of small amplitude transect the rock in many places and are marked by residues of organic matter and hematite. Chalcidony (1% of rock) occurs as a partial replacement of both framework grains and cements. Framework grains have a median size of 1.5 mm and maximum size of 5.0 mm. Elongate grains have a crude sub-parallel orientation.

The hand specimen is a massive rock in which orange and brown rock fragments stand out from the light gray background of fossils and micrite.

Although limestones with the texture and composition of this rock do not crop out in the Marathon region, the framework grains resemble those that occur in some coarse beds of Dimple Limestone. (BB-12)

5. Sandstone (very coarse sandstone: silicic and calcitic submature arkose). Grain size: maximum, 4.0 mm; median, 0.7 mm. The summary composition of the sandstone is: cement, 6%; matrix, 1%; framework: quartz, 71%; feldspar, 25%; rock fragments, 4%. The rock has trace amounts of muscovite, biotite, and iron oxides. Rock fragments include sandstone, slate, quartzite, and felsite. Complete mineral composition data are given in table 6.

The hand specimen is a brownish-gray weathering to orange-gray massive cobble in which pink feldspar and glassy quartz granules stand out from the remainder of the rock.

The sandstone is similar in texture and mineralogy to some Haymond sandstone. (BB-16; Pl. 20, D)

6. Sandstone (muddy medium sandstone: immature chlorite-bearing arkose). Grain size: maximum, 8.0 mm; median, 0.3 mm. A framework of angular granite or granodiorite (25%), perthitic alkali feldspar (45%), quartz (8%), and chlorite grains (2%) in a dark brown organic-rich clay matrix (20%) containing some quartz and feldspar silt. Feldspars are highly vacuolized and show incipient sericitization and partial replacement by calcite. Chlorite is present as pseudomorphs or primary ferromagnesian constituents. The rock is essentially an unsorted gruss with an organic-rich illite matrix. Some grain contacts are sutured owing to pressure-solution.

The hand specimen is dark green with scattered blotchy white grains of feldspar and granite up to 8 mm long. The weathered surface is brown-

ish green with white spots of weathered feldspar. The rock is massive and has no preferred orientation of grains. (BB-6, A-681)

7. Sandstone (medium sandstone: slightly silicic immature subarkose). Grain size: maximum, 0.5 mm; median, 0.2 mm. The summary composition is: cement, 3%; matrix, 8%; framework: quartz, 90%; feldspar, 6%; rock fragments, 4%. Point-count data are given in table 6. The sandstone is barely a subarkose bordering on quartzarenite. Although the sandstone is classed as immature owing to the clay matrix, the framework grains are well sorted and subrounded. The rock is bound by sparse quartz overgrowths, interlocking sutured grains, and reconstituted (?) matrix minerals.

The hand specimen is a 3-foot-long block of greenish-gray weathering to brownish-red massive sandstone that has numerous calcite-filled fractures up to 2 mm wide.

The color, texture, and mineralogy of the boulder are similar to sandstones of the Tesnus Formation. (BB-10; Pl. 21, A)

8. Metasandstone. Grain size: maximum, 0.4 mm; median, 0.15 mm. Fabric: epiclastic modified by some granulation of quartz and feldspar; elongate grains have a preferred orientation which defines bedding. The sandstone shows the effects of only incipient metamorphism: moderate crushing and recrystallization of quartz and feldspar grains; recrystallization of micaceous rock fragments and matrix clays to chlorite, sericite, or intergrowths of chlorite-sericite; and development of stylolite seams outlined by insoluble iron oxides and organic matter. Originally the rock was a fine sandstone: slightly silicic immature lithic subarkose. Summary composition is: cement, 2%; matrix, 17%; framework: quartz, 71%; feldspar, 16%; rock fragments, 13%. Point-count data are given in table 6.

The hand specimen is a banded greenish-gray weathering to greenish-brown pebble with numerous healed fractures. The dark bands are residue along stylolite seams that are parallel with bedding.

The unaltered sandstone was similar in composition and texture to sandstones in both the Tesnus and Haymond Formations. (BB-15; Pl. 21, B)

9. Quartzite. Slightly sheared coarse sandstone: silicic supermature quartzarenite. Grain size: maximum, 4.5 mm; median, 0.3 mm. The original rock was a sandstone composed of well-rounded and well-sorted grains (99%) tightly cemented by overgrowths of quartz. Chert, meta-quartzite rock fragments, feldspar (now largely sericite), and heavy minerals (tourmaline, leucocoxene, and iron ores) together comprise 1 percent of the rock. Point-count data are given in table 6. Compression of the rock resulted in granulation of quartz grains and cement along shear zones and at points of stress; the product is mosaics of strained quartz whose grain size ranges

from cryptocrystalline to 0.1 mm. Cementation by quartz occurred prior to deformation, because sutured quartz grains are absent.

The hand specimen is a white massive pebble with irregular patches stained pale brown by hematite. Authigenic grains of hematite up to 1 mm in diameter, probably pseudomorphs of pyrite, stand out in relief on 1 percent of the weathered surface of the pebble.

This type of sandstone is unlike Paleozoic sandstone in the region, (BB-14; Pl. 21, C)

10. Metasandstone. Grain size: maximum of uncrushed grains, 4.0 mm; median of uncrushed grains, 0.3 mm. Uncrushed framework grains of quartz (25%) and feldspar (5%) are encased in a fine-grained mixture of quartz, feldspar, muscovite, biotite, chlorite, and traces of iron ores. Uncrushed feldspar grains are highly vacuolized and have aligned sericite fibers. Former sedimentary(?) rock fragments are now composed of a mosaic of quartz and micas. Micaceous grains rarely exceed 0.04 mm in length. The fine-grained minerals are largely reconstituted products of the original sandstone; the dark color of the mixture is caused by organic matter and iron-ore dust. Foliation imparted by original bedding has been amplified by the development of microstylolite sutures and narrow discontinuous shear zones. The composition and texture of the rock indicate the parent sandstone was a graywacke rich in feldspar.

The hand specimen is a dark greenish-gray weathering to orange-gray pebble with an obscure foliation. (BB-1a, A-672)

11. Metasandstone(?) breccia. Grain size: breccia particles, 0.05 mm to 2.0 mm; matrix grains, cryptocrystalline to 0.3 mm. Fabric: brecciated, microgranular. Quartz and alkali feldspar (75%), chlorite-sericite (24%), leucoxene (1%), iron ores (tr). The breccia texture shows well in the greenish-gray weathering to light-brown hand specimen and in the thin section when viewed by eye against sunlight. Breccia particles are a mosaic of quartz and feldspar grains in which chlorite-sericite intergrowths occur chiefly as isolated clusters (15%); the breccia matrix differs in that chlorite-sericite is more abundant (33%) and is evenly distributed, and the quartz-feldspar mosaic has more abundant cryptocrystalline grains.

The parent rock was probably a fine-grained lithic arkose that underwent severe brecciation and low-grade metamorphism. Relic epiclastic texture is visible in several breccia clasts (lamination is distinct in one particle in the hand specimen), where approximately one-half the detrital grains have undergone granulation and crushing. Chlorite-sericite clumps are probably recrystallized rock fragments. The finer grain size of the matrix and greater abundance of chlorite-sericite is attributed to more extensive brecciation and alteration of feldspars and rock fragments. (BB-13; Pl. 21, D)

12. Granite bordering on granodiorite. Grain size: 0.1 to 4.0 mm. Fabric: xenomorphic granular. K-feldspar (40%), albite-oligoclase (35%), quartz (16%), muscovite (4%), biotite (4%); apatite, sericite, calcite, and garnet all have trace amounts. About one-half the feldspars have a brownish cast owing to moderate vacuolization. K-feldspar is characterized by spindle-shaped twin lamellae; grid twinning is rare. A few grains of microcline micropertite are present. Much plagioclase shows oscillatory zoning; the center of such grains contains aligned muscovite fibers. Much biotite is rimmed by muscovite. Numerous grains have undergone incipient replacement by calcite. (BB-3; Pl. 22, A)

13. Altered rhyodacite(?). Grain size: groundmass, microcrystalline; phenocrysts, 0.1 to 2.0 mm. Fabric: porphyritic, holocrystalline. Groundmass (55%), alkali feldspar (20%), oligoclase (15%), quartz (6%), chlorite (4%); hematite, calcite, zircon, and apatite all have trace amounts. Quartz phenocrysts are strongly resorbed; grains have deep embayments, whereas only rounded cores remain of other grains. Feldspars are moderately vacuolized; oligoclase shows incipient replacement by calcite. Phenocrysts of colorless to pale-green chlorite grains have abundant rectangular hematite inclusions; chlorite is probably pseudomorphous after biotite. The groundmass is a mixture of feldspar, quartz, and chlorite. Curved fractures or microstylolites lined with hematite cut randomly across the groundmass.

The hand specimen is a dark-gray weathering to light-tan pebble that lacks foliation. Phenocrysts are clearly visible. (BB-13A, A-696; Pl. 22, B)

14. Rhyolite porphyry. Grain size: groundmass, cryptocrystalline to 0.1 mm; phenocrysts, 2.0 mm. Fabric: porphyritic microgranular. Groundmass (77%), albite? (11%), quartz (8%), saussurite? (3%), pyrite (1%); chlorite and sericite have trace amounts. The groundmass is a micro-mosaic of alkali feldspar and quartz that is cloudy owing either to saussurite or altered ferromagnesian minerals. Phenocrysts are subhedral to euhedral; albite is slightly antiperthitic and vacuolized and shows carlsbad, pericline, and albite twins; quartz, in places embayed, commonly has inclusions of chlorite which pseudomorph an older mineral. Irregular fractures (1% of rock) are marked by iron-oxide stains and flakes of chlorite and sericite(?). Pyrite euhedra are cemented along a few fractures but also occur disseminated through the rock.

In hand specimen the rock is dark greenish gray that weathers to greenish brown; quartz phenocrysts are glassy, whereas feldspar phenocrysts are milk white. (BB-4; Pl. 22, C)

15. Cataclasite; metarhyolite porphyry. Grain size: groundmass, 0.01 to 0.1 mm; porphyroclasts, 0.01 to 2.0 mm. Fabric: cataclastic, porphyroblastic, porphyroclastic. Groundmass mosaic of quartz and alkali feldspar (78%), feldspar por-

phyroclasts (10%), quartz porphyroclasts (7%), biotite and chlorite (5%); leucoxene, hematite, muscovite, apatite, and sphene occur in trace amounts. Foliation is well defined by lenses of brown biotite (largely altered to chlorite) and by augen of quartz and feldspar. Augen of recrystallized quartz and partly crushed albite porphyroclasts stand out from the finer-grained groundmass. Zones of strongest crushing are richer in biotite and chlorite than the remainder of the rock.

Portions of the hand specimen, a greenish-gray weathering to orange-gray and distinctively foliated rock, have milky white feldspar and glassy quartz phenocrysts typical of undeformed samples of porphyritic rhyolite (*see* description of BB-4, No. 14 above). Samples from the boulder bed member include rock types gradational between those of BB-4 and BB-7; hence the interpretation that this rock is a cataclastically altered porphyry seems warranted. (BB-7; Pl. 23, A, B)

16. Cataclasite; meta-arkose or metarhyolite. Grain size: 0.01 to 0.6 mm. Fabric: cataclastic, porphyroblastic. Micromosaic of quartz and alkali feldspar (87%), quartz porphyroclasts (8%), biotite and muscovite (5%); chlorite, leucoxene, and iron oxides make up trace amounts. The mosaic of quartz and feldspar which forms the bulk of the rock is well foliated; bands of grains with slight differences in grain size and tiny fibers of well-oriented micas provide the foliation. Parts of the rock show a preferred orientation of quartz grains when tested with a gypsum plate. Mica flakes are scattered through the slide but are chiefly concentrated in layers. Muscovite occurs as tiny flakes (0.05 mm long); brown biotite, which is coarser and occurs in clusters, has rims of chlorite. Augen composed of mosaics of quartz are all recrystallized, although the core of one augen of alkali feldspar is a remnant of the original rock.

The hand specimen is composed of alternating lenses of white and dark gray layers up to 2 mm thick.

The parent of this rock was probably either an arkose or rhyolite. (BB-5; Pl. 23, D)

17. Cataclasite. Grain size: porphyroclasts, 0.1 to 3.0 mm; groundmass mosaic, 0.005 to 0.05 mm. Fabric: cataclastic, porphyroclastic. Alkali feldspar porphyroclasts (20%), quartz porphyroclasts (10%); micromosaic of quartz, feldspar, and chlorite (70%); leucoxene and muscovite are present in trace amounts. A strong foliation is produced by aligned chlorite platelets, trains of crushed quartz grains, and "tails" trailing from the porphyroclast augen. The foliation is curved around many porphyroclasts, indicating the latter have undergone rotation during deformation. The rock has undergone severe cataclastic deformation and is approaching a mylonite. The parent rock was apparently a rhyolite porphyry similar to BB-4; this rock represents the highly sheared

end-member of the sequence of metaporphry cobbles.

The hand specimen is a dark, glassy, nearly black pebble that weathers to orange tan. Foliation is present but faint. Porphyroclasts stand out distinctly as light-colored grains in the dark groundmass. (BB-10A, A-690; Pl. 23, C)

18. Graphite metaquartzite. Grain size: groundmass, 0.01 to 0.06 mm; porphyroblasts, 0.1 to 0.4 mm. Fabric: cataclastic, porphyroblastic, feebly schistose. Groundmass of quartz and feldspar(?) (83%), graphite (10%), quartz porphyroblasts (5%), tourmaline (1%), muscovite and biotite (1%), pyrite (tr.). The principal foliation is defined by graphite layers and stretched quartz porphyroblasts; a slip cleavage marked by graphite forms a secondary cleavage athwart the principal one. Minute mica flakes (0.02 mm) are scattered throughout without preferred orientation. Porphyroblasts of tourmaline are the largest grains in the rock.

The hand specimen is coal black where fresh but weathers bluish gray. The principal foliation is contorted. (BB-6; Pl. 22, D)

19. Muscovite-biotite schist. Grain size: 0.05 to 0.4 mm. Fabric: schistose. Quartz-alkali feldspar mosaic (50%), biotite (25%), muscovite (24%), iron ores (1%), chlorite (tr.). The rock has nearly uniform grain size and fabric except for several large clots (2.0 mm) of sericite that are pseudomorphs of feldspar(?). Schistosity is defined by the subparallel orientation of mica and layers of quartz; both minerals seldom more than one grain thick in each layer. Muscovite flakes reach 0.25 mm in length, about twice as long as most biotite flakes.

The hand specimen is dark orange brown weathering to a light orange brown. Dark (biotite-rich) lenses alternate with light lenses; the pod-shape of the dark lenses gives the weathered surface a spotted texture. (BB-8; Pl. 24, A, B)

20. Tourmaline-garnet gneiss. Grain size: 0.45 to 4.0 mm. Fabric: gneissic, coarsely foliated. Quartz (35%), alkali feldspar (35%), muscovite (28%), calcite (1%), tourmaline (1%); garnet, apatite, and hematite are present in trace amounts. Muscovite flakes up to 4.0 mm long are well oriented and are concentrated in irregularly spaced bands. Much quartz is strained, and some large grains are rimmed by a mosaic of finer grains. Feldspar, much of which is microperthite, is very cloudy owing to severe vacuolization and incipient replacement by calcite. Tourmaline and garnet have well-developed sieve textures.

The hand specimen is a light pink weathering to light gray pebble with a distinct foliation but absence of bedding.

The parent of this rock was probably granite. The foliation is not strong, and many feldspar grains have apparently not been recrystallized because they have a xenomorphic rather than granoblastic fabric. (BB-16, A-700; Pl. 24, C)

21. Spotted quartz-biotite-sillimanite schist. Grain size: 0.05 to 0.1 mm. Fabric: granoblastic with scattered "sunburst" spots of sillimanite. Quartz (60%), brown biotite (35%), sillimanite (4%), Muscovite (1%); chlorite, hematite, and apatite are present in trace amounts. Biotite occurs as subequant grains interstitial to quartz. Spots (15% of rock) are an intergrowth of quartz, long slender needles of sillimanite in

radial pattern, and minor muscovite. Spots have diameters up to 4 mm.

The hand specimen is a light pinkish-gray weathering to orange-brown pebble with a distinct foliation. This foliation is not visible in the thin section because the rock was cut perpendicular to the foliation. A sheared zone 2 mm wide cuts the pebble. (BB-24, A-674; Pl. 24, D)

APPENDIX B

LOCATION OF NUMBERED DATA LOCALITIES SHOWN IN FIGURE 3

Geographic features cited are shown on Plates 23 or 24 of P. B. King's 1937 report.)

LOCALITY

1. Northeast flank of Cochran Mountains; area $\frac{1}{4}$ mile square south of bladed ranch road.
2. Area $\frac{1}{4}$ mile square immediately northwest of old county road, $1\frac{1}{2}$ miles southeast of Monument Spring.
- 3A. Small outcrop 3 miles north of Monument Spring.
- 3B. Exposures in Dugout Creek at northwest edge of Payne Hills.
4. Area $\frac{1}{4}$ mile square southeast of Dugout Mountain.
5. Area $\frac{1}{4}$ mile square 4 miles southwest of Maxon.
6. Exposure by arroyo that flows out of the south end of Haymond Mountains syncline; $1\frac{1}{2}$ miles north of southern end of Dimple outcrop.
7. Vicinity of small arroyo $\frac{1}{2}$ mile southeast of the old Bennett Place ($1\frac{1}{4}$ miles southeast of Haymond) and immediately east of San Francisco Creek.
8. Exposures along San Francisco Creek from just south of the Southern Pacific Railroad tracks to $\frac{1}{2}$ mile north of the old Bennett Place, Haymond Mountains.
9. Railroad cut on north side of tracks 2 miles east of Haymond.
- 10A. Area $\frac{1}{2}$ mile square north of the windmill that is $1\frac{1}{2}$ miles west of southwest spur at top of Housetop Mountain.
- 10B. Area $\frac{1}{4}$ mile square at the base of Gap Peak.
11. Area $\frac{1}{8}$ mile square, $1\frac{3}{4}$ miles southeast of the old McFarland Place (which is $3\frac{1}{4}$ miles north-northwest of Haymond).
12. Area $\frac{1}{2}$ mile square south of Cedar Mountain and north of U. S. Highway 90.
13. Area $\frac{1}{4}$ mile square 5 miles south of the Arnold (now McGonigill) ranch headquarters.
14. Area $\frac{1}{4}$ mile square $5\frac{1}{4}$ miles south-southwest of the Arnold (now McGonigill) ranch headquarters just west of the Frog Creek thrust. Outcrop area misprinted as Tesnus on Plate 23 of P. B. King's 1937 report.
15. Area $\frac{1}{8}$ mile square $3\frac{1}{4}$ miles S. 10° E. of Arnold (now McGonigill) ranch headquarters; exposure is north of mesa capped by Cretaceous limestone.
16. Area $\frac{1}{8}$ mile square of exposure that straddles the Pecos-Brewster County boundary, 3 miles south of the Dimple Hills.
17. Exposure in *Chaetetes* hill, 2 miles south of Gap Tank.
- 18A. Vicinity around small conical hill, $1\frac{1}{3}$ miles south-southeast of the Allison ranch headquarters.
- 18B. Strip of outcrop $\frac{1}{4}$ mile long at base of rim of Cretaceous rock $2\frac{1}{2}$ miles southwest of the Allison ranch headquarters.
19. Area $\frac{1}{4}$ mile square on east side of county road, $4\frac{1}{4}$ miles southeast of the Allison ranch headquarters just northwest of Ellis Buttes.
20. Cut by county road $\frac{3}{4}$ mile south of the Allison ranch headquarters.

Plates 3-25

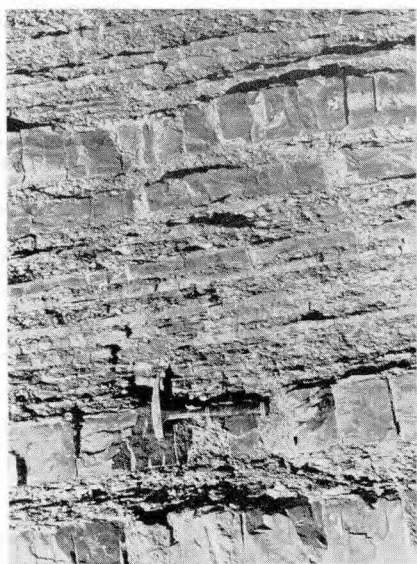
PLATE 3

Haymond outcrops showing the flysch character of the formation

- A. Nearly vertical interbeds of sandstone and shale exposed in road cut on U. S. Highway 90, 3/4 mile east of Lemons Gap. Stratigraphic top is to the right.
- B. Close-up of (A) showing detail of interbedded sandstone and shale. Sandstone beds as thin as 1/2 inch are visible.
- C. Nearly flat-lying section of Haymond flysch composed of alternations of very thin sandstone and shale beds. A thin interval of "microbeds" is visible in lower part of photograph. Locality: Dugout Creek at the west edge of the Payne Hills (Loc. 3B).
- D. Same as (C) but close-up showing detail of shale beds (dark) and sandstone beds (light); some of the latter have ripple-marked tops. A fault cuts the section by the hammer.

Sedimentary Petrology, Haymond Formation

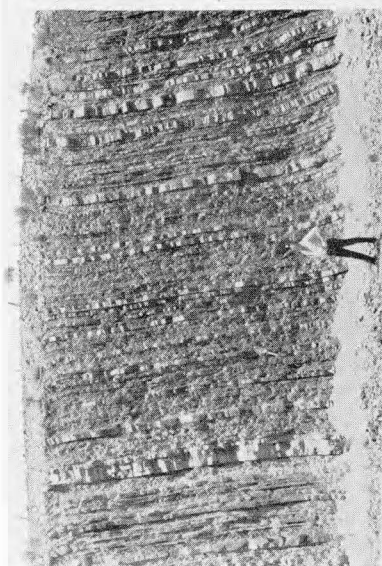
Plate 3



B



D



A



C

Sedimentary Petrology, Haymond Formation

Plate 4

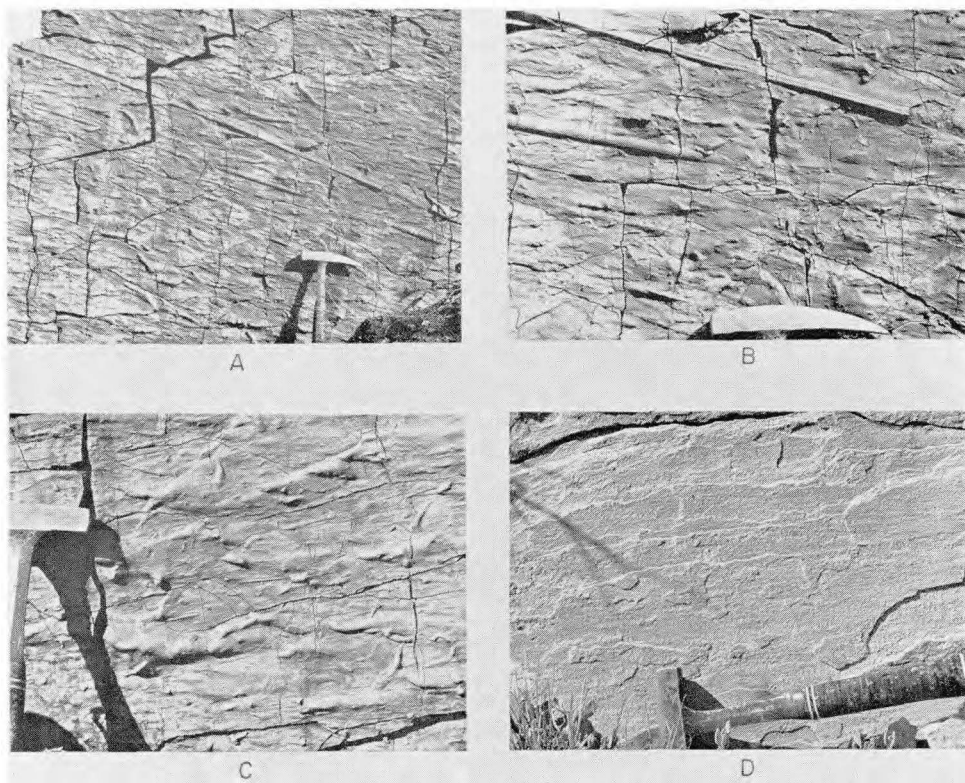


PLATE 4

Directional and other sedimentary structures in Haymond sandstones

- A. Sole (bottom bedding surface) of a sandstone bed showing groove casts (trending upper left to lower right) and pits and trails of trace fossils. Locality: south end of Haymond Mountains (Loc. 6).
- B. Same as (A) but close-up to show details.
- C. Sole of a bed showing short groove casts, shallow flute casts, and trace fossils. The flute casts show that the current moved left to right. Locality: same as (A).
- D. Parting lineation (parallel with hammer handle) exposed in a coarse sandstone bed. Locality: conical hill $\frac{1}{4}$ mile northwest of Clark Butte (Loc. 18A).

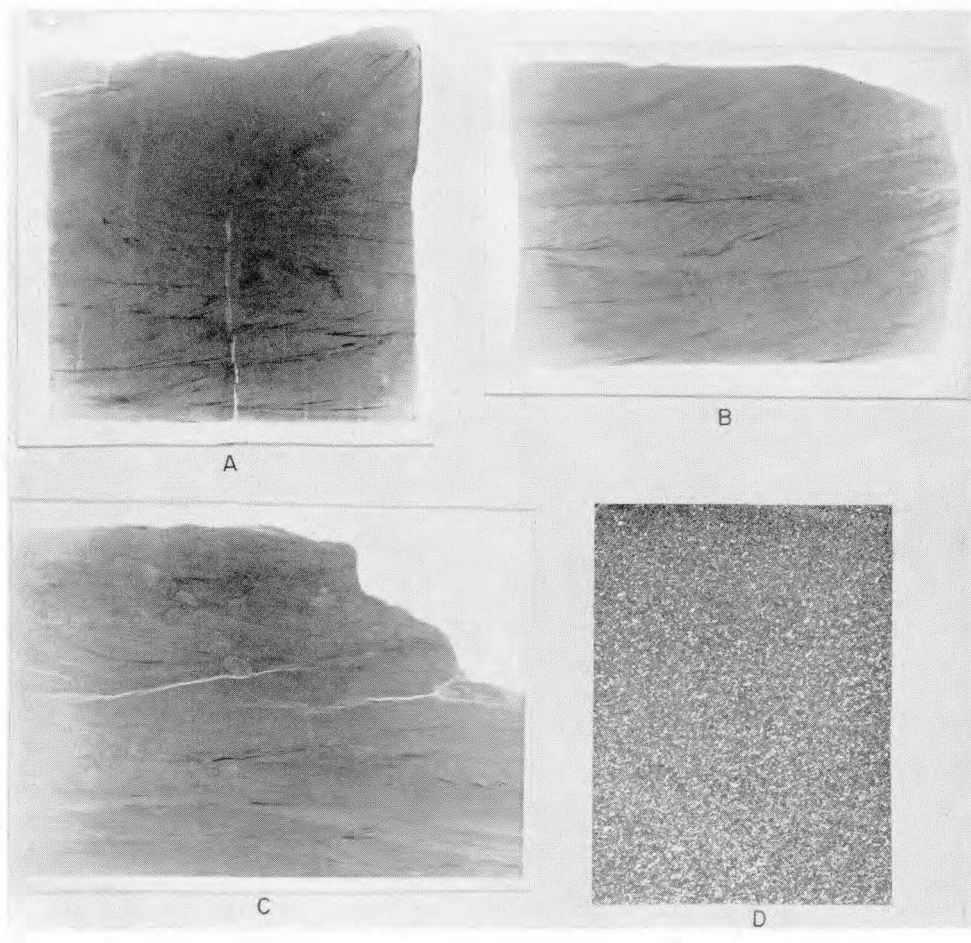


PLATE 5

X-radiographs and negative print of Haymond sandstones showing internal bedding structure
X-radiographs $\times 0.8$

- A. Sandstone bed showing climbing-ripple cross-lamination overlain by overturned cross-lamination grading upward into convoluted laminae. The vertical white streaks are healed fractures.
- B. Sandstone bed showing current-ripple cross-laminae throughout.
- C. Sandstone bed from near the top of the Haymond showing faint current-ripple cross-laminae and disturbed zones produced by burrowing animals (elliptical light patches). Locality: road cut 1 mile south of Allison ranch (Loc. 20).
- D. Graded bedding (fine sandstone at base to very fine sandstone at top) in layer $1\frac{1}{4}$ inches thick. The top $\frac{1}{2}$ inch spalled off during sampling. Photograph by direct enlargement of thin section. Locality 3B.

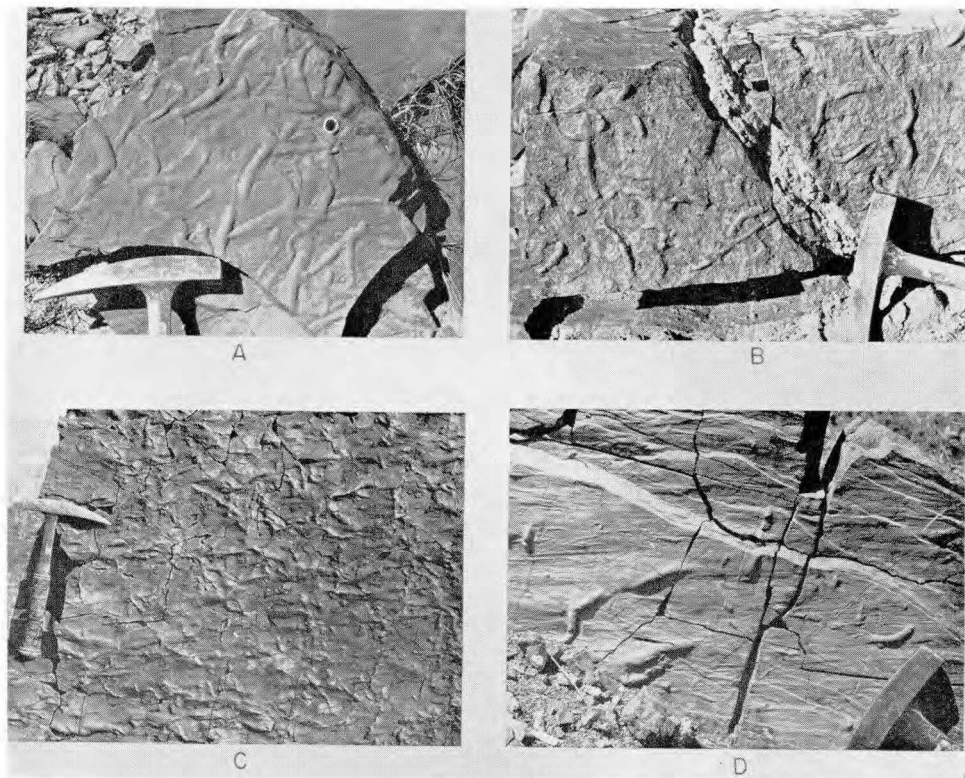


PLATE 6

Trace fossils, current structures, and soft-sediment faults in Haymond sandstones

- A. Sole showing pattern of burrow-fillings parallel to bedding on a float fragment. Locality 15.
- B. Sole showing pattern of burrow-fillings parallel to bedding. Sandstone bed is 8 inches thick. Locality: bed of San Francisco Creek (Loc. 8).
- C. Sole showing pattern of burrow-fillings parallel to bedding. Sandstone bed is 6 inches thick. Locality: south end of Haymond Mountains (Loc. 6).
- D. Sole with groove casts and burrow-fillings cut by soft-sediment normal faults of small displacement. Locality: same as (C).

Sedimentary Petrology, Haymond Formation

Plate 7

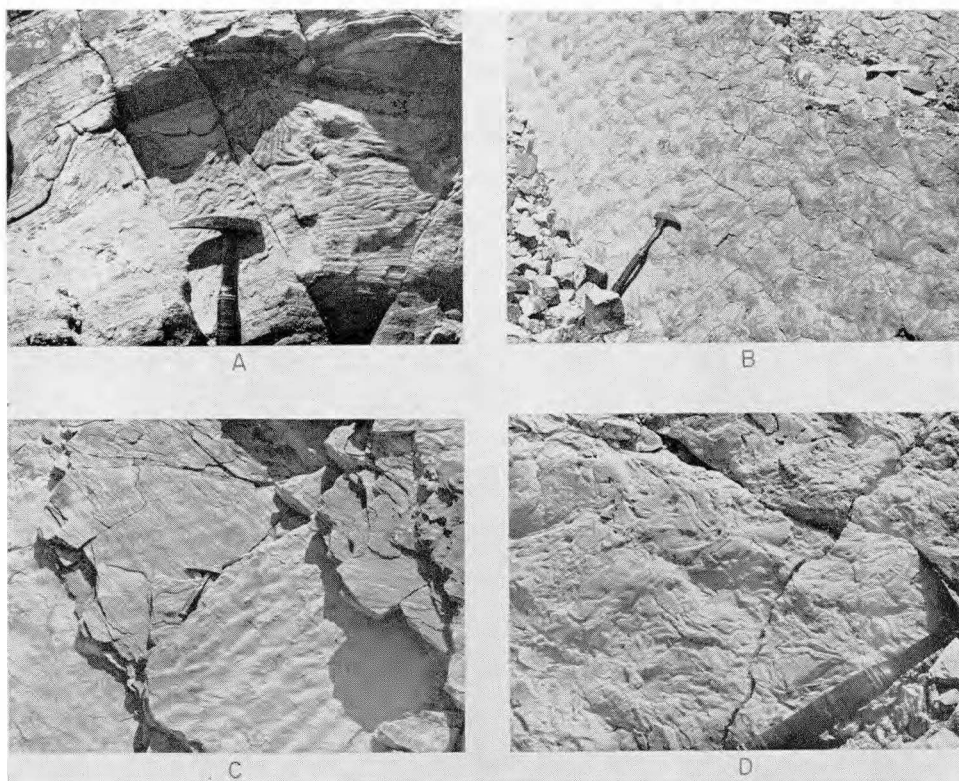


PLATE 7

Bedding features of Haymond sandstones

- A. Contorted laminae in a coarse sandstone bed. Locality: hill slope 1/3 mile northwest of Clark Butte (Loc. 18A).
- B. Unusual exposure of the upper surface of a flysch sandstone bed showing irregular current-ripple marks. Beds lower in the section show effects of soft-sediment deformation; hence it is uncertain whether the irregular ripple forms are the result of deformation or whether they are primary. Locality: 3½ miles south of Dimple Hills (Loc. 15).
- C. Directional features in Haymond sandstone in the Allison Ranch facies. The trend of current-ripples below the hammer is at right angles to parting lineation above the hammer. Locality: road cut 1 mile south of Allison ranch headquarters (Loc. 20).
- D. Top bedding surface showing high density of animal burrows in sandstone of Allison Ranch facies. Burrows are both parallel with and perpendicular to bedding. Locality: same as (C).

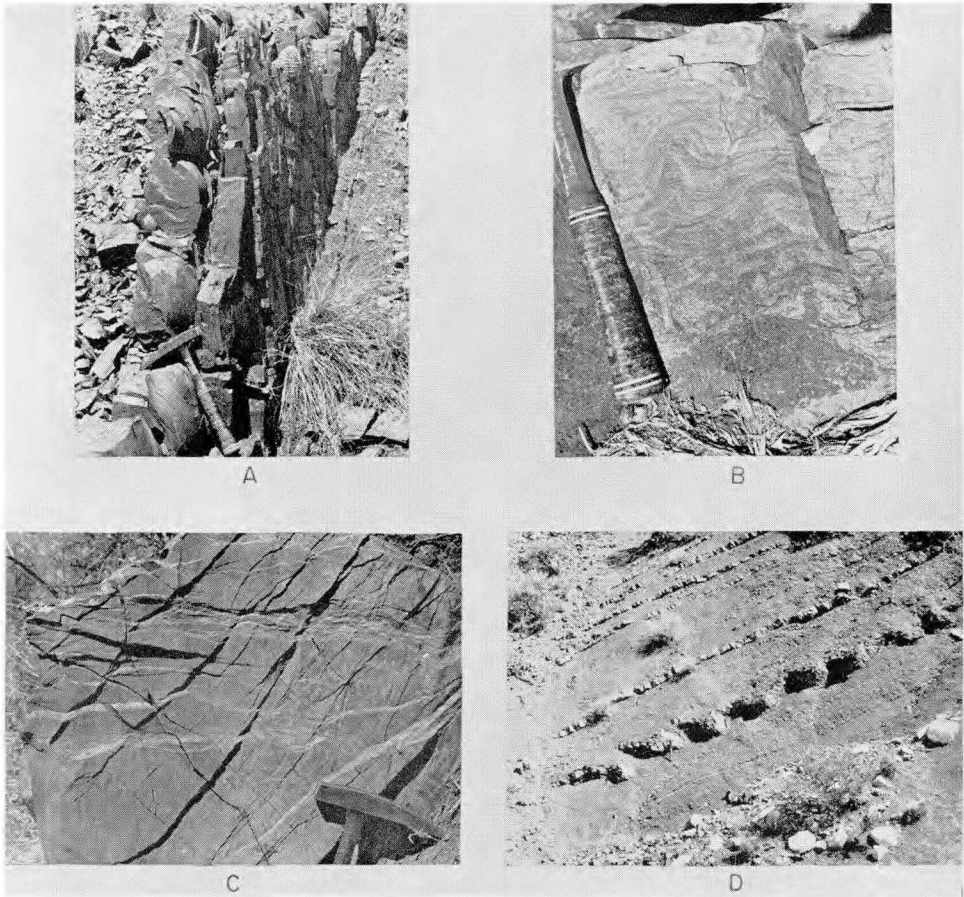


PLATE 8

Sole marks and features of soft-sediment deformation in Haymond sandstones

- A. Ball-and-pillow structure in a 6-inch-thick sandstone bed. Stratigraphic top is to the left. Locality: south end of Haymond Mountains (Loc. 6).
- B. Bed with horizontal laminae at the base and strong convolute laminae just below the top of the bed. Locality: unknown.
- C. Bed broken by two major sets of soft-sediment normal faults. Faint groove casts and a flute cast (extreme upper right) are offset by the faults. Locality: south end of Haymond Mountains (Loc. 6).
- D. Slump-fold involving 3 feet of interbedded sandstone and shale. Beds above and below the contorted zone are not disturbed except for regional dip. Slump motion was to the left. Locality: base of Housetop Mountain on the east limb of the synclinal fold (above the boulder bed member).

Sedimentary Petrology, Haymond Formation

Plate 9

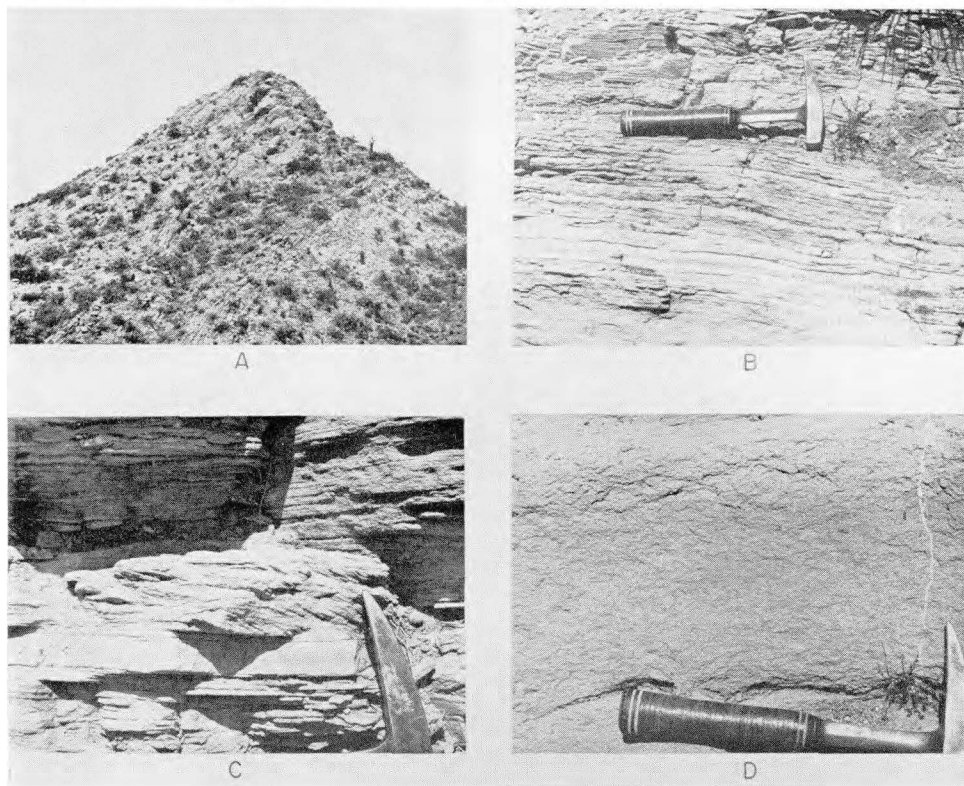
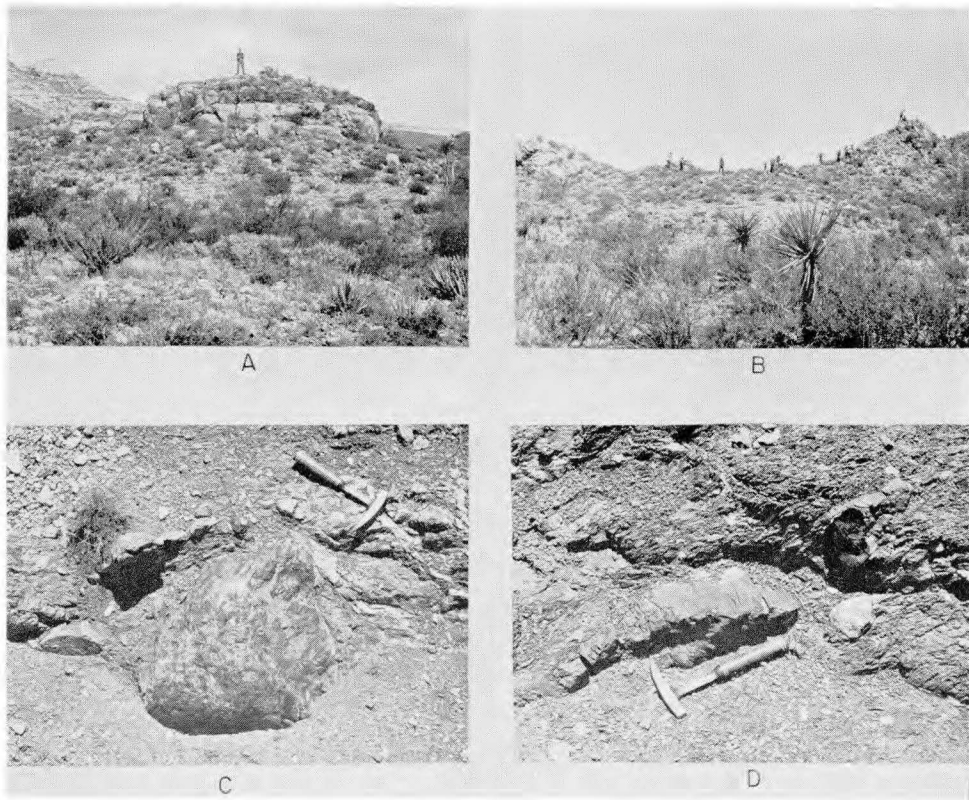


PLATE 9

Features of coarse (non-flysch) sandstone beds

- A. View toward the west showing hill supported by thick beds of coarse sandstone. The chief boulder-bearing unit is just outside the view of the photograph to the right. Man for scale.
- B. Horizontally laminated sequence in coarse sandstone beds.
- C. Three thin beds of current-ripple cross-laminae (cross-laminae inclined to the right) intercalated with horizontally laminated beds.
- D. Very coarse sandstone showing massive (structureless) bedding. True bedding is parallel with the length of the photograph. The white line is a calcite-filled joint.

All beds are on the conical hill $\frac{1}{2}$ mile northwest of Clark Butte (Loc. 18A).

**PLATE 10****Boulder bed member southwest of Housetop Mountain**

- A. Block of fossiliferous Pennsylvanian limestone 100 feet long. Bedding in the block is essentially parallel with bedding in the Haymond. Locality: 100 yards east of the windmill at the base of Housetop Mountain (Loc. 10A).
- B. Small knobs supported by erratic blocks in the boulder bed member. View looking northeast. Locality: same as (A).
- C. Rounded boulder of black Maravillas chert embedded in mudstone and contorted sandstone beds. Locality: arroyo 1/8 mile east of the windmill at the base of Housetop Mountain.
- D. Limestone cobble (white) and smaller fragments embedded in shale and mudstone with interbedded deformed sandstone (resistant layer of irregular thickness). Locality: vicinity 3/4 mile east of the windmill at the base of Housetop Mountain.

Sedimentary Petrology, Haymond Formation

Plate 11

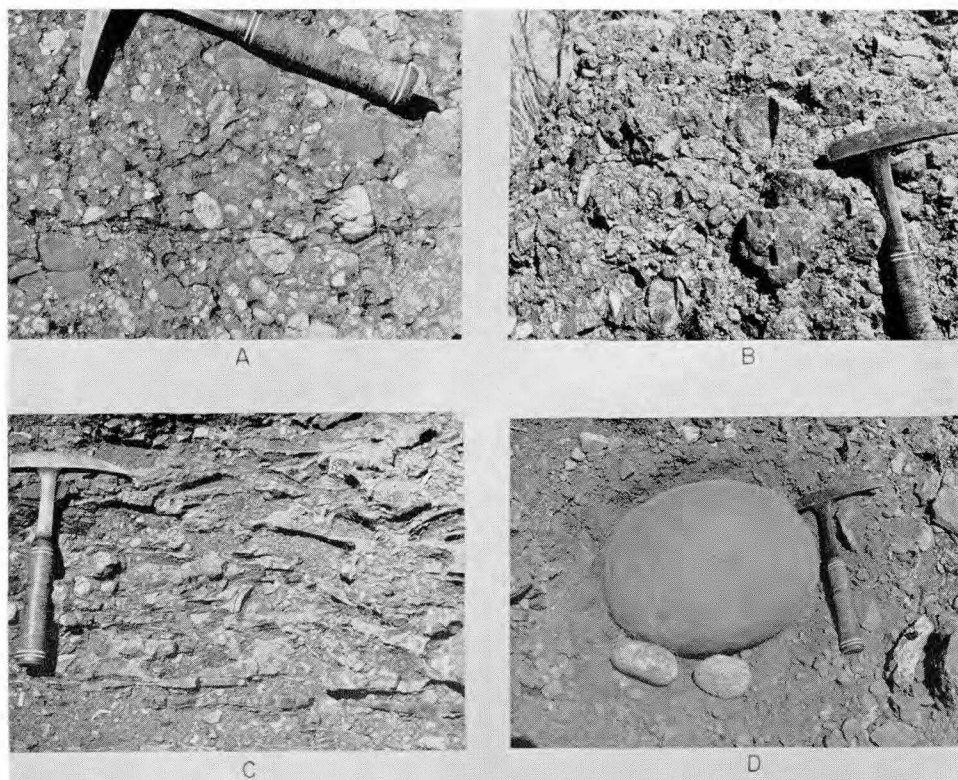


PLATE 11

Boulder bed member from the vicinity southwest of Housetop Mountain

- A. Polymictic conglomerate bed 3 feet thick in the lower part of the boulder bed unit. Most clasts are rounded pebbles of sandstone, metamorphic rock, and igneous rock unlike older Paleozoic rocks in the region. Matrix is muddy arkose. Locality: $\frac{3}{4}$ mile northeast of the windmill at the base of Housetop Mountain.
- B. Conglomerate bed (breccia bed of P. B. King) 4 feet thick composed chiefly of angular clasts of chert and novaculite derived from the Maravillas and Caballos Formations. Matrix is muddy arkose. Locality: $\frac{1}{2}$ mile northeast of the windmill at the base of Housetop Mountain (unit C south of section C-C' on P. B. King's (1937) Plate 10).
- C. "Shale-pod" conglomerate bed in the boulder bed member. Slabs of fragmented shale beds lie with subparallel orientation in a muddy arkose matrix. Scattered cobbles occur in this lithology. Locality: $\frac{1}{2}$ mile east-northeast of the windmill at the base of Housetop Mountain in the second arroyo north from the large gravel pediment.
- D. Boulder of quartzite and cobbles of metarhyolite (left) and granite (right) from the boulder bed member showing high degrees of roundness. The quartzite boulder exhibits an unusually high sphericity. Locality: same as (A).

Sedimentary Petrology, Haymond Formation

Plate 12

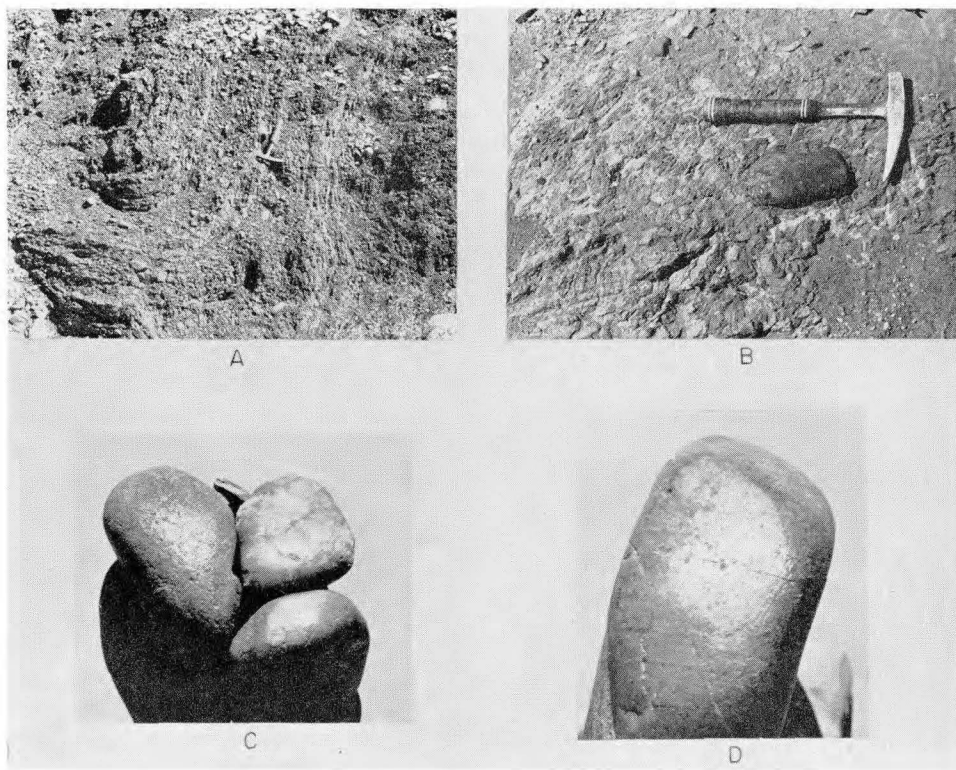


PLATE 12

Details of the boulder bed member and polished and striated pebbles

- A. Synclinal slump-fold in pebbly mudstone. Locality: west of Housetop Mountain, 2 miles northeast of the windmill at the base of the mountain.
- B. Close-up of chert pebble encased in mudstone. The irregular jointing in the mudstone reflects the absence of bedding. Locality: west of Housetop Mountain, vicinity $\frac{1}{2}$ mile east of the windmill at the base of the mountain.
- C. Pebbles with polished surfaces. The sandstone (left), vein quartz (top right), and quartzite pebbles were encased in mudstone. About 0.4 natural size.
- D. Polished and striated quartzite pebble removed from mudstone. About 0.8 natural size.

Sedimentary Petrology, Haymond Formation

Plate 13

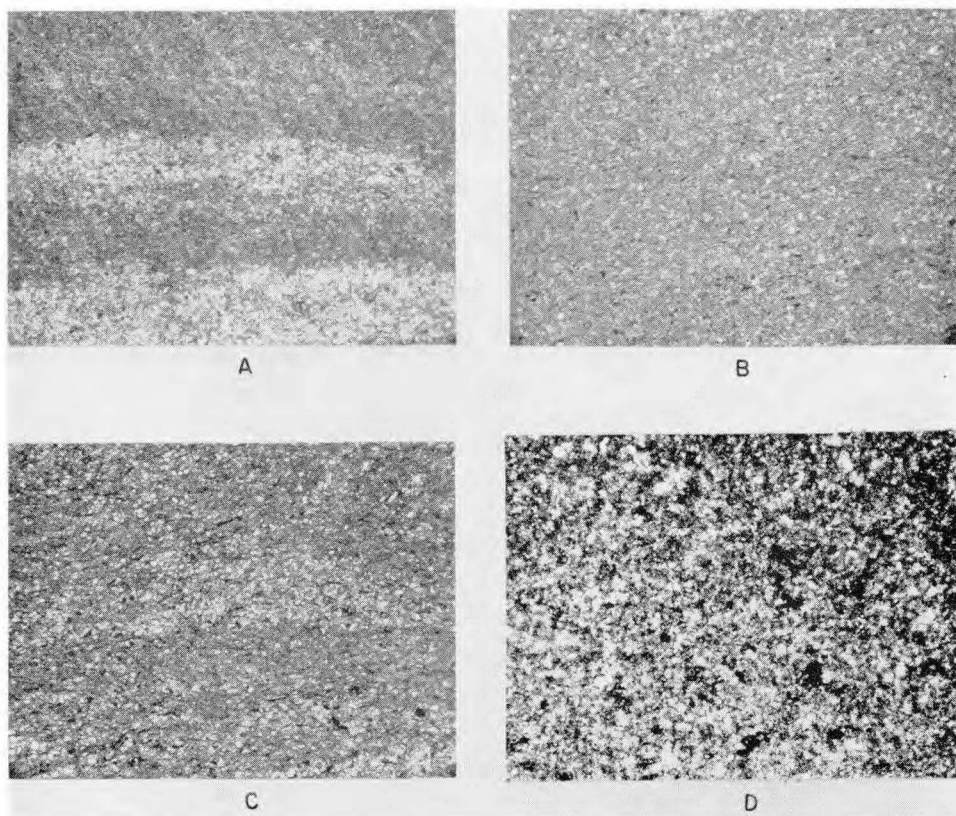


PLATE 13

Photomicrographs of Haymond shales
All $\times 19$, plain light

- A. Clay-shale with silt laminae. This sample shows negligible effects of burrowing animals. Diagonal streaks are saw marks on the thin section. (Hs-24A)
- B. Clay-shale. No vestige of bedding remains in this intensely burrowed shale. (Hs-28A)
- C. Silt-shale. A vestige of original bedding is preserved in this moderately burrowed shale. Black particles are plant fragments. (Hs-13)
- D. Carbonaceous clay-shale. Plant fragments make up from 10 to 15 percent of this shale. (Hs-20)

Sedimentary Petrology, Haymond Formation

Plate 14

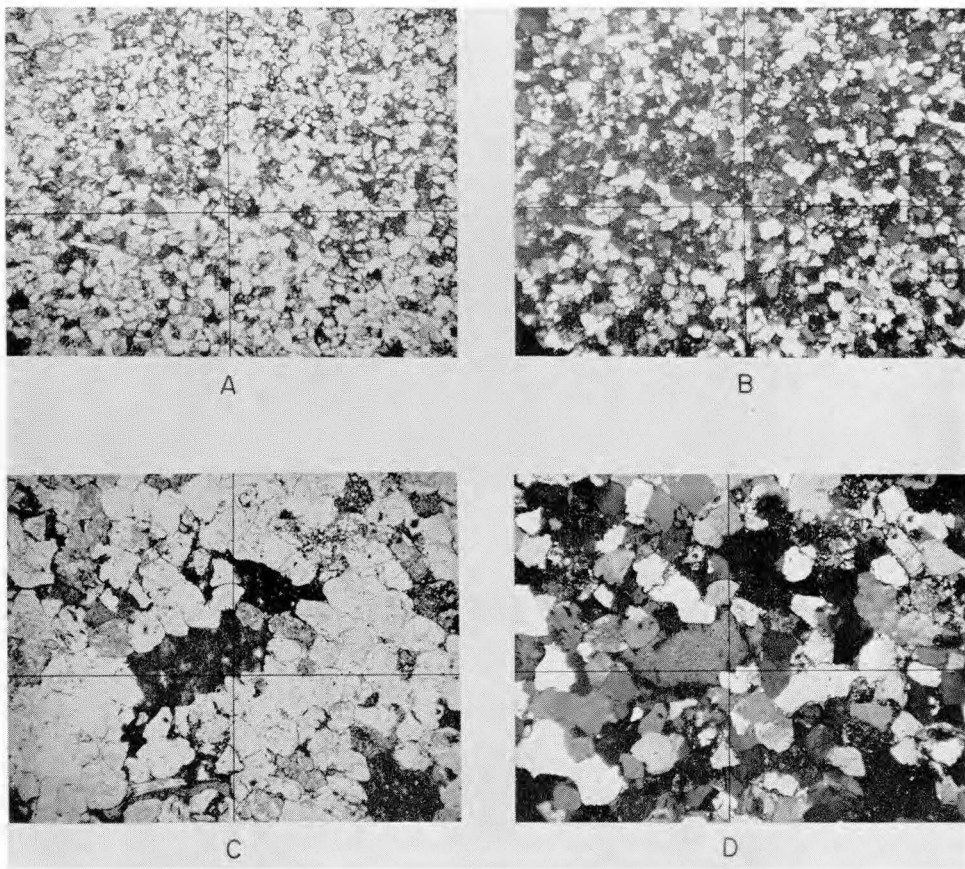


PLATE 14

Photomicrographs of flysch sandstones from below the coarse sandstone and boulder beds
All $\times 19$

- A. Laminated very fine and fine sandstone: calcitic immature lithic arkose.¹⁶ Laminae trend parallel with the east-west cross-hair. Plain light. (H-36)
- B. Same as (A) but with crossed nicols.
- C. Medium sandstone: silicic immature feldspathic sublitharenite. Dark grains are SRF's (shale). Strong compaction effects are shown by crinkled mica (lower left quadrant) and by SRF's embayed by quartz (at cross-hairs). Plain light. (H-10)
- D. Same as (C) but with crossed nicols.

¹⁶Sandstone descriptions follow the five-fold scheme of Folk (1954), as follows: (grain-size term): (cement) (textural maturity) (miscellaneous transported constituents) (clan name).

Sedimentary Petrology, Haymond Formation

Plate 15

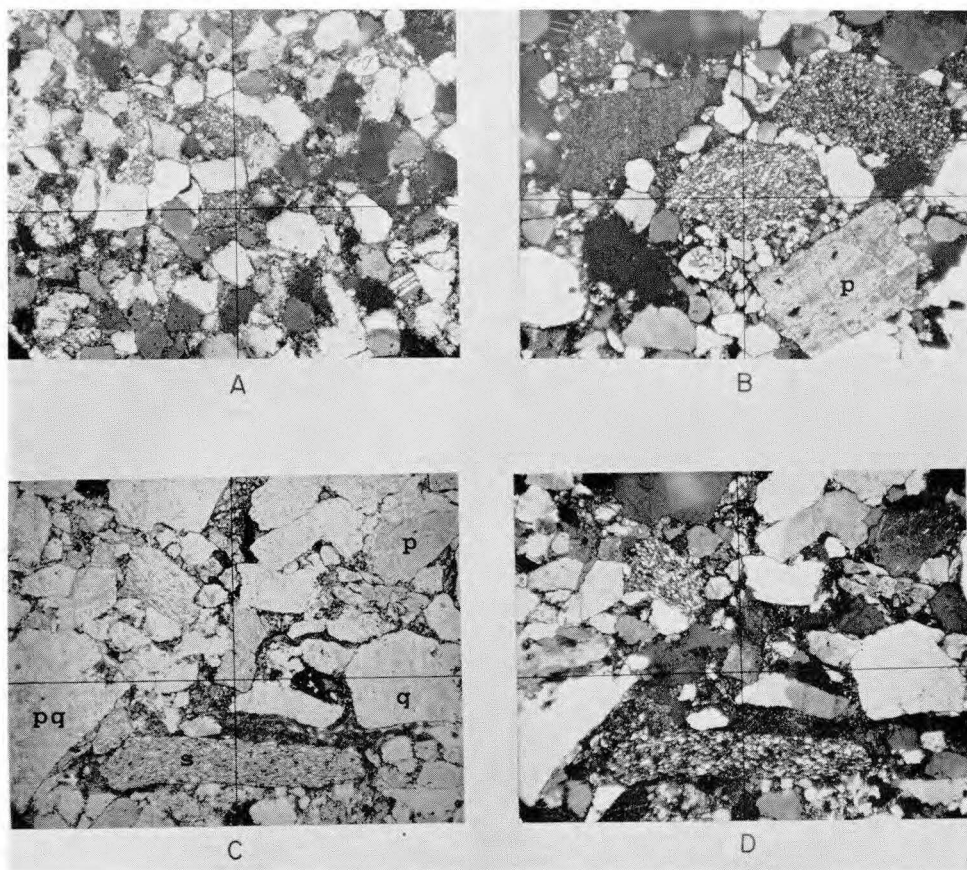


PLATE 15

Photomicrograph of sandstones from below the boulder bed member

All $\times 19$

- A. Medium sandstone: immature subarkose. Cross-hairs rest on a feldspar grain replaced by calcite. Crossed nicols. (H-28)

Photomicrographs of coarse (non-fiysch) sandstone

- B. Very coarse sandstone: immature feldspathic sublitharenite. Cross-hairs rest on a sheared VRF; the large grain in the upper right quadrant is a siltstone fragment. Crossed nicols. (H-105)
- C. Coarse sandstone: immature lithic arkose. Numerous grains have sutured contacts. Plain light. (H-30)
- D. Same as (C) but with crossed nicols.

Q, quartz; P, plagioclase; S, schist; Pq, polycrystalline quartz

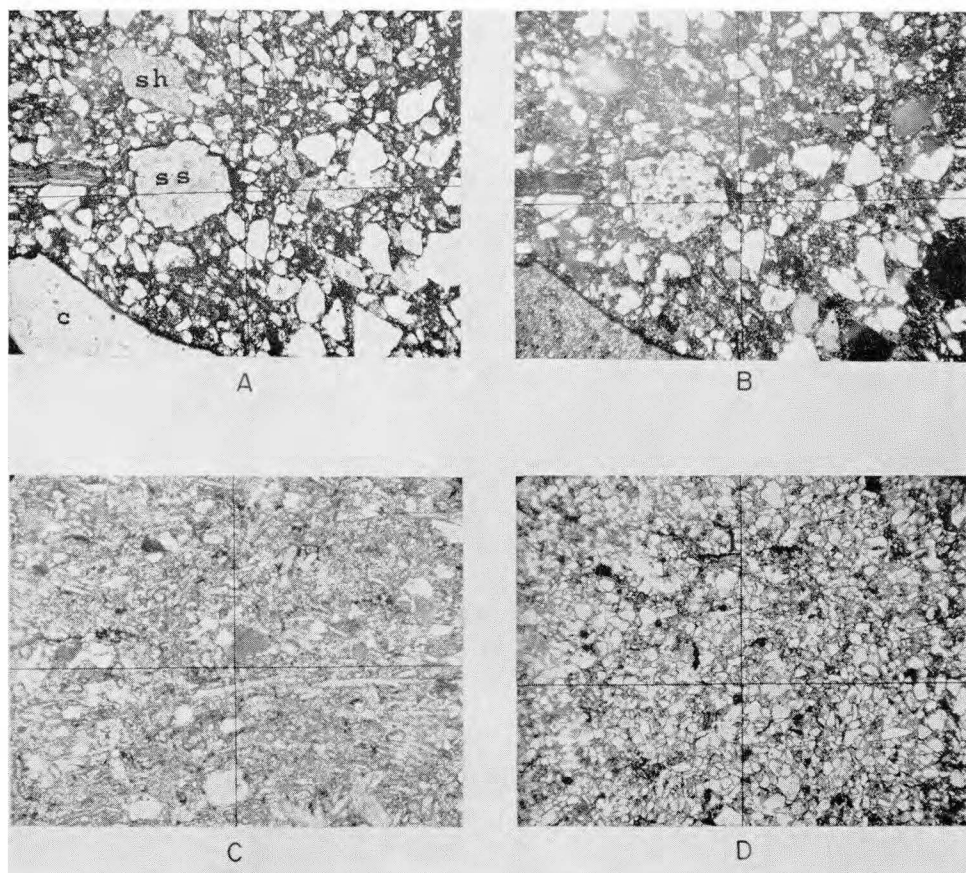


PLATE 16

Photomicrographs of mudstone from the boulder bed member

- A. Mudstone (muddy sandstone). Dark matrix is organic-rich clay. Plain light. $\times 19$. (H-91)
- B. Same as (A) but with crossed nicols.

Photomicrograph of the spicule (?) bed from the Dugout Mountain area

- C. Spicular limestone. The calcite spicules have a preferred orientation parallel with the east-west cross-hair (parallel with bedding). Plain light. $\times 60$. (H-114A)

Photomicrograph of a burrowed sandstone from above the boulder bed member

- D. Clayey fine sandstone. Grains and plant fragments show no preferred orientation. The east-west cross-hair is parallel with bedding. Plain light. $\times 19$. (H-231)

C, chert; Ss, siltstone; Sh, shale

Sedimentary Petrology, Haymond Formation

Plate 17

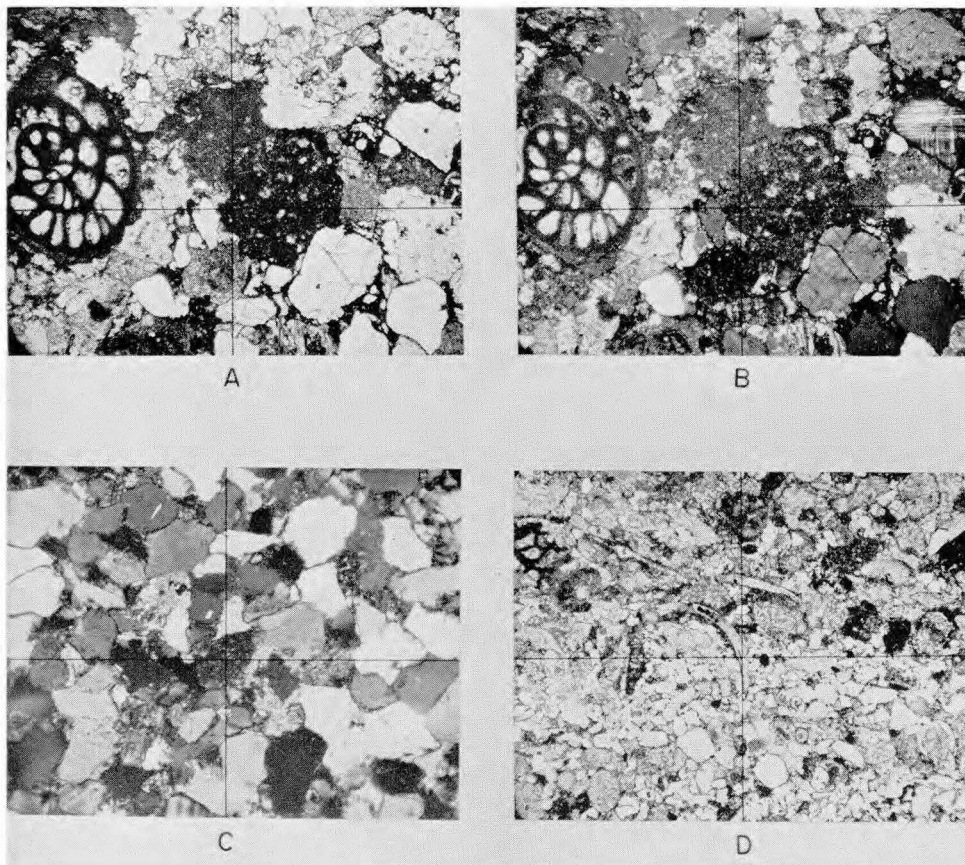


PLATE 17

Photomicrographs of sandstones from the Dugout Mountain area

All $\times 19$

- A. Coarse sandstone: calcitic feldspathic litharenite. Cross-hairs rest on a limestone fragment. A cross section of a fusulinid is at the extreme left. Plain light. (H-115)
- B. Same as (A) but with crossed nicols.
- C. Medium sandstone: calcitic and silicic submature lithic arkose. Cross-hairs rest on a VRF. Crossed nicols. (H-109)
- D. Interlaminated calcarenite (above east-west cross-hair) and calcarenitic arkose (below cross-hair). Coarse-grained laminae are rich in carbonate detritus, whereas fine-grained laminae are rich in silicate mineral detritus. Plain light. (H-114)

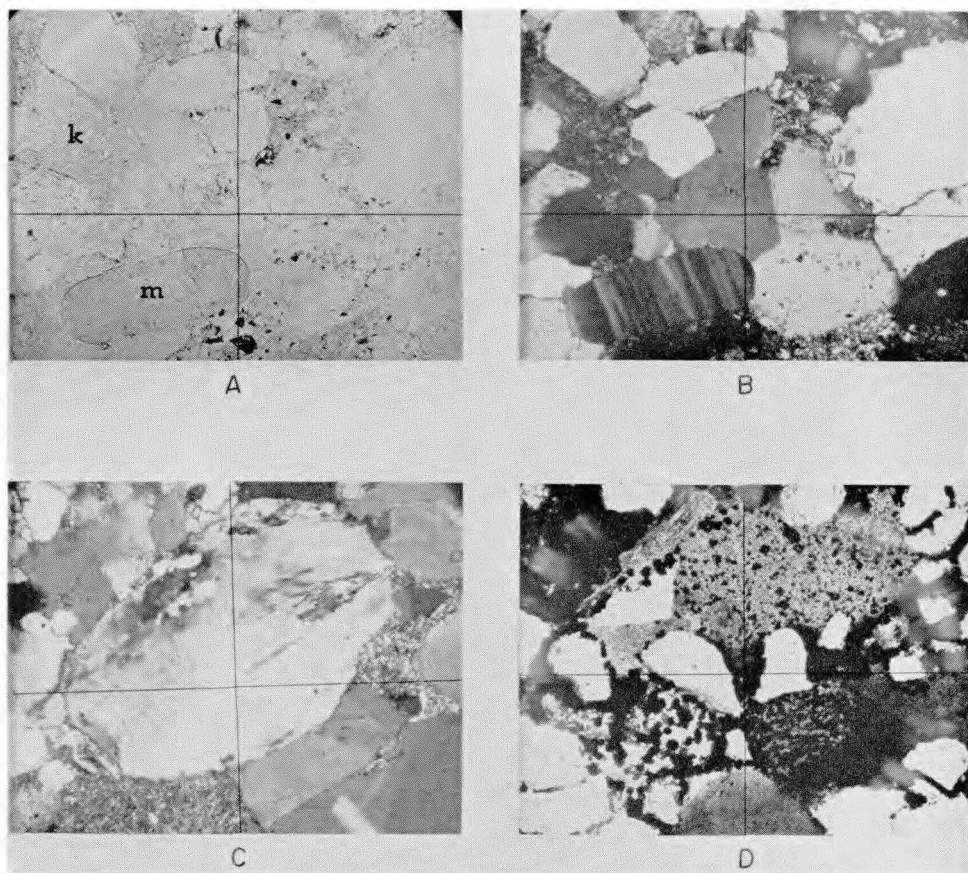


PLATE 18

Photomicrographs of sandstones showing diagenetic features

All $\times 60$

- A. Sandstone cemented by quartz overgrowths. Overgrowths can be distinguished from detrital cores only where the cores are rimmed by hematite "dust." A small patch of authigenic kaolinite which appears to be a pore-filling is shown in the upper left quadrant. Plain light. (H-97)
- B. Same as (A) but with crossed nicols.
- C. Large polycrystalline quartz grain showing sutured contacts with adjacent grains. Crossed nicols. (H-97)
- D. Tiny opaque hematite grains are pseudomorphs of ankerite or siderite rhombs. Large dark grains are SRF's (shale). The shale grain above the cross-hairs is deeply embayed by more resistant quartz grains. Plain light. (H-95)

M, microcline; K, kaolinite

Sedimentary Petrology, Haymond Formation

Plate 19

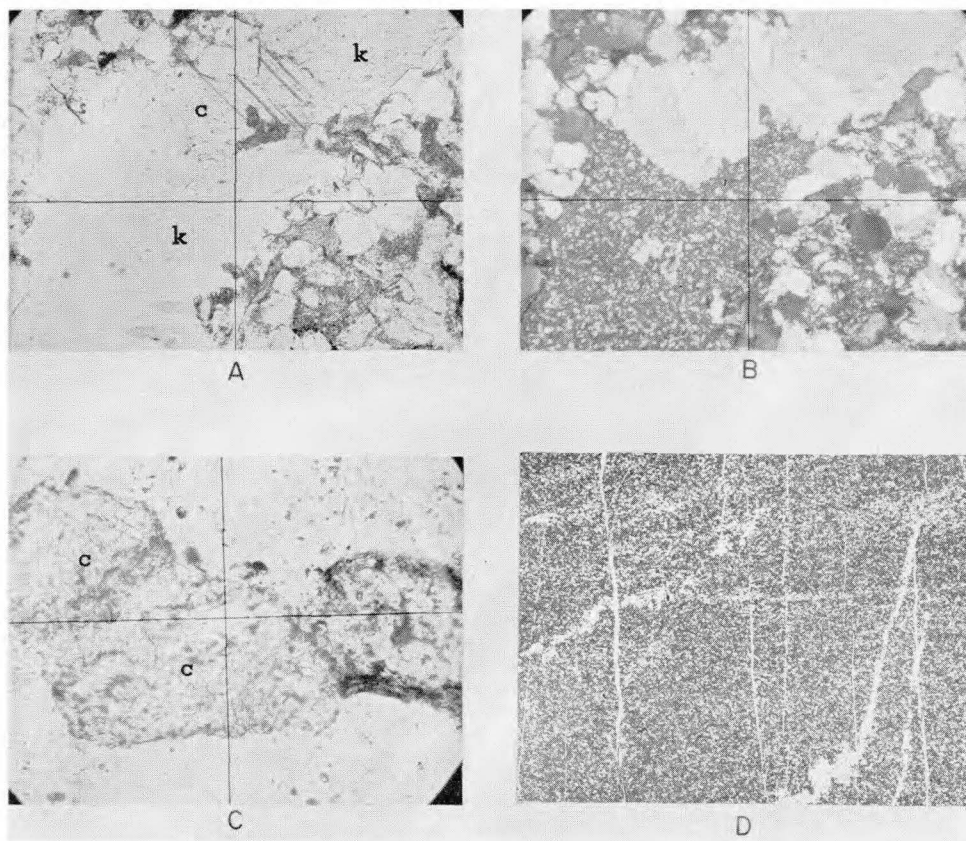


PLATE 19

Photomicrographs and negative print of sandstones showing diagenetic features

- A. Kaolinite-cemented sandstone. Authigenic kaolinite fills pores and a fracture that trends upper right to lower left. Calcite (C) is younger than kaolinite (K). Plain light. $\times 19$. (H-212)
- B. Same as (A) but with crossed nicols.
- C. Calcite (C) pseudomorphs of feldspar grains (at cross-hair and at left). Cross-hair rests on unreplaced core of feldspar. Dark grain at right is a VRF. Plain light. $\times 235$. (H-4)
- D. Negative print of fine-grained sandstone. Narrow vertical white lines are joints filled with ankerite-siderite and quartz; larger sinuous zones are where ankerite-siderite has replaced the host rock. About one-half the carbonate has been altered to iron oxides. $\times 3$. Crossed nicols. (H-216)

Sedimentary Petrology, Haymond Formation

Plate 20

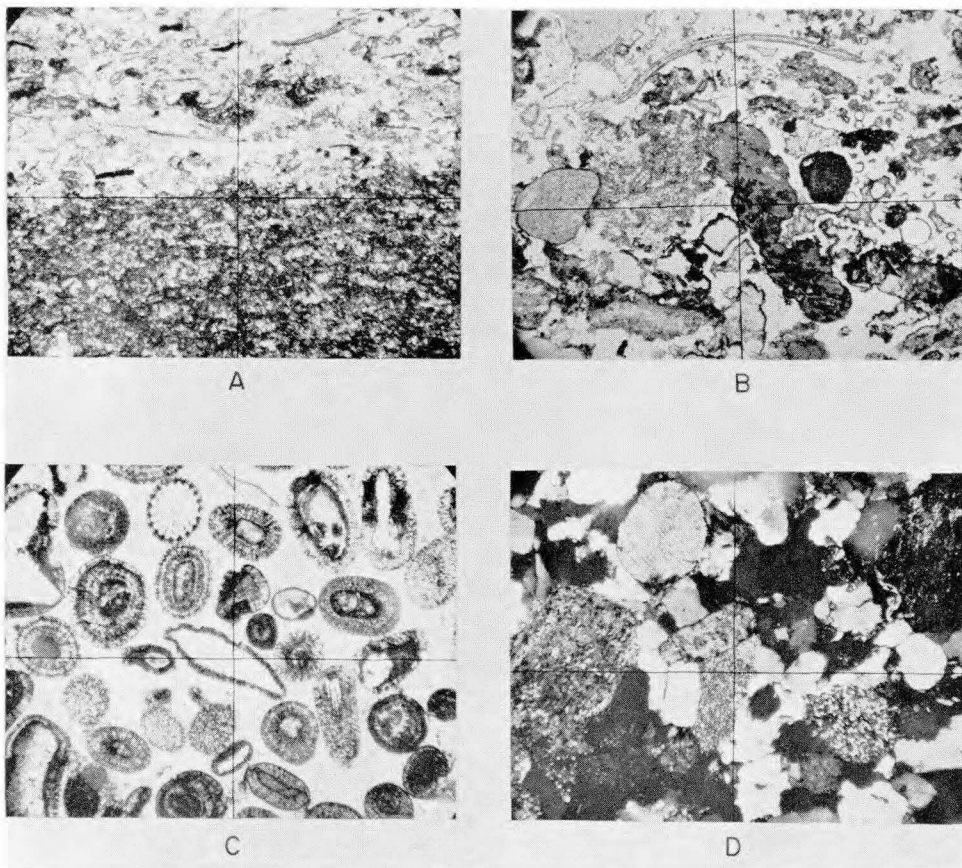


PLATE 20

Photomicrographs of sedimentary rocks from the boulder beds
All $\times 19$

- A. Limestone. Organic-rich microsparite in lower part and biosparite in upper part. Plain light. (No. 1)¹⁷
- B. Chertified limestone. White interstitial material is chalcedony. Cross-hairs rest on a phosphate grain. Plain light. (No. 2)
- C. Limestone (oosparite). Clear cement is sparry calcite. Cross-hairs rest on an echinoderm fragment that has a superficial oolite coating. Plain light. (No. 3)
- D. Sandstone. Coarse arkose. The field shows several rock fragments. Crossed nicols. (No. 5)

¹⁷ Numbers on Plates 20-24 refer to the sequence of rocks described in Appendix A.

Sedimentary Petrology, Haymond Formation

Plate 21

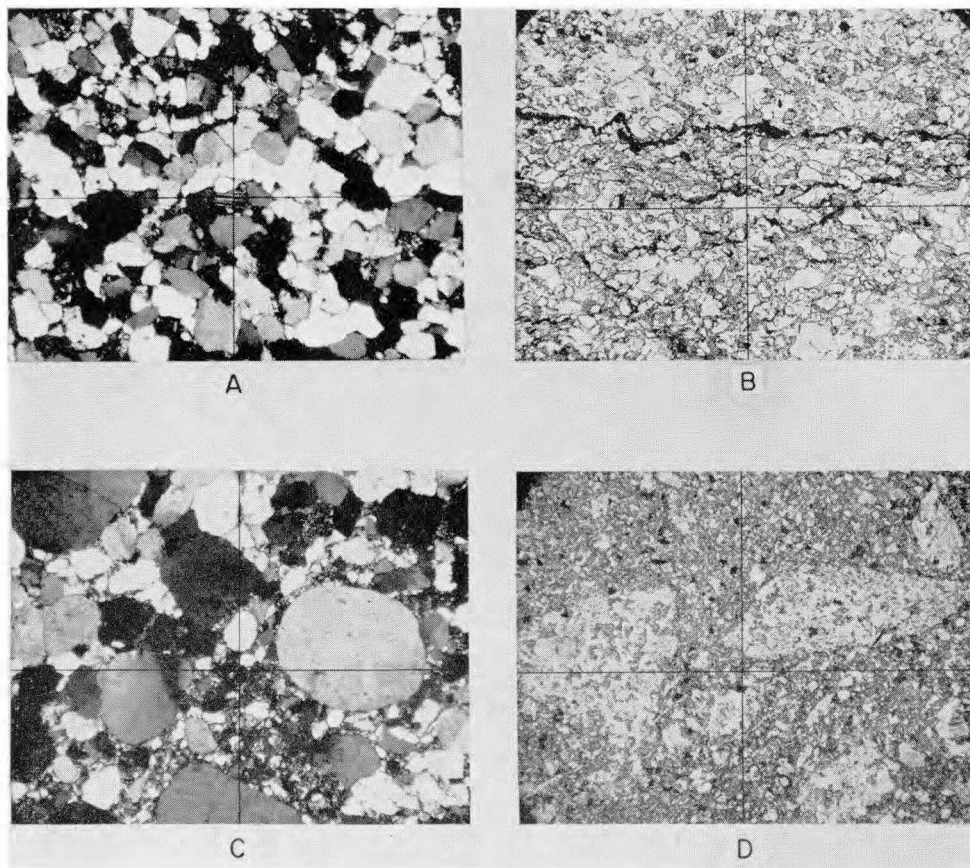


PLATE 21

Photomicrographs of sandstones and metasandstone from the boulder bed member
All $\times 19$

- A. Sandstone. Medium-grained: slightly silicified immature subarkose. Crossed nicols. (No. 7)
- B. Slightly sheared sandstone. Fine-grained: immature lithic subarkose. Dark bands that are parallel with the east-west cross-hairs are microstylolites. Plain light. (No. 8)
- C. Quartzite. Coarse-grained: silicified supermature quartz-arenite. The fine-grained matrix is crushed quartz. Crossed nicols. (No. 9)
- D. Metasandstone breccia. Large particles are breccia fragments of fine-grained sandstone. Darker colored background is the "paste" of crushed grains. Plain light. (No. 11.)

Sedimentary Petrology, Haymond Formation

Plate 22

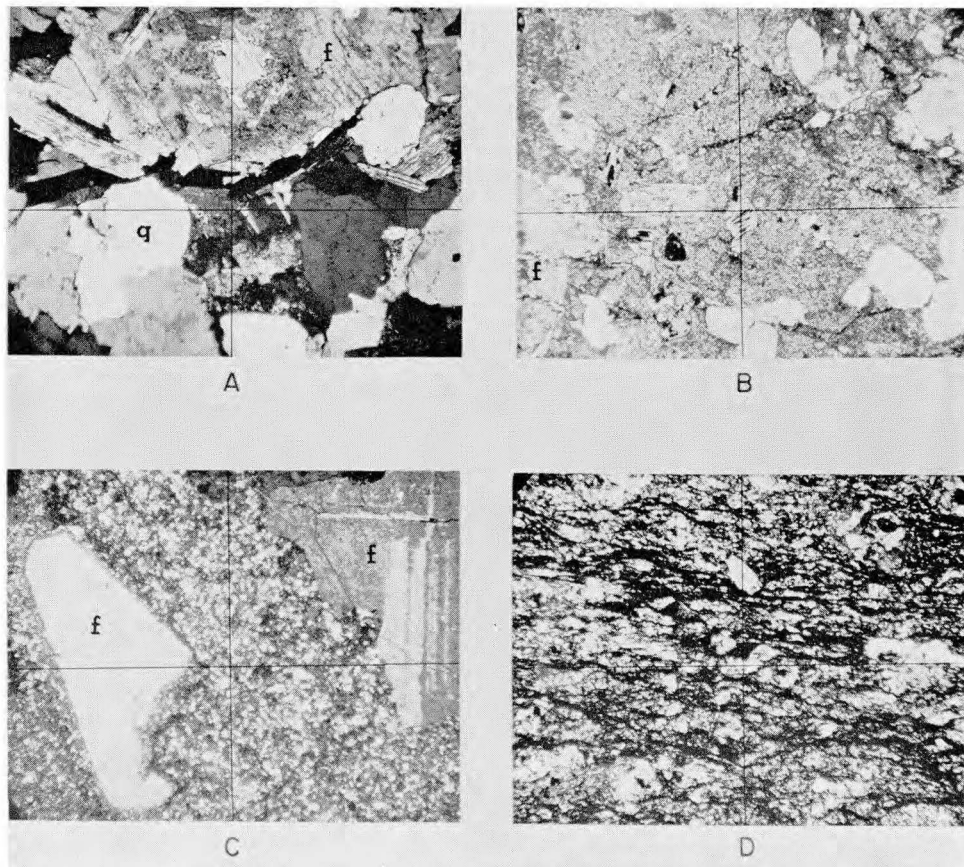


PLATE 22

Photomicrographs of igneous and metamorphic rocks from the boulder bed member
All $\times 19$

- A. Granite. Crossed nicols. (No. 12)
- B. Altered rhyodacite (?). Cross-hairs rest on a chlorite grain with aligned hematite inclusions. Plain light. (No. 13)
- C. Rhyolite porphyry. Crossed nicols. (No. 14)
- D. Graphitic metaquartzite. The clear grain cut by the top vertical cross-hair is a tourmaline porphyroblast. The dark areas are graphite. Plain light. (No. 18)

Q, quartz; F, albite and alkali feldspar

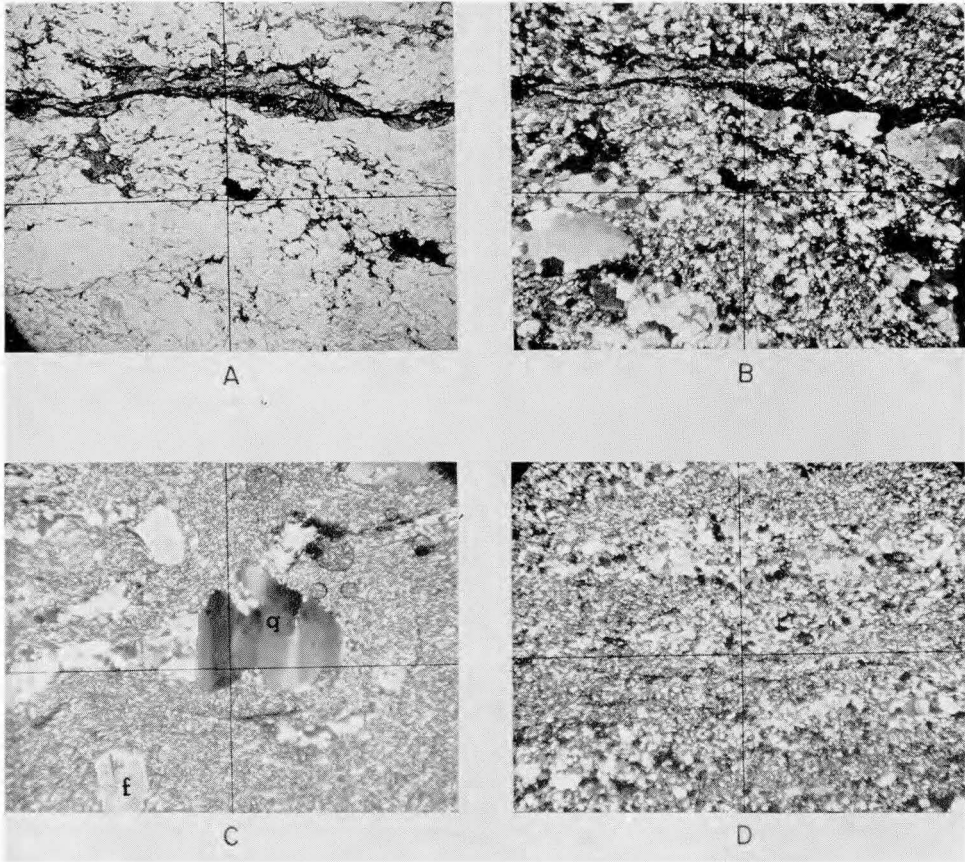


PLATE 23

Photomicrographs of metamorphic rocks from the boulder bed member
All $\times 19$

- A. Cataclasite; metaporphyry. (No. 15)
- B. Same as (A) but with crossed nicols.
- C. Cataclasite; metaporphyry. Section shows arcuate "tails" of recrystallized quartz around the porphyroblast. Spherical patches are bubbles in the Canada balsam. Crossed nicols. (No. 17)
- D. Cataclasite. Crossed nicols. (No. 16)

Q, quartz; F, alkali feldspar

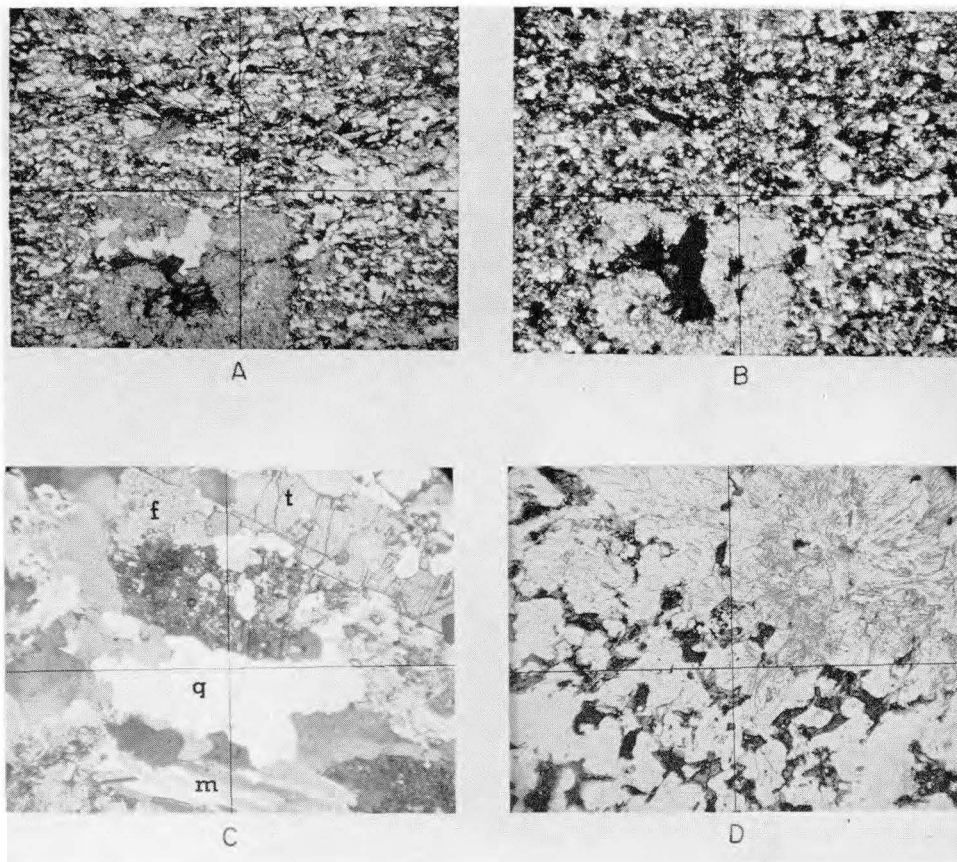


PLATE 24

Photomicrographs of metamorphic rocks from the boulder bed member
All $\times 19$

- A. Muscovite-biotite schist. Plain light. (No. 19)
- B. Same as (A) but with crossed nicols.
- C. Tourmaline-garnet gneiss. Crossed nicols. (No. 20.)
- D. Spotted quartz-biotite-sillimanite schist. The porphyroblast in the upper right quadrant is an intergrowth of quartz, muscovite, and sillimanite. The thin section is cut perpendicular to the foliation and lineation and thus the schistose fabric is not apparent. (No. 21)

Q, quartz; T, tourmaline; F, feldspar; M, muscovite

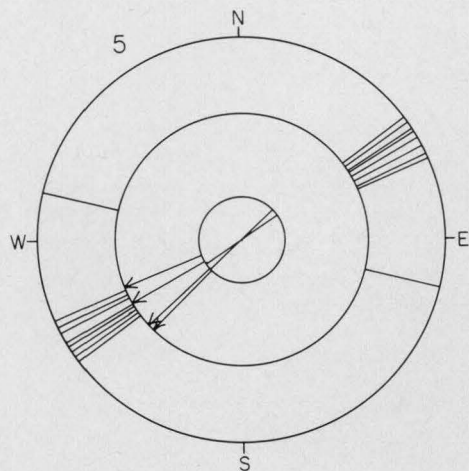
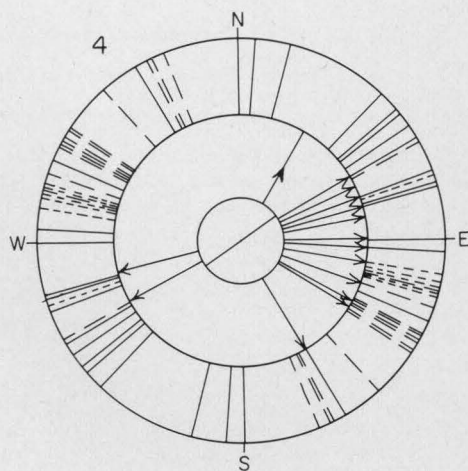
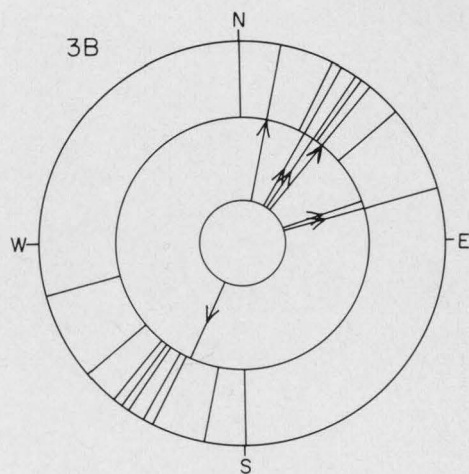
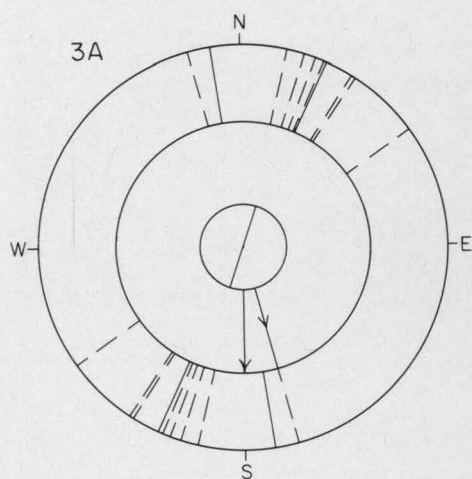
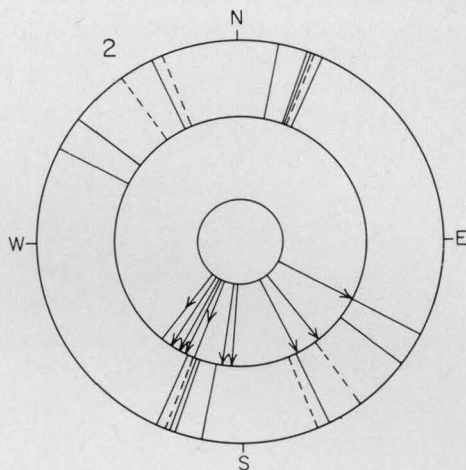
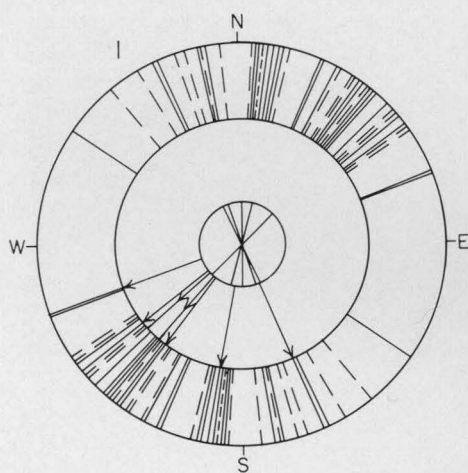
PLATE 25

Diagrams showing orientation of directional sedimentary structures

(Location of stations is shown in figure 3.)

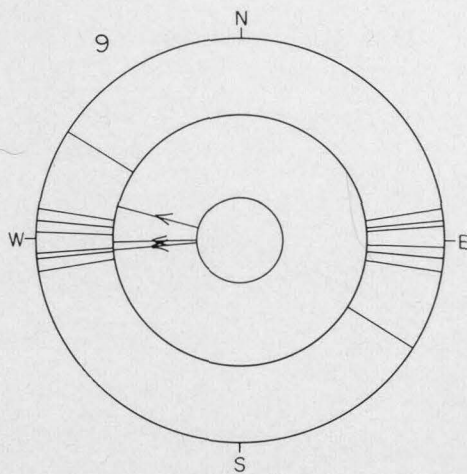
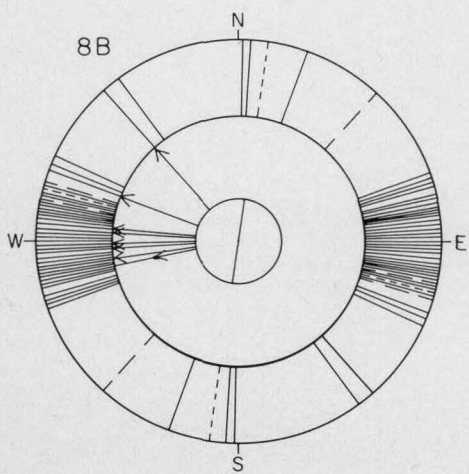
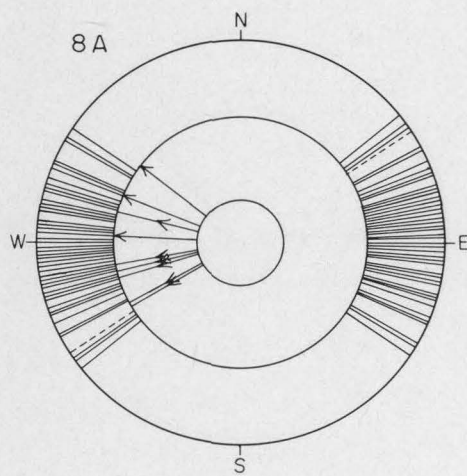
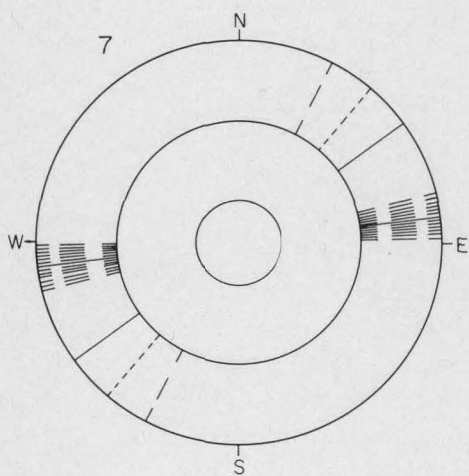
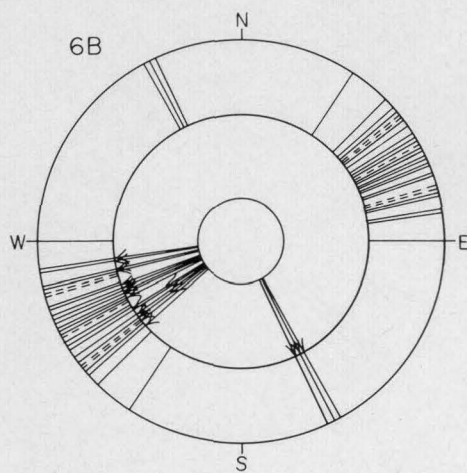
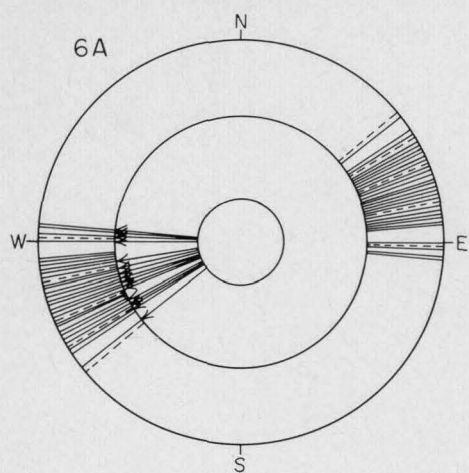
Sedimentary Petrology, Haymond Formation

Plate 25



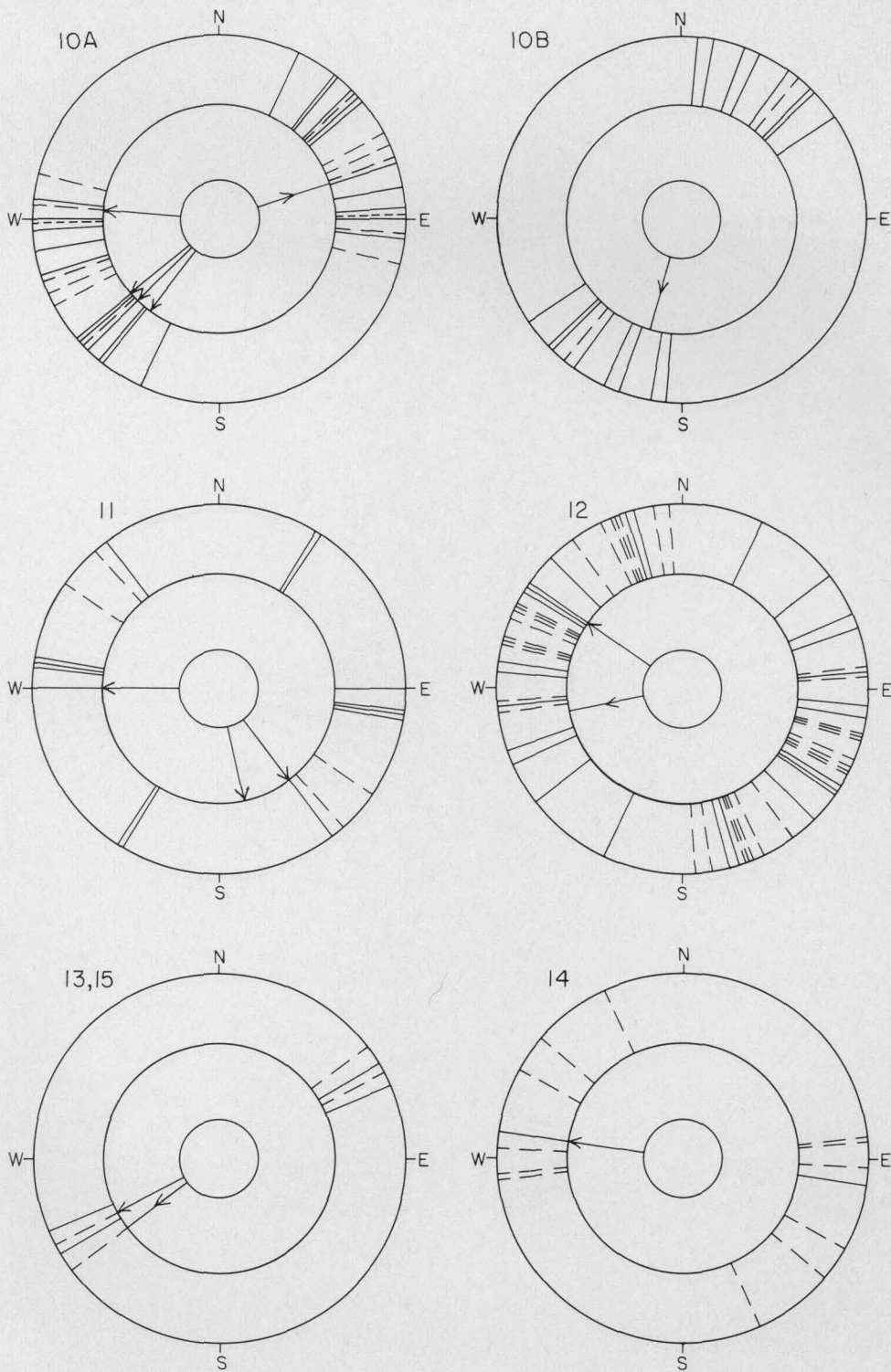
Sedimentary Petrology, Haymond Formation

Plate 25



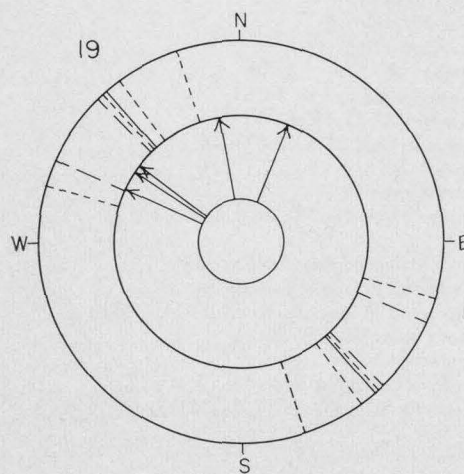
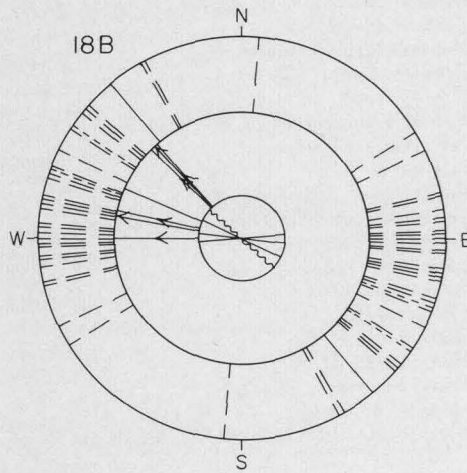
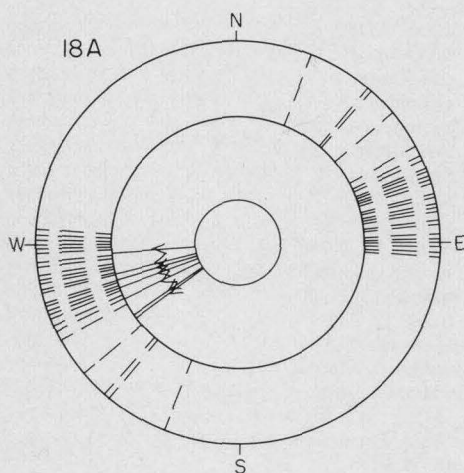
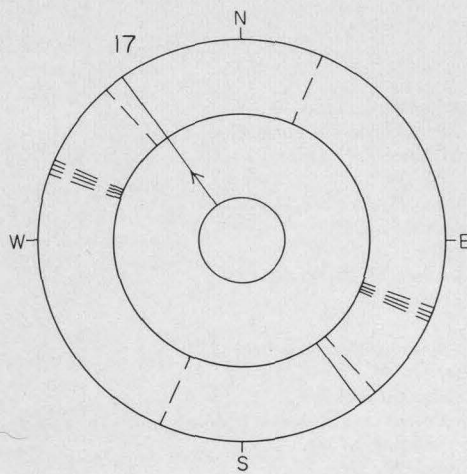
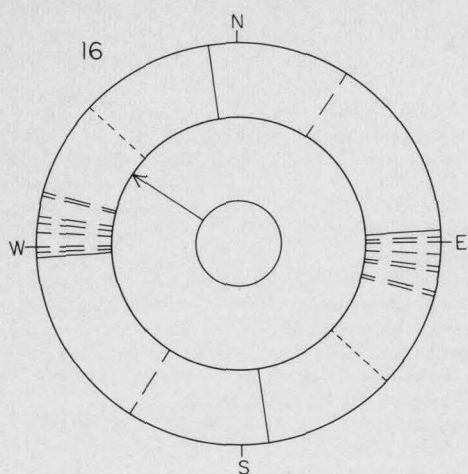
Sedimentary Petrology, Haymond Formation

Plate 25



Sedimentary Petrology, Haymond Formation

Plate 25



KEY TO DIAGRAMS

OUTER CIRCLE

GROOVE CAST

PARTING LINEATION

FLUTE LINEATION

MIDDLE CIRCLE

FLUTE CAST

GROOVE CAST; DIRECTION FROM
CROSS-BEDS

INNER CIRCLE

PLANT ORIENTATION

RIPPLE MARK

Index

- acknowledgments: 6
- age of Haymond Formation: 15, 16
- Allison Ranch facies: 10, 16, 17, 22-24, 30, 46-48, 55, 59, 61
- ankerite-siderite: 32, 33, 44
- apatite: 37, 39
- aplite: 26
- arkose: 23, 24, 66-68
- Atokan: 16

- ball-and-pillow structure: 21
- barite: 44
- basement rocks: 6
- bedding. *See* massive bedding and structureless bedding,
- biomicrite: 65
- biosparite: 65
- boulder beds: 3, 6, 10, 12, 24-29, 34, 37, 40, 49-53, 59, 65-69
- Bouma's turbidite model: 46
- Brewster County: 58

- Caballos Novaculite: 25, 28, 29, 34, 57, 60, 61, 65
- calcarenite: 65
- calcite: 44
- Callixylon* cf. *newberryi*: 29
- carbonate rock fragments: 32
- carbonate rocks: 65
- cataclasite: 2, 6, 57, 67, 68
- cement: 33, 40
- Chaetetes* Hill: 14
- chalcidony: 44, 52
- chert: 28, 29, 31, 37
- cherty limestone: 39
- chlorite: 30, 32, 33
- Clark Butte: 10, 12, 23, 24, 28, 51, 53, 56, 59, 60, 65
- clay minerals: 30
- Coahuila peninsula: 58
- coarse sandstone: 10, 17, 23, 24, 34, 39, 43, 50, 53, 59, 60
- cellophane: 66
- compaction: 44
- conglomerate: 25, 26, 57, 59
- convolute lamination: 18, 19, 20, 23, 46
- correlation coefficient: 41
- cross-lamination: 18-22, 23, 24, 46-48, 54, 59
- current work: 3

- Desmoinesian: 16
- Diablo Platform: 58, 60
- diagenetic features: 44
- Dimple Limestone: 3, 12, 14-16, 25, 39, 47, 50, 57-59, 61, 65, 66
- Dugout Mountain: 12, 14, 15, 21, 32, 33, 39-41, 44, 54-56, 61

- environment of deposition: 6

- epidote: 37, 39
- erratic rocks: 3, 15, 26, 34, 59, 65
- exotic rocks: 3, 15, 24-26, 28, 34, 51, 59, 65

- fabric: 33
- faulting: 44
- feldspar: 44
- flute casts: 18, 20, 21, 23, 54, 56, 60
- flute lineation casts: 20, 54
- fluxoturbidite: 56, 60
- flysch: 3, 8, 14, 15, 17, 45, 47, 59
 - deposition of: 45, 49, 59
 - facies: 8, 10, 12, 17-22, 48, 50
 - sandstone: 17, 23, 31-34, 39, 40, 41, 43, 48, 53
 - shale: 17
 - thickness of beds: 17
- folding: 44
- fossils: 8, 15, 32, 65
 - algae: 15, 32
 - brachiopods: 15, 32
 - conodonts: 16
 - crinoids: 32
 - echinoderms: 32
 - foraminifera: 31, 32
 - fusulinids: 6, 8, 15, 16, 32
 - molluscs: 15
 - pelecypods: 32
 - plants: 15, 27, 30, 59
 - sponge spicules: 31, 59
 - spores: 15, 31, 59
 - trace: 15, 21
- framework: 40
- Fusulina* sp.: 15
- Fusulinella haymondensis*: 15

- Gaptank Formation: 12, 14, 16, 23, 32, 33, 39, 46, 48, 59, 61
- garnet: 37, 39, 44
- gas rings: 23, 48
- glacial origin: 49
- glauconite: 65
- gneiss: 68
- graded bedding: 18, 46, 53
- granite: 25, 57, 59, 60, 66, 67
- granodiorite: 25, 57, 59, 60, 66, 67
- gravel: 50, 51
- graywacke: 67
- groove casts: 18, 20, 22, 23, 48, 54, 60

- haymondensis*, *Fusulinella*: 15
- Haymond Formation: 3, 61, 66
- Haymond Mountains syncline: 10, 12, 20, 23
- heavy minerals: 37-39
- hematite: 44
- horizontal laminations: 18, 19, 20, 22, 24
- Housetop Mountain: 16, 23-26, 28, 49, 59, 65

- igneous rocks: 6, 65

- illite: 30, 32
- imbrication: 34
- induration: 44
- introduction: 3
- jointing: 44
- K-feldspar: 31, 32, 41, 43
- kaolinite: 30, 32, 44
- laminated: 24, 46–48, 53, 59
- Las Delicias-Acatita: 58
- Lebensspuren*: 15
- limestone: 15, 25, 28, 65, 66
- lithology: 6
- lithostratigraphy: 8
- Llanoria: 57, 60, 61
- load deformation: 21
- load pockets: 18, 21
- Marathon—
 - Basin: 3, 22, 54, 56, 59
 - Formation: 65
 - geosyncline: 3, 57
 - town of: 17
- Maravillas Formation: 25, 29, 34, 50, 57, 65
- massive bedding: 19, 23, 46, 53, 59
- matrix: 19, 32, 33, 40, 43
- maximum grain size: 40
- measured sections: 8, 10
- megascopic features: 17–29
- metamorphic rock fragments: 31, 43
- metamorphic rocks: 6, 65
- metaquartzite: 31, 68
- metarhyolite: 59
- metasandstone: 66, 67
- microfaults: 21
- microsparite: 65
- molasse: 8, 61
- monazite: 37, 39
- montmorillonite: 30, 33
- mudstone: 10, 21, 23, 27, 33, 34, 50, 51, 59
- novaculite: 28, 29
- newberryi*, *Callxylon*: 29
- old Bennett Place: 10, 17, 23, 65
- oosparite: 65
- oriented grains: 22
- oriented plants: 21
- Ouachita—
 - geosyncline: 3, 59, 61
 - orogeny: 8
 - structural belt: 3, 57, 59
- paleocurrents: 50, 54–56, 57, 60
- parting lineation: 18, 20, 23, 54, 60
- Pennsylvanian: 15
- petrography: 30–43
- phyllite: 57
- plagioclase: 31, 32, 41, 43
- plant fossils: 15, 30
- polycrystalline quartz: 31, 43
- Precambrian: 28, 57
- previous work: 3
- problems: 8
- prod casts: 20
- provenance: 57–58, 60
- pyrite: 44
- quartz: 31, 41, 43, 44
- quartzarenite: 66
- quartzite: 59, 66
- radiometric age: 28, 60
- rhyodacite: 25, 67
- rhyolite: 26, 29, 60, 67, 68
- ripple marks: 17, 18, 20, 22, 45, 47
- rock fragments: 32
- roll-mark casts: 20
- rutile: 37, 39
- San Francisco Creek: 17
- sandstone: 25, 26, 31–34, 57, 59, 60, 65, 66
- sandstone dikes: 18, 21, 22
- sandstone sills: 21
- schist: 26, 57, 59, 60, 68, 69
- sedimentary rock fragments: 31, 43
- sedimentary structures: 18
- sedimentologic history: 59–61
- shale rock fragments: 33
- Sierra del Carmen: 58
- skeletal debris: 65, 66
- slump structures: 21, 44
- soft-sediment deformation: 50
- sole marks: 15, 20, 21
- sphene: 37, 39
- spring pits: 23, 46, 48
- stratigraphic petrographic variability: 39
- stratigraphy: 3, 6, 8–16, 59
- structure: 3
- structureless bedding: 18, 19, 21
- subarkose: 66
- submarine slumps and slides: 50–52, 59, 61
- summary: 59–61
- syenite: 26
- tectonic history: 60–61
- Tesnus Formation: 3, 8, 25–27, 29, 45, 57, 61, 66
- texture: 33
- thickness: 3
- tool-mark casts: 20
- tourmaline: 37, 39
- Trans-Pecos Texas: 3
- turbidite: 14, 15, 18, 20, 46–48, 50, 53, 55, 56, 60, 61
- turbidity current: 15, 45–47, 49–51, 53–54, 56–59, 61
- Val Verde basin: 61
- varves: 45
- volcanic rock fragments: 31
- wild-flysch: 59
- X-radiographs: 19
- X-ray diffraction: 30
- zircon: 37, 39